Characterization of tumor-infiltrating lymphocytes in ovarian cancer and development of a peptide-based anti-cancer vaccine

Charakterisierung von Tumor-infiltrierenden Lymphozyten des Ovarialkarzinoms und die Entwicklung einer peptid-basierten Krebsimpfung

Dissertation

der Mathematisch-Naturwissenschaftlichen Fakultät

der Eberhard Karls Universität Tübingen

zur Erlangung des Grades eines

Doktors der Naturwissenschaften

(Dr. rer. nat.)

vorgelegt von

M.Sc. Kevin Röhle

aus Zeitz

Tübingen

2017

Gedruckt mit Genehmigung der Mathematisch-Naturwissenschaftlichen Fakultät der Eberhard Karls Universität Tübingen.

Tag der mündlichen Qualifikation:	10.11.2017
Dekan:	Prof. Dr. Wolfgang Rosenstiel
1. Berichterstatter:	Prof. Dr. Stefan Stevanović
2. Berichterstatter:	Prof. Dr. Hans-Georg Rammensee

Ich erkläre hiermit, dass ich die zur Promotion eingereichte Arbeit mit dem Titel: „Characterization of tumor-infiltrating lymphocytes in ovarian cancer and development of a peptide-based anti-cancer vaccine“ selbständig verfasst, nur die angegebenen Quellen und Hilfsmittel benutzt und wörtlich oder inhaltlich übernommene Stellen (alternativ: Zitate) als solche gekennzeichnet habe. Ich erkläre, dass die Richtlinien zur Sicherung guter wissenschaftlicher Praxis der Universität Tübingen (Beschluss des Senats vom 25.5.2000) beachtet wurden. Ich versichere an Eides statt, dass diese Angaben wahr sind und dass ich nichts verschwiegen habe. Mir ist bekannt, dass die falsche Abgabe einer Versicherung an Eides statt mit Freiheitsstrafe bis zu drei Jahren oder mit Geldstrafe bestraft wird.

Tübingen, den

Table of contents

Abbreviations

aAPC	artificial antigen presenting cell
Ab	antibody
ACN	acetonitrile
BSA	bovine serum albumin
CA-125	cancer antigen 125
CD	cluster of differentiation
CRABP	cellular retinoic acid-binding protein
CTL	cytotoxic T lymphocyte
DC	dendritic cell
DMSO	dimethylsulfoxide
DNA	deoxyribonucleic acid
ELISpot	enzyme linked immuno spot assay
EOC	epithelial ovarian cancer
ER	endoplasmic reticulum
EYA2	eyes absent homolog 2
Fa	formic acid
FIGO	International Federation of Gynecology and Obstetrics
FOLR1	folate receptor alpha 1
FSC	forward scatter
HLA	human leukocyte antigen
ICS	intracellular cytokine staining
IDO1	indoleamine 2,3-dioxygenase 1
IFN	interferon
IL	interleukin
KLK	kallikrein
LGALS1	galectin-1
MHC	major histocompatibility complex
MMP	matrix metalloproteinase
MS	mass spectrometry
MSLN	mesothelin
MUC16	mucin 16
OvCa	ovarian cancer
PBMC	peripheral blood mononuclear cell

PMP	patients with malignant progression
PNP	patients with no malignant progression
PTTG	pituitary tumor transforming gene
RNA	ribonucleic acid
SSC	side scatter
TAA	tumor-associated antigen
TFA	trifluoroacetic acid
Th1	T helper cell type 1
TIL	tumor infiltrating lymphocyte
TMEM158	transmembrane protein 158
Treg	regulatory T cell
TSA	tumor-specific antigen

Summary

This thesis is about the characterization of tumor-infiltrating lymphocytes (TILs) and the development of a therapeutic peptide-based anti-cancer vaccine against ovarian cancer. The thesis is divided into three parts. The first part is about tumor-infiltrating lymphocytes and their expression of co-inhibitory and co-stimulatory receptors on the cell surface. For a more precise differentiation CD8+ cytotoxic T cells were separated from CD4+ T cells and the latter were further differentiated into regulatory T cells and T-helper cells. The co-inhibitory and co-stimulatory receptors CD137, cytotoxic T lymphocyte protein (CTLA-4), lymphocyte activation gene 3 (LAG-3), programmed cell death protein 1 (PD-1) und T cell immunoglobuline (TIM-3) were analyzed separately in the three different groups of regulatory T cells, cytotoxic T cells and T-helper cells. To evaluate the expression levels of the co-receptors on tumor-infiltrating lymphocytes, they were compared to lymphocytes from the peripheral blood (PBMCs) of each patient and PBMCs from healthy donors. It was shown that most of the receptors remained absent or of low expression besides PD-1 that apparently plays a dominant role in the immunosuppressive tumor microenvironment. Besides PD-1, CD137 shows low to moderate expression across the different patients being an interesting target for immunotherapy.

The second part focusses on the isolation of natural HLA ligands from ovarian tumor tissue. The eluted peptides and their respective source proteins were compared to source proteins and their peptides of benign ovarian tissue and a database that contains autopsies of different benign tissues. Through comparative profiling tumor-exclusive source proteins were determined.

At the end of the thesis these naturally presented tumor-exclusive ligands were used to treat patients who have no further therapy options. The treatment was able to induce HLA class I and HLA class II mediated reactions. The reactions were monitored through the course of therapy *via* IFN-γ ELISpot. Overall three patients were analyzed. In the first patient treated, we were able to induce a HLA class II mediate immune response. We were able to induce an HLA class I and II mediated immune response. The third patient has shown a pre-existing immune response against one HLA class I peptide and an immune reaction was induced against three HLA class II restricted peptides.

Zusammenfassung

Die vorgelegte Doktorarbeit befasst sich mit der Charakterisierung von tumorinfiltrierenden Lymphozyten und der Entwicklung einer therapeutischen peptidbasierenden Krebsimpfung beim Ovarialkarzinom. Der erste Part befasst sich mit tumorinfiltrierenden Lymphozyten und deren Expression von costimulatorischen und coinhibitorischen Rezeptoren auf der Zelloberfläche. Für eine präzisere Auftrennung wurden CD8+ zytotoxische T-Zellen von CD4+ T-Zellen unterschieden und diese wiederum wurden ihrer Funktion ein weiteres Mal unterteilt in T-Helferzellen und regulatorische T-Zellen. Die kostimulierenden und koinhibierenden Rezeptoren CD137, zytotoxisches T-Lymphozyten Protein 4 (CTLA-4), Lymphozyten-Aktivierungsgen 3 (LAG-3), programmierter Zelltodprotein (PD-1) und T-Zellimmunoglobulin (TIM-3) wurden in den drei Gruppen regulatorische T-Zellen, T-Helferzellen und zytotoxische T-Zellen separat betrachtet und ausgewertet. Um die Expression der Rezeptoren auf tumorinfiltrierenden T-Zellen bewerten zu können wurden diese mit Zellen des peripheren Blutes (PBMCs) der entsprechenden Patienten und PBMCs von gesunden Spendern verglichen. Es konnte gezeigt werden, während fast alle Rezeptoren nur gering exprimiert wurden und dass PD-1 eine dominante Rolle im immunsupprimierten Umfeld des Tumors einnimmt. Mit geringer oder moderater Expression ist CD137 ein valides Ziel für Immuntherapie.

Im zweiten Teil wird die Isolation von natürlichen HLA-Liganden von Ovarialtumoren beschrieben. Die dabei gefunden Peptide und deren Quellproteine wurden im Kontext von gutartigen Ovarien betrachtet. Darüber hinaus wurden Vergleiche mit einer Datenbank gezogen, die isolierte HLA-Liganden aus unterschiedlichen gutartigen Geweben beinhalten. Durch die Analyse der vergleichenden Ligandenprofile konnten Quellproteine bestimmt werden, deren Liganden ausschließlich auf dem HLA von Ovarialkarzinomen aber nicht auf dem HLA von anderem Gewebe gefunden wurden.

Am Ende der Arbeit wurden diese natürlichen tumorexklusiven Liganden dazu genutzt, um austherapierte Patientinnen im Heilversuch mit peptidbasierenden Impfungen zu behandeln. Hierbei konnte die Behandlungsstrategie zwischen den Patientinnen angepasst und verbessert werden. Dabei konnten sowohl HLA Klasse I-als auch HLA Klasse II-vermittelte Immunreaktionen nachgewiesen werden. Die Reaktionen wurden mittels 12-Tagesstimulation mit anschließendem ELISPOT-Test überprüft.

1. Introduction

1.1 Ovarian cancer: origin, incidence, mortality

Located on each side of the uterus, ovaries produce eggs that travel through the fallopian tube, where fertilization and the first mitotic cycles may occur. Fertilized zygotes then pass into the uterus, implant, and continue prenatal development.
The ovary consists of three different cell types. The epithelial cells form the outer boarder of the ovary, while the stroma cells embed the germ cells and form the surrounding tissue. These cells also produce female body hormones estrogen and progesterone. Stromal cells also produce the hormones estrogen and progesterone. Germ cells are progenitors to the eggs that develop in follicles that will eventually burst, allowing the eggs to leave the ovary. Although each of the three ovarian cell types can give rise to ovarian cancer, epithelial ovarian cancers (EOC) account for up to 90% of all OvCa, and will be the focus of this thesis. EOC can be subdivided into two main types. Type I tumors arise from ovarian epithelium and include the germ cell layers. They are thought to turn into endometroid, mucinous, clear cell and well-differentiated serous tumors, all of which typically show slower clinical progression. Type II tumors arise from the fallopian tube and give rise to poorly differentiated serous carcinomas, which grow more aggressively and are more prone to metastasis. Both types of EOC preferentially metastasize into the peritoneal cavity, where they can affect multiple organ systems.
The International Federation of Gynecology and Obstetrics (FIGO) collaborates with world's leading scientist in obstetrics and gynecology and frequently updates tumor staging and optimal treatment approaches. The staging comprises four stages considering the spread of disease with the organ of origin, the spread to other organs or vessel systems. Early stages of disease are largely symptom free, leading most patients to be diagnosed at a later stage (FIGO III or IV).EOCs can also metastasize through the lymphatic system via the retroperitoneal lymph nodes that are located close to organs and blood vessels [1].

OvCa is a gynecological malignancy and the fifth leading cause of cancer related death in women in Germany (Figure 1) [2]. The American Cancer Society reports over 22

200 estimated new cases and over 14 000 estimated deaths in the United States in 2017 [3].

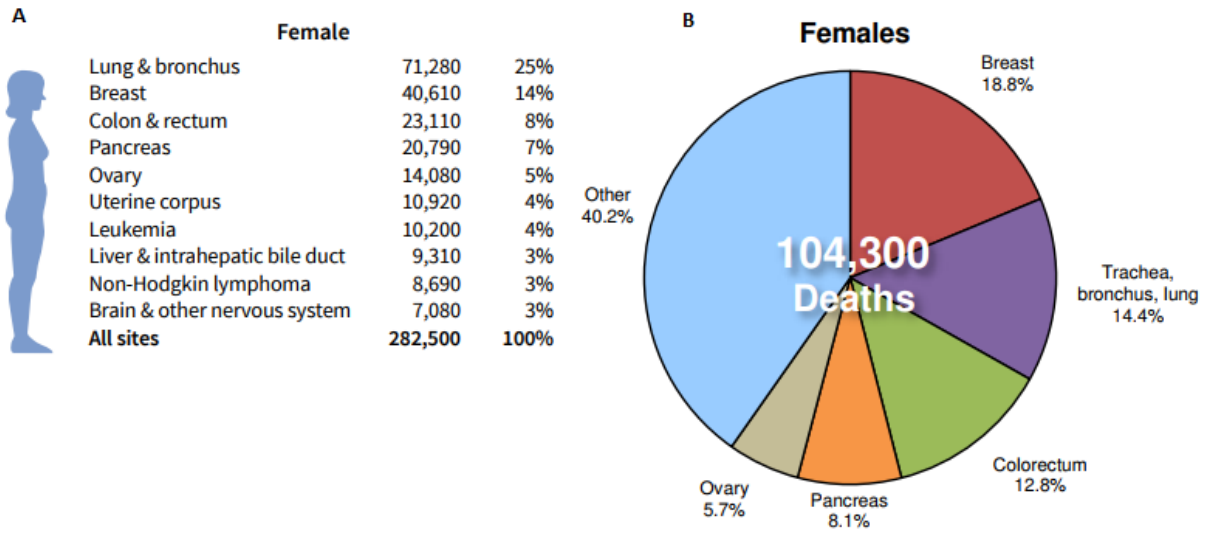

Figure 1 Comparison of estimated deaths in women in the United States (A) and Germany (B) [2].

The overall 5 year survival rate for all ovarian cancer types is 45%. The tumor type and stage, the age at diagnosis and the responsiveness to chemotherapy are crucial factors influencing overall survival. The five year relative survival of OvCa patients with an early stage diagnosis (FIGO IA and IB) is 92% but around 85% of the patients are diagnosed at an advanced stage cancer.

Table 1
Carcinoma of the ovary: FIGO nomenclature (Rio de Janeiro 1988)

Stage I	Growth limited to the ovaries	
	Ia	Growth limited to one ovary; no ascites present containing malignant cells. No tumor on the external surface; capsule intact
	Ib	Growth limited to both ovaries; no ascites present containing malignant cells. No tumor on the external surfaces; capsules intact
	Ic[a]	Tumor either Stage Ia or Ib, but with tumor on surface of one or both ovaries, or with capsule ruptured, or with ascites present containing malignant cells, or with positive peritoneal washings
Stage II	Growth involving one or both ovaries with pelvic extension	
	IIa	Extension and/or metastases to the uterus and/or tubes
	IIb	Extension to other pelvic tissues
	IIc[a]	Tumor either Stage IIa or IIb, but with tumor on surface of one or both ovaries, or with capsule(s) ruptured, or with ascites present containing malignant cells, or with positive peritoneal washings
Stage III	Tumor involving one or both ovaries with histologically confirmed peritoneal implants outside the pelvis and/or positive retroperitoneal or inguinal nodes. Superficial liver metastases equals Stage III. Tumor is limited to the true pelvis, but with histologically proven malignant extension to small bowel or omentum	
	IIIa	Tumor grossly limited to the true pelvis, with negative nodes, but with histologically confirmed microscopic seeding of abdominal peritoneal surfaces, or histologic proven extension to small bowel or mesentery
	IIIb	Tumor of one or both ovaries with histologically confirmed implants, peritoneal metastasis of abdominal peritoneal surfaces, none exceeding 2 cm in diameter; nodes are negative
	IIIc	Peritoneal metastasis beyond the pelvis >2 cm in diameter and/or positive retroperitoneal or inguinal nodes
Stage IV	Growth involving one or both ovaries with distant metastases. If pleural effusion is present, there must be positive cytology to allot a case to Stage IV. Parenchymal liver metastasis equals Stage IV	

[a] In order to evaluate the impact on prognosis of the different criteria for allotting cases to Stage Ic or IIc, it would be of value to know if rupture of the capsule was spontaneous, or caused by the surgeon; and if the source of malignant cells detected was peritoneal washings, or ascites.

IJGO Vol. 95, Suppl. 1 FIGO Annual Report, Vol. 26

Figure 2 FIGO staging of ovarian cancer. Stage I tumors are limited to the ovary with progression within the ovaries. Stage II tumors can progress into the tubes, uterus or pelvic space also including ruptures or metastasis and ascites formation. By increasing spread of metastasis into the peritoneum stage III tumors are defined. By stage IV distant metastases occur [4].

Later stage diagnosed patients have a less than 40% five year survival chance, emphasizing the importance of early diagnosis methods and routine medical checks. Transvaginal sonography can be used to detect even minor morphological changes. Additionally abdominal sonography gives insight in the presence of ascites, adhesions and other pathological findings in the abdomen. Magnetic resonance imaging (MRI) can be used to assess patients in poor condition or with difficult to assess cancers [5], however the cost and time involved in obtaining MRI readings makes this technique not optimal for routine monitoring. In later staged tumors cancer antigen 125 (CA 125) can be used as a blood biomarker, which can be used to track overall tumor burden.

1.2 Standard therapy

Standard therapy for OvCa patients involves tumor debulking surgery followed by platinum-based chemotherapy. Often the ovary is completely removed during surgery to increase maximal cytoreduction. The importance of good surgical tumor tissue removal should not be underestimated since it was shown that the more tissue was removed, the better the overall survival [6]. Carboplatin is used as the standard of care chemotherapy since it is less toxic and equally efficient as cisplatin [7]. Platinum-based drugs such as cisplatin or carboplatin enter the cell and undergo hydrolysis. The reactive platinum molecules bind nucleophilic groups containing oxygen, nitrogen and sulfur which can be found in amino acid side chains and the purine bases of RNA and DNA. The binding of the DNA is thought to be the mechanism of action since platinum-DNA adducts interfere with transcription and induce a DNA-damage response resulting in tumor cell apoptosis [8, 9]. Chemotherapy is further extended by giving taxane such as paclitaxel, which increases overall survival and progression free survival with an acceptable safety profile [10]. Paclitaxel is FDA approved for the treatment of ovarian, breast and lung cancer. It is a microtubule-stabilizing drug meaning it promotes the assembly and prevents the disassembly of microtubules. The constant assembly of microtubule induces cell arrest followed by apoptosis [11].

1.3 Risk factors of OvCa

In general cancer is an age-related disease. OvCa is rare in women younger than 40 years old, with over half of all OvCas occurring at the age of 63 or older. The highest OvCa rates are in post-menopausal women aged 55-64 years. One in 75 women will suffer from ovarian cancer [1], making OvCa among the highest probabilities of cancer development [12]. Despite the etiology of ovarian cancer remaining largely unknown, several risk factors can contribute to the development of OvCa including age, nulliparity, infertility, ovulation-inducing drugs. Use of oral contraceptives and hysterectomy both significantly reduce the risk of OvCa [13, 14]. Furthermore nutrition is also taken into account concerning the risk of developing ovarian cancer. Obesity significantly increases the OvCa incidence [15].

1.4 T cell development

Haematopoietic stems cells in the bone marrow differentiate into common lymphoid progenitors, which migrate and colonize the thymus. These developing progenitor cells are called thymocytes. Their maturation steps can be identified based on their surface marker expression. Most of the T cells developing in the thymus are αβ-T cells. Only a small amount of about 5% bear the γδ-TCR. The thymocytes interact with the stromal cells of the thymus. During their maturation process thymocytes wander through the thymus that consists of the inner medulla and the outer cortex. In the beginning thymocytes neither express CD4 nor CD8 and are therefore called double negative (DN).

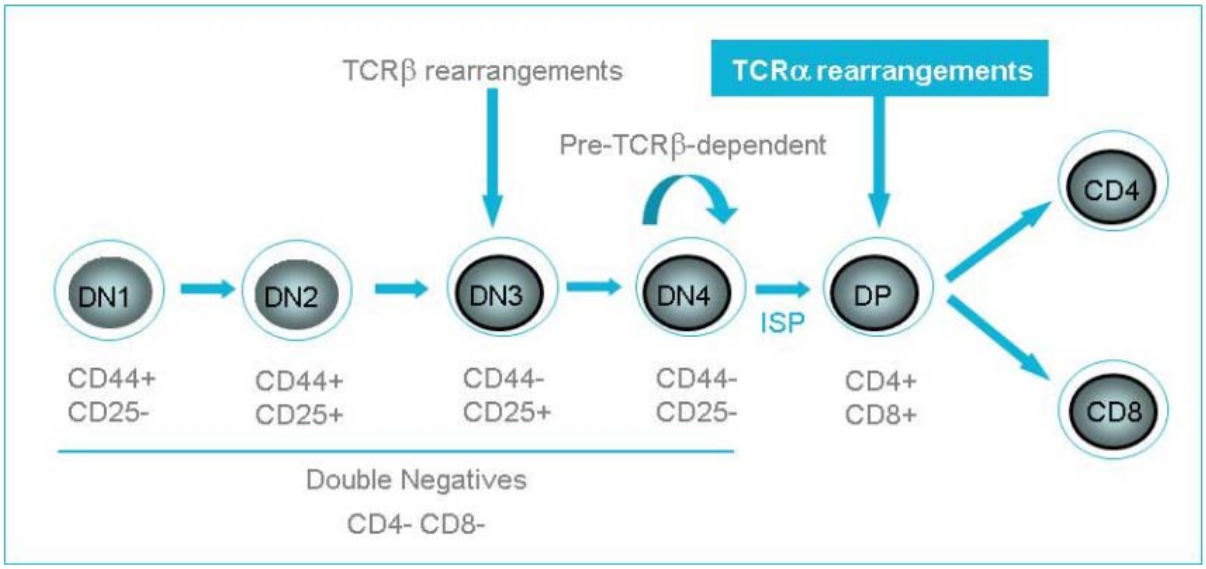

Figure 3 Different stages of T cell development. T cells start as CD4-CD8- double negative thymocytes, change the expression profile of different surface markers, rearrange α- and β-TCR loci and undergo multiple selections to develop into either cytotoxic CD8+ T cell or into CD4+ T cells with either helper or regulatory function [16].

During the DN stage, thymocytes express RAG1/2 and undergo V(D)J recombination to produce a functional TCR. For αβ T cells, the TCR β locus rearranges first. To test for production of a functional TCR β theβchain pairs with a surrogate TCR α chain to form a pre-TCR that complexes with CD3. Following this complex formation, thymocytes express survival and proliferation signals, stopβ-chain loci rearrangements, and begin rearranging the TCR α locus. T cells expressing a paired TCR αβ also express CD4 and CD8. The majority of CD4+CD8+ double positive

cortical thymocytes (DP) die in thymus due to failure to bind peptide-MHC complexes. This process, which eliminates useless T cells, is called death by neglect. DP cells with TCRs that are capable of binding MHC undergo positive selection in the outer cortex of the thymus. During positive selection the TCR weakly binds to MHC-peptide complexes presenting self-antigens allowing for signaling through the TCR, leading to upregulation of BCL-2 and rescue from default apoptosis. However, too strong signaling through the TCR, as would occur for autoreactive specificities, results in a negative selection step eliminating thymocytes that migrated into the medulla and whose interaction between TCR and self-antigen MHC complex is too strong. During the last step of development, one of the co-receptors is downregulated turning thymocytes into CD4 or CD8 single positive T cells. About 3% of all thymocytes leave the thymus to roam the peripheral blood and lymphoid tissues as naïve T cells [17, 18].

1.5 The role of tumor infiltrating lymphocytes in cancer

Early prediction models of disease progression and survival rates were developed and based on factors such as tumor thickness, radial or vertical growth. As the role of the immune system in controlling tumor growth has become more appreciated, tumor-infiltrating lymphocytes and cytokines that influence the tumor microenvironment were recently shown as important factors for clinical outcome across a wide range of malignancies. Halpern and Schuchter described prognostic models for melanoma and the importance of TILs and cytokines as prognostic factors [19]. Further studies have shown the importance of intratumoral T cells and their association with progression-free and overall survival. The potential of TILs was also shown in breast cancer [20], renal cell carcinoma [21] and colorectal cancer [22]. In esophageal carcinomas, activated, IFN-γ secreting CD8+ T cells were associated with a good prognosis in squamous cell and adenocarcinomas [23]. For OvCa, a cohort of epithelial ovarian cancer (EOC) patients was analyzed by immunohistochemistry for the presence of CD3-positive intratumoral T cells and progression-free and overall survival was significantly increased in patients with high amounts of TILs [24]. Collectively, these studies suggest the importance of intratumoral lymphocytes in solid tumors and also suggest that increasing intratumoral lymphocytes may be a desirably aim for OvCa therapy.

1.6 T-cell priming: the three signals for T cell activation

In order to prime naïve T cells, three different signals are required. The first signal conveys antigen specificity and is created by binding of the T cell receptor (TCR) to the peptide-MHC complex on an antigen presenting cell. Although many cells express MHC molecules, dendritic cells are particularly suited to priming naïve T cells. Activated dendritic cells also upregulate the chemokine receptor CCR7, allowing them to traffic to the draining lymph node and interact with naïve T cells. Naïve T cells that recognize their cognate antigen presented on MHC (signal 1) are simultaneously given a second signal through the interaction of CD80/CD86 binding to CD28 on T cells as a co-stimulatory signal to the TCR-MHC-interaction (Figure 4) [25].

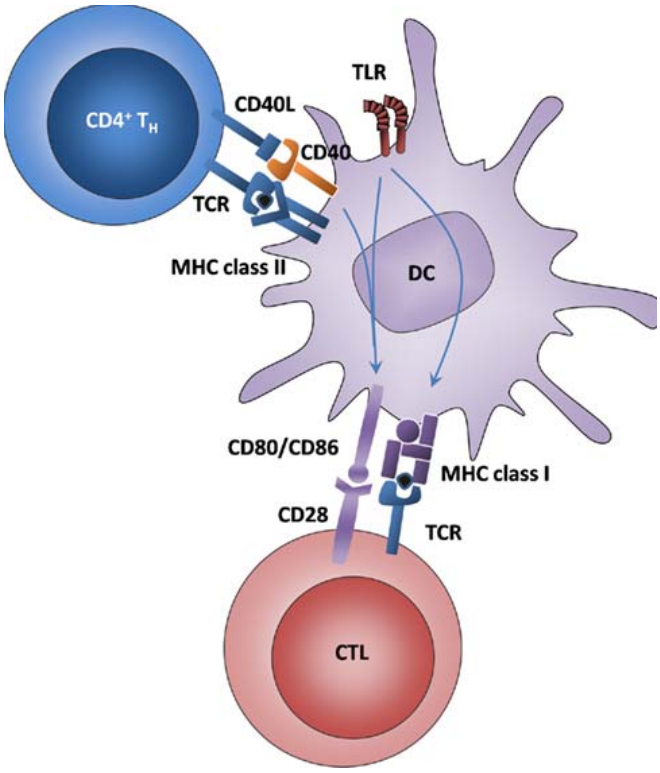

Figure 4 Schematic depiction of interaction between APC and cytotoxic TL (CTL) and T-helper cell (TH). The TCR-complex of CTL interacts with the MHC class I and TCR-complex of CD4 TH binds MHC class II. TCR engagement is the first signal for successful T cell activation. The second signal is created by CD28 that binds its ligand CD80/CD86 [26].

Signal 1 and signal 2 are needed for proper T cell priming. Cytokines such as IL-12 secreted by the dendritic cell may also influence T cell effector function. The cytokine milieu present at the time of naïve T cell priming is called signal 3 and is critically

important for formation of CD4 helper T cell subsets. Successful activation of the T cell leads to cytokine production and proliferation, and in the case of CD8 T cells, acquisition of cytotoxic ability [27]. Effector T cells leave the lymph node and travel to inflamed tissues where they can reencounter antigen as peptide-MHC complexes and, in the case of CD8 T cells, kill virally infected or transformed cells. Importantly, effector CD8 T cells require only TCR:peptide/MHC engagement (signal 1) and can kill their targets in a costimulation independent manner. Cytotoxic reaction can be induced by perforin and proteases such as granzyme B. Additionally the targeted cell can undergo apoptosis caused by the interaction of Fas and Fas-ligand [28].

In case of cancer the immune system can distinguish the myriad of genetic and epigenetic alterations that are characteristic to the cancer cells and differentiate them from normal tissue counterparts. The quality and amplitude of the immune response depends on an interplay of co stimulatory and co-inhibitory signals, called immune checkpoints (Fig. 5). Immune checkpoints are critical for preventing autoimmunity by inducing self-tolerance and protecting the tissue from taking damage in case of infection. Cancerous tissue on the other hand can induce a dysregulated expression of immune-checkpoint proteins and therefore manipulate the immune system and prevent an anti-cancer immune response [29].

Chemotherapies, radiation and targeted therapies all aim at the malignant cell directly and induce tumor cell death. Another approach is cancer immunotherapy, here therapy targets the immune system rather than the malignant cell [30]. Immune-based therapies for cancer have shown major advances over the past years with adoptive T cell transfer, RNA- or peptide-based vaccines and antibodies or small molecules either targeting cancer antigens or key regulators of anti-tumor immunity.

1.7 Novel cancer immunotherapy: immune checkpoint blockade

Among the most promising of immunotherapies is the use of antibodies targeting co-inhibitory or co-stimulatory receptors. With steadily growing numbers of different receptors and increased understanding of their effector mechanisms, they became attractive targets for cancer immunotherapy. This thesis will focus on tumor necrosis factor receptor superfamily member 9 (TNFSR9, 4-1BB, CD137), cytotoxic T

lymphocytes associated antigen 4 (CTLA-4), programmed death1 (PD-1), lymphocyte-activation gene 3 (LAG-3) and T-cell immunoglobulin and mucin-domain containing-3 (TIM-3).

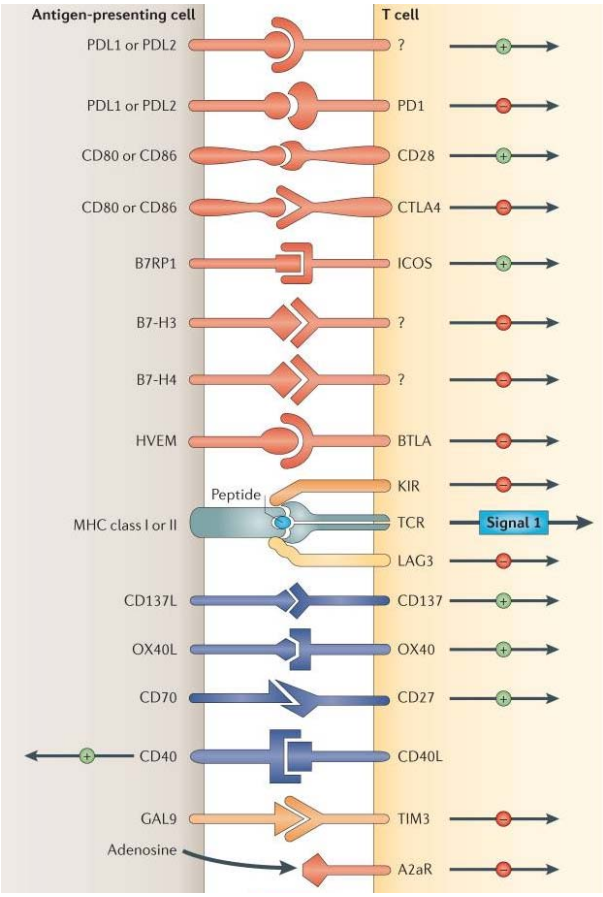

Figure 5 T cell response is modulated by numerous activating or inhibiting receptors. This interaction is further regulated by various receptor-ligand interactions. These responses can occur either upon initiation within the lymph node or in the peripheral tissue or tumor tissue. Up to now not all possible ligand receptor interactions are fully understood and different combinations might be possible. CD28 and CTLA-4 for example share the same ligand but expression of receptor occurs either in naive T cells, in case of CD28, or upon T cell activation in case of CTLA-4 (modified from [29]).

CD137 also called 4-1BB or tumor necrosis factor receptor superfamily member 9 (TNFRSF9) is expressed on activated T cells, Tregs, and natural killer (NK) cells. CD137 is a costimulatory receptor that belongs to the TNF receptor superfamily [31], and has been shown to enhance cytotoxic T cell responses. The treatment of tumor

inoculated mice with CD137 mAb lead to eradication of tumor and established memory response against the tumor with mice being immune to rechallenge with tumor cells [32]. Another study analyzed the effect of agonistic stimulating anti-CD137 antibody and the consequence of CD137 knockout in mice. KO mice are more susceptible to B16F10 lung metastasis, accompanied with shorter survival compared to similarly inoculated control mice. Likewise, treatment with an agonistic stimulatinganti-CD137 antibody, extends survival in the B16F10 lung metastasis model [33]. The immunomodulatory function of CD137 appears to affect naïve T cell priming by dendritic cells. The adjuvant role of CD137L was assessed by using the extracellular domain of CD137 ligand (CD137L). In combinational of peptide loaded dendritic cells and CD137L strongly increased cytotoxic T cell function measured by T-cell proliferation, activation and survivals well as IL-2 and IFN-γ production [34]. An anti-CD137 mAb in a vaccination setting enhances presentation of tumor antigens by dendritic cells, leading to reduced tumor recurrence and improved survival [35]. In addition anti-CD137 mAb can even reduce the number of tumor-infiltrating Tregs, although the mechanism for this Treg reduction is not fully elucidated [36, 37].

CTLA-4 was the first immune checkpoint to be clinically targeted [38]. It is exclusively expressed on T cells where it regulates T cell activation as an antagonist to the CD28 co-stimulatory receptor. CTLA-4 and CD28 share the same ligands CD80 and CD86. Upon engagement of the TCR to the peptide-MHC complex, CD28 strongly amplifies TCR signaling subsequently. The expression of CTLA-4 on the T cell surface outcompetes the binding to the two ligands because it shows a higher avidity for CD80 and CD86 than CD28 and therefore dampens the T cell response by delivering inhibitory signals [29, 39]. The importance of CTLA-4 in controlling the immune response is underscored by the lethality of CTLA-4 knockout in mice causing massive lymphoproliferation and fatal multi organ tissue destruction [40]. Despite CTLA-4 being expressed on CD8+ T cells, the major function of anti-CTLA-4 immunotherapy appears to be depletion of CD4+ intratumoral Tregs, which have higher surface expression of CTLA-4 than any other cell in the body [41].

PD-1 is an inhibitory receptor found on T cells, B cells, dendritic cells and NK cells. PD-1 has so far two known ligands, programmed deathligand1/2 (PD-L1/2). PD-L1 is found on APCs, some somatic and cancer tissues whereas PD-L2 is selectively

expressed on activated monocytes and dendritic cells [42, 43]. The Food and Drug Administration (FDA) approved blocking antibodies to the PD-1/PD-L1 pathway, pembrolizumab, nivolumab, and atezolizumab. Topalian and colleagues have shown that blockade of PD-1 is a potent way of reactivating an immune response in their cohort for 18% of the non-small-cell lung carcinoma patients, 25% of the melanoma patients, and 27% among patients with renal-cell cancer [44]. Many clinical trials using blocking antibodies targeting PD-1 or its ligands and combining it with different types of other antibodies or treatments are currently in progress. PD-1 and LAG-3 have been shown to work synergistically to prevent autoimmunity in mice [45].

Lymphocyte activation gene-3 (Lag-3) is up regulated on both CD4+ and CD8+ T cells. Lag-3 deficient mice revealed Lag-3 to be a negative regulator of T cell expansion. Despite LAG-3 and CD4 sharing less than 20% amino acid sequence homology, the structure of Lag-3 is quiet similar to CD4 [46]. Thus Lag-3 likewise to CD4 binds MHC class II and acts as a negative competitor [47]. Lag-3 is also expressed by regulatory T cells. Studies have shown that modulation of LAG-3 can enhance or abrogate Treg activity [48].

T cell immunoglobulin-3 (Tim-3) is a cell surface molecule expressed on IFN-γ producing CD4+ T helper cells, CD8+ cytotoxic T cells, Tregs and innate immune cells such as dendritic cells, natural killer cells and monocytes [42]. Tim-3 functions as a negative regulator of type 1 immunity. Mice treated with anti-TIM-3-antibody have exacerbated experimental autoimmune encephalomyelitis, a mouse model of multiple sclerosis [49].

Being the only cell type in the human organism capable of producing antibodies B cells play an important role in creating an immune response. Additionally they serve as antigen presenting cells and express co-inhibitory and co-stimulatory receptors on the cell surface. Furthermore B cells can secret cytokines overall having multiple ways to influence the immune response [50].

B cells have been shown to be reasonable prognostic factors in cancer patients such as node-negative breast cancer [51] metastatic melanoma [52]and advanced ovarian

cancer [53]. Within these cancers the amount of infiltrating B cells positively correlated with progression-free and overall survival.
In addition to that a regulatory B cell (Bregs) phenotype has been described, remaining yet to be fully understood [50]. They have been reported to be able to suppress IFN-γ and TNF-α secretion by T cells and their proliferation. CD19(+)CD24(hi)CD38(hi) B cells were able to inhibit naïve T cell differentiation into TH1 and TH17 cells and mediate Treg-properties [54]. These properties have been shown to be induced through immunosuppressive cytokines such as IL-10 and TGF-β and induction of FoxP3 and CTLA-4 expression [55].

Besides the known high impact of the adaptive immune system there is increased evidence of tumor surveillance by natural killer cells (NK cells). Early studies have shown NK cells are able to discriminate tumor cells from normal tissue and eradicate the tumor. Tumor cells may lose expression of MHC molecules, which can be detected by NK cells. Furthermore, tumor cells upregulate the stress ligands MICA/B, which can be recognized by activating NK receptors, inducing NK mediated killing. A rechallenge following a first sensitization of NK cells leads to persistent rejection of tumor [56]. Besides that depletion of NK cells in mice through NK1.1 binding antibodies lead to a higher susceptibility to B16 melanoma and increasing mortality of NK cell depleted mice. However depletion did not influence distribution of other lymphocyte subsets [57]. NK cells control cancer either by direct interacting with tumor cells or augmenting the activities of other tumor cells in the tumor microenvironment. NK cells may directly release perforin and granzyme, leading to tumor cell lysis [58]. Furthermore NK cells can induce tumor cell death through death receptor-mediated pathways such as FasL and TRAIL [59-61].

Another problem than overcoming the immunosuppressive tumor microenvironment is to stimulate T cells. A major focus in current research are cytotoxic T cells capable of directly eradicating tumor cells. Antigen processing, presentation and isolation are key points in the selection process of vaccination peptides.

1.8 Major histocompatibility complex

The MHC molecules present peptide fragments derived from pathogens or mutated proteins on the cell surface. In the consequence the infected or mutated cells are killed, macrophages and B cell are activated. B cells subsequently produce antibodies that are eliminating or neutralizing extracellular pathogens.

The MHC is polygenic meaning there are several different MHC class I and MHC class II genes that create a set of MHC molecules with different ranges of peptide-binding specificities in each individual. Secondly MHC molecules are polymorphic meaning there are multiple variants of each gene within the population as a whole. The MHC is located on chromosome 6 in humans and contains more than 200 genes whereas the genes for the β_2-microglubulin and the invariant chain are located on chromosomes 15 and chromosome 5. The genes for the α-chain of MHC class I and the α and β chain for MHC class II are linked within the gene complex. In humans the MHC is called human leukocyte antigen (HLA) since they were first discovered as differences in leukocytes between individuals.

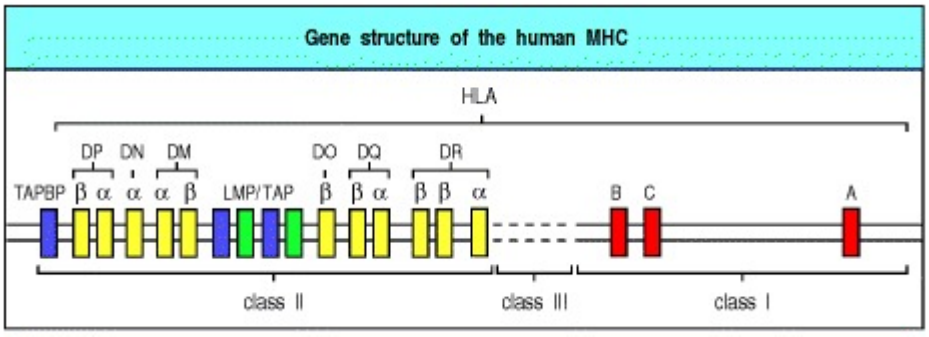

Figure 6 Gene structure of MHC class I and MHC class II on human chromosome 6. There are three HLA class I genes (HLA-A, -B and -C) as well as three pairs of MHC class II α and β chain genes (HLA-DR, -DP, -DQ) (adapted from [62]).

The combination of MHC alleles found on a single chromosome is called MHC haplotype with MHC genes being codominantly expressed with both HLA alleles of each locus to produce molecules that present peptides at the cell surface. The

treatment of cells with interferons-α, -β, -γ leads to an upregulation of MHC-α chain and β_2-microglubulin genes as well as genes encoding the proteasome, tapasin and TAP.

Peptides bind MHC class I through specific anchor residues with the sidechains of these residues anchoring binding pockets along the peptide binding groove of the MHC class I molecule. Each MHC class I molecule has a specific preferred sequence motif allowing the prediction of potential MHC binders from a given protein sequence. MHC class II also has different allelic variants that have a certain preferred peptide sequence motif. In contrast to MHC class I the peptide-binding groove is bigger allowing the binding of longer peptides and an overall greater flexibility in peptide binding. Concluding it is more difficult to predict MHC class II binding peptides [62].

The process of antigen presentation shows the current state of the cell. Here antigens are presented at the cell surface to be recognized by the immune system. These peptides are either presented by major histocompatibility complex class I (MHC I) molecules by all nucleated cells to CD8+ T lymphocytes. Alternatively the peptides can be presented by major histocompatibility complex class II (MHC II) to CD4+ T lymphocytes by antigen presenting cells (APC) such as dendritic cells (DC), macrophages and B lymphocytes. In general peptides presented by MHC I are derived from intracellular peptides. Peptides presented on MHC II are derived from source proteins from the extracellular space.

Vaccinating and immunizing patients with peptide-based vaccines can be achieved in two ways: either Peptides can be predicted with bioinformatitional tools such as SYFPEITHI or NetMHCpan-3.0. These tools predict the binding probability (SYFPEITHI) or binding affinity (NetMHCpan-3.0) of a peptide to a certain HLA of interest. Predicted peptides sometimes fail to induce proper immune responses, especially if the source protein is low abundant or the HLA of interest has a natural low affinity to its peptides in general.

Therefore isolating peptides via liquid chromatography-coupled mass spectrometry is a more suitable approach to identify peptides that can be used as vaccination peptides. These peptides are naturally presented HLA ligands and since they are isolated from

the ligandome of, in this case, tumor tissue they are potential targets for cancer immunotherapy.

1.9 OvCa relevant target proteins

The following peptides were shown to be OvCa associated in preliminary work of our lab. Additionally they were put in context for tumor development and progression in other tumor entities.

Mucin16 (MUC16) also called cancer antigen125 (CA125) is a commonly used ovarian cancer serum marker. It is a very large type-1 transmembrane mucin with about 22152 amino acids [63, 64]. First of all Muc16 can be used for early detection of OvCa, additionally it can be used to monitor the response the response to OvCa treatment and control for tumor recurrence. Despite its important role in OvCa MUC16 is overexpressed in breast, pancreatic and colorectal cancer [65] and being mutated in other tumor types as well [66].

The cellular retinoic acid-binding proteins-1 and-2 regulate the access of retinoic acid to the nuclear retinoic acid receptors. It was early described that CRABP is present in tissue of patients with large bowl cancer [67]. CRABP 2 seems to be involved in the inhibition of tumor growth since the activation of retinoic acid receptor with retinoic acid leads to expression of ant proliferative genes [68]. Yet its complete function in tumorigenesis still remains to be fully understood.

Indoleamine 2,3-dioxigenase 1 (IDO1)is the main enzyme that catalyzes the first rate limiting step in the metabolic cascade that converts the essential amino acid L-tryptophan into L-kynurenine. IDO-1 is constitutively expressed by tumor tissue cells. The metabolic pathway has been shown to establish peripheral tolerance and creating a tumor suppressive microenvironment. This feature makes it an attractive target for cancer immunotherapy [69, 70].

Matrix metalloproteinase 11 (MMP11 or stromelysin-3) has been reported to be involved in in the development and progression of a variety of malignancies. In general matrix metalloproteases are key regulators in the metabolism of connective tissue matrices. MMP11 exerts collagenolytic functions. In cancer they can promote

oncogenic transformation and angiogenesis supporting tumor growth and metastasis [71].

Human pituitary tumor-transforming gene (PTTG or securin) is a proto-oncogene in the development invasion and metastasis in a variety of different tumor types including OvCa. Its overexpression induces cellular transformation and tumor development in mice. Furthermore PTTG overexpression correlates with worse differentiation in OvCa [72]. Short interfering RNAs (siRNA) reduced expression of PTTG mRNA and protein and subsequently to a 50% reduction in cell proliferation. Mice constitutively expressing siRNA against PTTG lead to a reduction in tumor development and tumor growth [73]. In humans PTTG expression correlated with invasiveness and vessel density [74, 75].

Eyes absent homolog 2 (EYA2) functions as a protein phosphatase and transcriptional coactivator for SIX1. SIX1 has been shown to be dependent on EYA2 expression to mediate epithelial-mesenchymal transition (EMT) and induction of cancer stem cell formation (CSCs). In breast cancer patients EYA2/SIX1 expression correlated with shortened time of relapse, metastasis and overall survival. Whereas EYA2/SIX1 are expressed only in a few adult tissues making them attractive targets for cancer therapy [76].

Galectin-1 (LGALS-1) belongs to the family of galectin proteins binding galactoside. LGALS1 is highly expressed in various tumors and their oncogenic processes. Galectin-1 is highly expressed in colon [77], glioma [78], breast [79], lung [80], head and neck [81], ovarian [82] and prostate carcinoma [83] being associated with metastasis and tumor growth [84].

The folate receptor α (FOLR1) transports folate into the cells which is needed in cell metabolism. Overexpression of FOLR1 is associated with increased tumor growth by increased folate uptake. In an attempt to target FOLR1 antibodies and conjugates have been developed in order to treat OvCa and lung cancer whereas FOLR1 is also overexpressed in breast, brain and colorectal cancer [85].

KLK10 also called kallikrein-related peptidase 10 is one of 15 highly conserved serine proteases. They are potential biomarkers of prostate, breast, ovarian, gastrointestinal, head and neck, lung and brain cancer. Most famous kallikrein is the prostate specific antigen (PSA or KLK3) that is used as a biomarker for prostate cancer [86].

The transmembrane protein 158 (TMEM158) was overexpressed in OvCa and a knockdown of TMEM158 RNA leads to significantly inhibition of cell proliferation. This inhibition may be caused by an increased G1-phase arrest due to its interaction with Ras that induces senescence. Silencing of
TMEM158 inhibited cell adhesion, cell invasion as well as tumorigenicity [87].

Mesothelin and MUC16 were found to be upregulated in the infiltrating compartment of pancreatic ductal adenocarcinoma impaling their involvement in migration and metastasis [88].

Tumor exclusive ligands are seemingly the best to use in cancer immunotherapy. The ideal application consists of a selection of peptides for each individual separately. To set up such an individualized therapy a warehouse of preselected peptides is needed. The warehouse idea comprises the possibility of having a big number of peptides available for cancer patient treatment. Each peptide is restricted by a certain HLA. Depending on the patients HLA up to 10 peptides are chosen, selecting the most immunogenic and best suiting ones for each patient, combining them into a cocktail. With this off-the-shelf use of peptides maximum flexibility is granted allowing individual and ideal therapy.

In order to establish the warehouse properly, compassionate use of peptides was not only dependent on HLA-genotype of each patient but also was a MS-analysis performed. Peptide lists of patients were searched for warehouse peptides. A cocktail of ten peptides was assembled accordingly.

1.10 Adjuvants in cancer immunotherapy

Adjuvants in cancer immunotherapy can give an additional boost to the immune system, priming an immunereaction and support the effectivity of the applied drug drastically. The ideal adjuvant provides optimal availability of the antigen by regulating its persistence, location, concentration and presentation [89].
Incomplete Freund's adjuvant (IFA), does not contain heat-killed Mycobacteria tuberculosis to avoid acute granulomatous lesions at the site of vaccination. IFA is a water-in-oil emulsion and is characterized by its depot effect and slow release of emulsified antigen inducing strong cellular and humoral immune reaction. Especially the vaccination with long peptides induced cytokine production and efficient T cell priming through DCs [90]. Accordingly the persistent activation and attraction of T cells prevent them from entering the tumor site and subsequently resulting in T cell exhaustion and Fas/Fas-L mediated cell death [91].

Aluminum-based adjuvants such as aluminum hydroxid (Alhydrogel™) and aluminum phosphate (Adjut-phos™) are used in virus vaccines against influenza, tetanus, diphtheria, pertussis, poliomyelitis and HPV [92]. Aluminum-based adjuvants are characterized by a depot effect. It has been reported that aluminum-based adjuvants induce intense antibody production [93].

Micro- and nanoparticles have advantageous features such as protection of their cargo against degrading factors such as serum/tissue peptidases or proteases increasing the half-life of their cargo. Furthermore these particles can be engineered by charge, rigidy, size or added ligands on particle surface to target certain tissues types or organs [89]
As vaccines changed from vaccinating with attenuated or dead pathogens towards recombinant artificial subunits scientists discovered the family of highly conserved pattern recognition receptors (PRR) called Toll-like receptors (TLR) [94] Since then more PRRs have been discovered such as NOD-like receptors (NLR), C-type lectin receptors and retinoic acid inducible gene (RIG)-1-like receptors (RLR) and with this adjuvants have been developed to additionally stimulate the immune system and promote effectiveness of vaccines[95-97]. TLR2 can be engaged by bacterial lipopeptides or palmitic acid. Stimulation of TLR2 lead to DC maturation [98]and up-regulation of co-stimulatory signals (such as CD80 and MHC class II) [99], B-cell

activation [100], enhanced T-cell response and pro-inflammatory cytokine secretion such as IFN-γ or TNF-α [101-103].

TLR3 agonists such as double-stranded RNA or the synthetic analog polyinosine-polycytidylic acid (poly I:C) can engage TLR3 in in the endosome DCs, macrophages and on the surface of epithelial cells [104]. It can induce the production of inflammatory cytokines, type 1 interferons followed by upregulation of co-stimulatory signals [103]. Despite its short half-life poly I:C has been shown to enhance cross-presentation by DC to CD8+ T cells [102].

TLR4 is expressed on the surface of DCs, macrophages, fibroblasts and epithelial cells. TLR4 activation strongly promotes TH1 response [105]. Since LPS is potentially dangerous to the patient it has been replaced with less toxic synthetic derivates such as monophosphory lipid A (MPLA) which has been tested in combination with other antigens in clinical trials for melanoma [106], lung [107] and prostate cancer [108].

TLR7 and TLR8 recognize single stranded RNA (ssRNA) in the endosomal compartment.TLR7/8 are expressed by antigen presenting cells. It has been shown that signaling from TLR7/8 gets DCs to migrate from the skin to the lymphnode presenting antigens to CTLs and T helper cells. Imiquimod is an imidazoquinoline amine and known as a potent immune response modifier inducing anti-viral and anti-tumor activity. Imiquimod was FDA approved to treat basal cell carcinoma and genital warts. It stimulates the production and release of cytokines such as interferon-α (IFN-α), interleukin-6 (IL-6) and tumor-necrosis factor-α (TNF-α9: Cytokine production was induce after topical application to the skin of hairless mice. Additionally it was shown that Imiquimod activates macrophages to secrete cytokines. It was applied epicutanously on the vaccination site. Additionally there have been clinical studies using Imiquimod supporting their vaccines targeting melanoma [109], prostate cancer [110], chronic myeloid leukemia [111] and vulva intraepithelial neoplasia [112]. Summarizing Imiquimod supportively leads to cellular and humoral responses.

1.11 Peptide-based anti-cancer vaccines

Peptide-based anti-cancer vaccines are promising ways of treating different cancer entities. The manifold advantages of peptide vaccines are they are relatively easy to synthesize, relatively stable in storage and show no oncogenic potential. Nevertheless their application is complicated and numerous parameters have to be set. Thus until now peptides have shown only poor immunogenicity. The choice of antigen the peptides are derived from and the suppressive microenvironment are further hurdles to overcome in order to successfully establish an anti-tumor vaccine. Antigenic HLA ligands are derived from tumor associated antigens (TAA) or tumor-specific antigens (TSA) [113, 114]. TAAs are found on tumor and on benign tissue but are generally found in higher amounts on the benign tissue. TSAs are exclusively found on tumor cells and caused by viral infection or genetic mutations. TAAs can be divided into differentiation antigens, cancer/ testis antigens, and overexpressed antigens. Differentiated antigens such as melanoma Ag recognized by T cells (MART-1)/Melan A, gp100, tyrosinase, tyrosinase-related protein (TRP-1) and TRP-2 are used to treat melanoma. Cancer/testis antigens share expression between tumor and germ line cells. Theses antigens do not induce an immune response against benign testis cells since these do not express MHC making cancer testis antigens attractive targets in cancer immunotherapy. Well studied examples of cancer/testis antigens are MAGE-1 and NY-ESO-1. HER-2 is a classical representative of the overexpressed tumor antigens. HER-2 is expressed in higher amounts during embryonal development but expressed in low amounts on normal tissue in adults whereas HER-2 is highly overexpressed in breast, ovarian and non-small-cell-lung cancer [115].

Montanide™ ISA-51 is a mineral oil-based emulsifier that stays at the injection site and is progressively eliminated by immune cells such as macrophages. It is metabolized into its compounds of fatty acids, triglycerides, phospholipids and sterols [116]. The degradation process is long lasting. It was shown that only 30% of the mineral oil is degraded within the first month which was found out by using radioactive tracers [117]. Montanide™ ISA-720 is based on plant oil, thus easier to degrade by but still offering the storage capacity of an oil based adjuvant but less side effects than Montanide™ISA-51.

1.12 Aim of the study

Ovarian cancer patients are often diagnosed at later stage of disease since disease progression remains largely symptom free. Post-menopausal monitoring for malignant transformation is difficult and elaborate. The blood level of Muc16 also called cancer antigen 125 (CA125) can be used as a tumor marker to discover and monitor disease occurrence and progression. Nevertheless, with low overall 5 year survival of OvCa patients and a high tumor recurrence rate there is still an urgent need for optimized treatment. Recent advances in cancer immunotherapy utilized immune checkpoint blocking antibodies. The blocking antibodies inhibited the inhibitory receptors expressed by effector T cells supporting them to overcome immunosuppressive tumor microenvironment. A vast number of immune checkpoint inhibitors have been identified and tremendous efforts were made to create blocking antibodies. Best choice of antibody can be crucial for therapy success and reduction of side effects. To find the ideal target for checkpoint inhibitor blocking antibodies broad analysis of coinhibitory and costimulatory receptors are needed. Therefore this thesis will focus on the analysis of LAG-3, CTLA-4, PD-1, TIM-3 and CD137 expression on CD4+ regulatory T cells, CD4+ non-regulatory T cells and CD8+ cytotoxic T cells. These three T cell subsets are key players in the regulation and mediation of tumor growth, progression and eradication.

A major focus lies on the stimulation of cytotoxic T cells because of their ability to directly kill tumor cells. Stimulation of CTLs requires presentation of short 8-12 amino acids long peptides presented on the HLA as a first signal. The immune peptidome landscape of OvCa tissue will be surveyed by liquid chromatography coupled mass spectrometry. To distinguish OvCa related peptides and their respective source proteins from peptides presented by benign tissue comparative profiling will be used. With the so identified peptide sequences we are aiming to treat fully resected OvCa patients. Patients will receive multiple vaccinations. Supporting peptide vaccination different adjuvants are tested in order to improve therapy efficiency. Response against vaccinated peptides will be monitored via ELISpot throughout the course of therapy.

2. Material and methods

To compare the changes in expression profiles, blood samples were taken of each patient before tumor-debulking surgery and fresh tumor tissue was collected as part from the overall tumor mass. Tissue was mechanically minced with a scalpel into pieces of around 1 mm^3. Depending on the quality of the tissue, fatty adjacent benign tissue was removed as far as differentiable. The tumor tissue was enzymatically digested with collagenase IV to achieve a single cell suspension.

PBMCs were isolated by grade density centrifugation and stained along with the single cell suspension. Therefore, cell suspensions were layered onto Ficoll-Hypaque and centrifuged at 2000 rpm for 20 min without break. The cell layer containing both lymphocytes and monocytes was taken and further analyzed. Prelimenary experiments have shown high amounts of debris in flow cytometry analysis. Ficoll isolation of cells reduced debris and unspecific background staining.

Samples were analyzed via flow cytometry with a BD Fortessa. Co-receptor expression was compared between lymphocytes from PBMCs and TILs analyzing separately CD4+ non-Tregs, CD4+ Tregs and CD8+ cytotoxic T cells.

Statistical analysis was performed using Graphpad Prism software (version 7.03). Results were tested for normality by the D'Agostino & Pearson normality test and depending on the distribution either unpaired student t-test in case of normal distribution of data or Mann Whitney test in case of non-parametric data were used.

Staining with the first panel assesses the landscape of co-inhibitory and co-stimulatory receptors. It further allows a differentiation of CD4 and CD8 T cells and shows the different subsets of memory cells.

2.1 Antibody panels

Table 1 Antibody panel staining for coreceptors on PBMCs and TILs of OvCa. The first column contains the specificities followed by the bound fluorochrome and the antibody clone.

specificity	fluorochrome	clone	company	purpose/ population
CCR7	Brilliant Violet 421	G043H7	BioLegend	memory phenotype
CD127	Brilliant Violet 510	HIL-7R-M21	BD biosciences	Treg-gating
CD8	Brilliant Violet 605	RPA-T8	BioLegend	CTL
CD4	Brilliant Violet 711	OKT4	BioLegend	TH/Treg
CD45RO	Brilliant violet 650	UCHL1	BioLegend	memory phenotype
CD45	PerCP	HI30	BioLegend	lymphocyte
CTLA-4	PE		BDbiosciences	checkpoint inhibitor
CD25	PeCy7	M-A251	BDbiosciences	Treg-gating
PD-1	APC Cy7	EH12.2H7	BioLegend	checkpoint inhibitor
TIM-3	APC	F38-2E2	BioLegend	checkpoint inhibitor
CD137	Alexa Fluor 700	4B4-1	BioLegend	checkpoint inhibitor
LAG-3	FITC	17B4	ENZO Life Sciences	checkpoint inhibitor

The second panel was used to get a better overview of cellular composition of TILs. More specifically CD19 was used as a marker for B-cells, NKp46 as a marker for NK cells. Epithelial cell adhesion molecule (EpCAM) was used to stain tumor cells.

Table 2 Antibody panel staining for lymphocyte subsets and tumor cells.

specificity	fluorochrome	clone	company	purpose / population
CD3	PeCy7	UCHT1	BioLegend	T cell
CD45	PerCP	HI30	BioLegend	lymphocyte
CD19	Pacific Blue	HIB19	BioLegend	B cell
NKp46	FITC	L9E2	BioLegend	NK cell
EpCAM	APC		MiltenyiBiotec	tumor cell marker
PD-L1	PE	MIH1	BD biosciences	checkpoint inhibitor ligand

For the staining of coinhibitory and costimulatory receptors isotype controls with the respective fluorochrome were used to exclude the background staining.

Table 3 Isotype controls used in flow cytometry analysis.

Isotype control-fluorochrome	clone	company
FITC-IgG1	MOPC-21	ENZO Life Sciences
PE-IgG2a	MOPC-173	BioLegend
APC/Cy7-IgG1	MOPC-21	BioLegend
APC-IgG1	MOPC-21	BioLegend
AF700-IgG1	MOPC-21	BioLegend

2.2 Devices and software

Analytical balance	Sartorius
Cell culture hood	Technoflow, Integra Biosciences
Centrifuge	Eppendorf
Cryo freezing container	Nalgene
ELISPOT reader Immunospot	cellular Technologies Ltd (Software Immunospot 3.2)
Flow cytometer FACS-Fortessa (incl. software FACS DIVA)	Becton Dickinson
Incubator for cell cultures (Heraeus BB6220 CU)	Heraeus
Light microscope	Zeiss
Mass Spectrometer (LTQ Orbitrap XL)	Thermo scientific
Neubauer counting chamber, depth 0.1mm	LO-Laboroptik
Peristaltic pump (LKB P-1)	GE-healthcare
Pipettes	Abimed
Potter glass tube	novodirect
Precision balance	Sartorius
Proteome discoverer 1.3	Thermo scientific
Speed vac vaccum concentrator	Bachofer
Spinning wheel	Bachofer
Water bath	GFL

2.3 General materials

50 ml reagent reservoir	Corning
6-well and 24-well plates	Greiner bio-one
96-well plates (F-bottom)	Corning
96-well plates (U-bottom)	Corning
Cell culture flask (75 cm^2, 175 cm^2)	Greiner bio-one
Cryotubes (2 ml)	Greiner bio-one
ELISPOT plates, 96 well (MSHAN4B)	Millipore

FACS tubes (5ml)	Becton Dickinson
NMWL 10,000 ultrafiltration tube (Amicon Ultra-15)	Millipore
NMWL 10,000 ultrafiltration tube (Amicon Ultra-4)	Millipore
Petri dish	Greiner bio-one
Safe-lock tubes (0.5 ml, 1.5 ml, 2 ml)	Eppendorf
Surgical disposable scalpel	Braun
Tubes (15 ml, 50 ml)	Greiner bio-one
ZipTip (µ-C_{18}, 10 µl)	Millipore

2.4 Chemicals, reagents and complete solutions

2-propanol (isopropanol)	Merck
4-(2-hydroxyethyl-1-piperazineethanesulfonic acid (HEPES)	Gibco (Life technologies)
Acetonitrile (MS-grade)	Thermo scientific
Alkaline phosphatase (avidine conjugated)	Sigma-Aldrich
Anti-human HLA class I, mouse, clone W6/32	in house production by C. Falkenburger
Anti-human HLA-DR, -DP and –DQ, mouse, Clone L243	in house production by C. Falkenburger
Anti-human HLA-DR, -DP and –DQ, mouse, Clone Tü-39	in house production by C. Falkenburger
BCIP/NBT tablet	Sigma-Aldrich
Bovine Serum Albumin (BSA)	Sigma-Aldrich
CHAPS	AppliChem
CNBR-activated sepharose	GE-Healthcare
Collagenase Type IV	Gibco
Complete protease inhibitor tablet	Roche
Dimethyl sulfoxide (DMSO)	WAK-Chemie
DMEM (Dulbecco´s Modified Eagle Medium)	Gibco
DNase	Roche
Ethanol	SAV LP
Ethylenediaminetetraacetic acid (EDTA)	Roth

Ficoll (Biocoll)	Millipore
Human IL-2	R&D Systems
IMDM (Icove`s Modified Dulbecco`s Medium)	Lonza
Ionomycin	Sigma-Aldrich
Pen/Strep	Sigma-Aldrich
Phosphate buffered saline (PBS)	Gibco (Life technologies)
Phytohaemagglutinin (PHA)	Sigma-Aldrich
RPMI	Gibco (Life Technologies)
Trifluoroacetic acid (TFA)	Apllied biosystems
Trypan Blue	Gibco (Life Technologies)
Tween 20	Merck
Water (MS-Grade)	Baker

2.5 Composition of media and buffers

Coupling buffer	0.1 M $NaHCO_3$, 0.5 M NaCL in ddH_2O
DMEM medium	1% Pen/Strep, 10% FCS in DMEM
Desalting solution	1% (v/v) formic acid in H_2O (MS-Grade)
Elution solution	1% (v/v) formic acid, 50% (v/v) acetonitrile in H_2O (MS-Grade)
FACS buffer	0.01% NaN_3, 2 mM EDTA, 2% FCS in PBS
Freezing medium	10% DMSO in FCS
Loading solvent	0.05% TFA, 1% acetonitrile in H_2O (MS-Grade)
PBS-BSA	0.5% BSA in PBS
PBS-Tween	0.05% Tween in PBS
Solulibisation buffer	1 tablet complete protease inhibitor 400 mg CHAPS in 33 ml PBS
Solvent B	0.05% TFA, 80% acetonitrile in H_2O (MS-Grade)
T Cell Medium	10% human plasma in IMDM

Thawing medium	3 µg/ml DNase, 1% Pen/Strep, 10% human plasma

2.6 Isolation of natural presented ligands on OvCa tissue

To isolate natural presented ligands, snap frozen tumor tissue is mechanically and chemically degraded with a scalpel and solubilization buffer. The sample-buffer solution is then transferred to a potter tube and degraded with a potter. After another incubation step of pottered tissue, the suspension was sonicated with ultrasound to lyse cellular membranes. The lysate was incubated once more and centrifuged to separate MHC-complexes in suspension from cellular debris and tissue fragments. Followed by immunoprecipitation of peptide-MHC complexes using the W6/32 [118] capture-antibody for HLA-class I molecules and a combination of the L243 [119] and Tue-39 [120] capture antibodies for HLA-class II that were coupled to an activated CNBr-sepharose matrix. The peptides were then eluted by mild-acidic elution using 0.2% trifluoroaceticacid (TFA) and analyzed by liquid-chromatography coupled mass spectrometry. Peptide spectra were searched against the human proteome (Uniprot/Swissprot 130927) using Seaquest search engine with a precursor mass of 5 ppm and a fragment mass tolerance of 0.02 Da. False discovery rate (FDR) of peptide spectrum hits was calculated using percolator.

The identified peptides with a FDR < 5% were then further processed and evaluated for their capability to bind to an HLA allotype of each patient/donor. Peptides with a binding score of ≥ 50% of the maximal score of SYFPEITHI and a binding affinity of ≤500 nM on NetMHC were defined as binders. Peptides were filtered in length of 8-12 amino acids length for HLA class I and 12 to 25 for HLA class II.

In order to determine tumor exclusiveness of cancer proteins a waterfall plot is generated, comparing benign ovary to OvCa source proteins and respective peptide lists that contain ligandomat determined binders of each patients HLA type. The source proteins that were determined to be tumor exclusive were filtered and corresponding peptides were selected for further analysis.

2.7 Vaccination peptide selection

Peptides were selected from a warehouse (table 12) containing HLA-matched tumor exclusive peptides. The author of this thesis contributed sequences to this warehouse. All OvCa IDs numbered 99 or higher are contributions of the author of this thesis while the others are preliminary work by Dr. Heiko Schuster and Dr. Janet Peper. The warehouse contains the information of source protein, peptide sequence and HLA restriction [121]. HLA typings of all three patients vaccinated are shown in the supplemental data (table 8). Furthermore peptides are rated depending on frequency of presentation on different OvCa samples and immunogenicity in T cell primings using artificial antigen presenting cells (aAPCs). The immunogenicity was assessed via T cell priming with aAPCs in healthy donors. Artificial antigen presenting cells are microbeads that have MHC:peptide complexes covalently bound on their surface. For the T cell priming CD8+ T cells are isolated from whole blood donations. Subsequently they were alternatingly stimulated every 3 to 4 days with IL-2 and aAPCs. The readout was done with tetramer staining and ICS. The immunogenicity testing was performed by Dr. Janet Peper and the warehouse was set up in cooperation with Dr. Heiko Schuster.

Patients chosen for compassionate use therapy were fully resected (R0) and tumor free at the beginning of treatment.

2.8 Immunomonitoring

The effectiveness of peptide vaccination was assessed by a twelve day stimulation of PBMCs isolated right before every injection of vaccination.

Therefore, PBMCs were isolated as described in chapter 1 and cryopreserved. The frozen cells are thawed quickly using DNase-containing thawing medium. After transferring cells into T-cell medium with 5% human serum they are rested overnight. The following day cells were pool-stimulated with target peptides and an HLA-matched negative control viral peptide at a final concentration of 1 µg/ml for HLA-class I peptides and 3 µg/ml for HLA class II peptides. At day three, six and eight cells were stimulated with 20 U/ml IL-2. After a medium exchange on day 10 the IFN-γ capture antibody coated ELISpot plate was loaded on day 13 and stained on day 14. 500,000 cells were

seeded per well and re-stimulated again with peptide, or as additional controls with either PHA or medium.

3. Results and discussion

To analyze the immunological landscape of OvCa, TILs and PBMCs of each patient were freshly isolated the day of tumor debulking surgery. The amount of receptor positive cells was based on CD4 and CD8 expression. CD4+ T cells were subdivided into Tregs and non-Tregs via the CD25+ CD127low staining.
As an additional control 10 volunteer women (HD) aged 52-59 years donated blood for PBMC analysis in order to determine changes in the expression pattern of receptors that might be altered on PBMCs of patients.

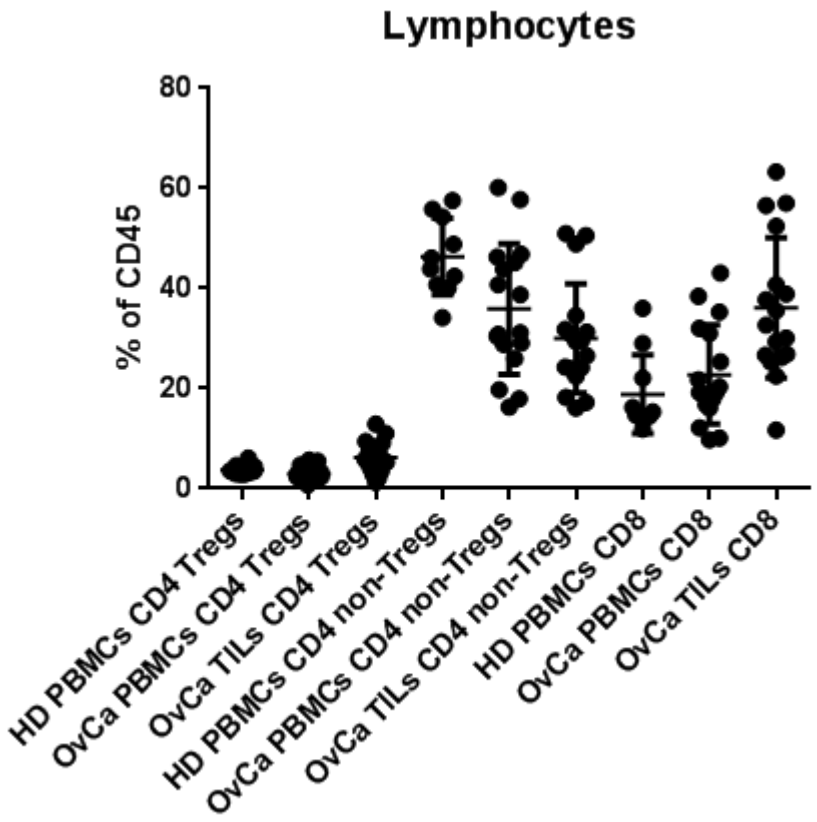

Figure 7 Differences in amounts of CD8+ and CD4+ Tregs and non-Tregs. Shown are cells from 10 healthy donors (HD) and 17 OvCas. Different subsets are shown as part of CD45. Each group was homogenous within itself and did not differ significantly between the three groups regardless if Tregs, non-Tregs or CTL.

Treg groups do not differ and form very homogenous cluster in healthy donors (HD), and PBMCs as well as Tregs of patients. The spread in abundance of CD4+ non-Tregs and CD8+ T cells is wider but there are no drastic differences between different

samples. In addition to that, no significant difference was observed between the abundance of CD+ non-Tregs and CD8+ T cells between HD and patients.

3.1 Co-receptor expression on regulatory T cells of PBMCs and TILs

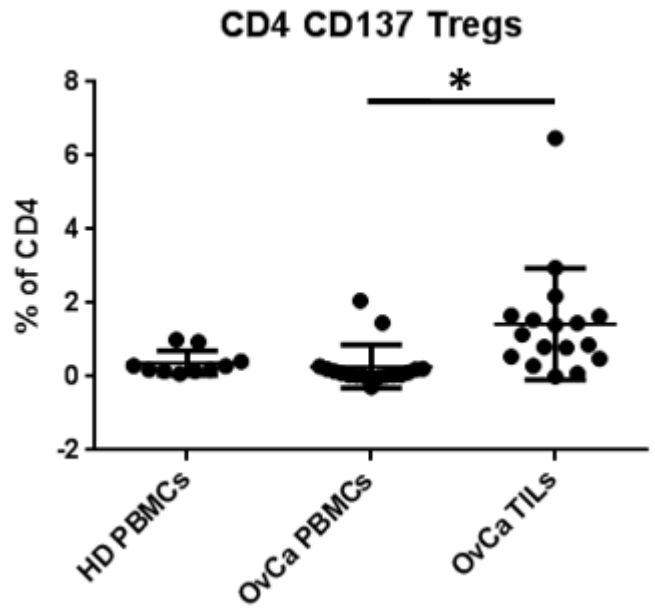

Figure 8 Comparison of CD4+ Tregs expressing CD137. Shown are results of 10 healthy donors (HD) and 17 OvCas. HD and OvCa PBMCs did not differ but there was a significant difference between PBMCs and TILs.

TILs from half of the patients had moderate amounts of regulatory T cells expressing CD137. Thus the other half of patients were characterized by low amounts or no Tregs expressing CD137. In healthy donors no Tregs expressed CD137. The expression of immune checkpoint inhibitors on Tregs remains broadly unknown. Adoptively transferred CD137+ Tregs in a lymphoma mouse model had significant impact on tumor progression. CD137+ Tregs suppressed proliferation of effector cells while Tregs persisted after the transfer in the host mice. The Tregs were inhibited tumor rejection. The study suggest to isolate Tregs prior to adoptive transfer of cells in lymphoma treatment [122].

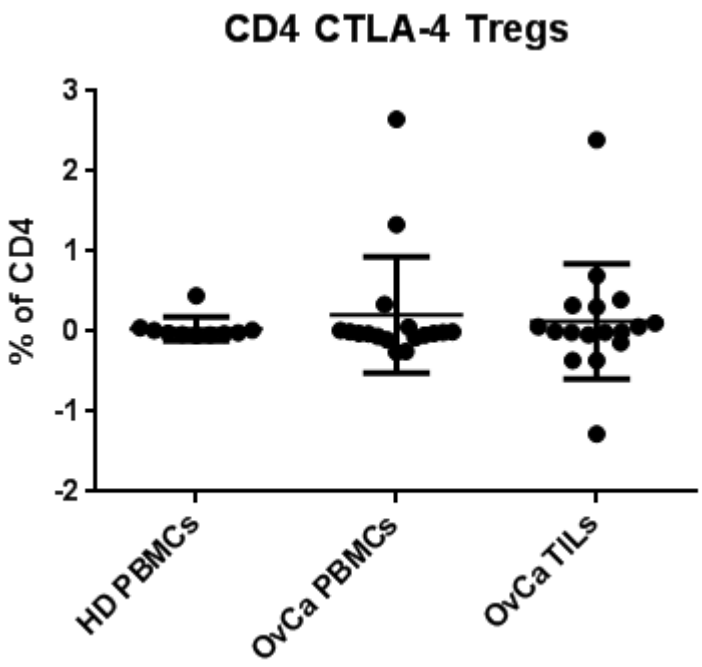

Figure 9 Comparison of CD4+ Tregs expressing CTLA-4. Shown are 10 healthy donors (HD) and 17 OvCas. HD did neither differ from OvCa PBMCs nor from TILs. No CD4+ Tregs were found CTLA-4 positive.

CTLA-4 is needed in Tregs to function as suppressor [123]. The blockade of PD-1 and CTLA-4 *in vitro* using blocking antibody followed by a transfer of treated cells enhanced effector infiltration and activation. However it was reported that the blockade ultimately affected Tregs inhibiting them in their suppressor function [124]. Comparing CTLA-4 among regulatory T cells of PBMCs and TILs, neither of the two groups were expressing CTLA-4. Only one patient was found to be positive in around two percent of PBMCs derived Tregs and her respective TILs.

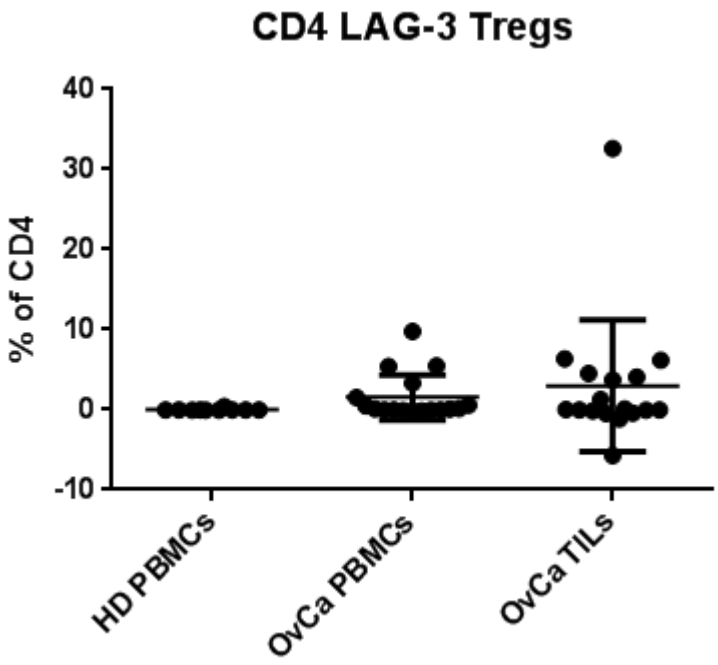

Figure 10 Comparison of CD4+ Tregs expressing LAG-3. Shown are 10 healthy donors (HD) and 17 OvCas. HD remain completely negative for LAG-3 expression. OvCa PBMCs and TILs were mostly negative for LAG-3 expression.

Equal to the expression of CTLA-4 samples were broadly negative for the expression of LAG-3 in Tregs derived from PBMCs and TILs, whereas three patients had between 5 to 10% of positive Tregs among their PBMCs. Those three patients were among the 5 samples with 5 to 10% of positive Tregs of TILs. One outlier was recorded to even have more than 30% of positive Tregs in her isolated TILs. At this point little is known about the role of LAG-3 expression by Tregs in the context of tumor progression. A study has shown that LAG-3 expression by Tregs are able to suppress the production of autoantibodies in a lupus mouse model [125]. Therefore LAG-3 seems to have a drastic influence on Treg function in general but was not found in HD or OvCa.

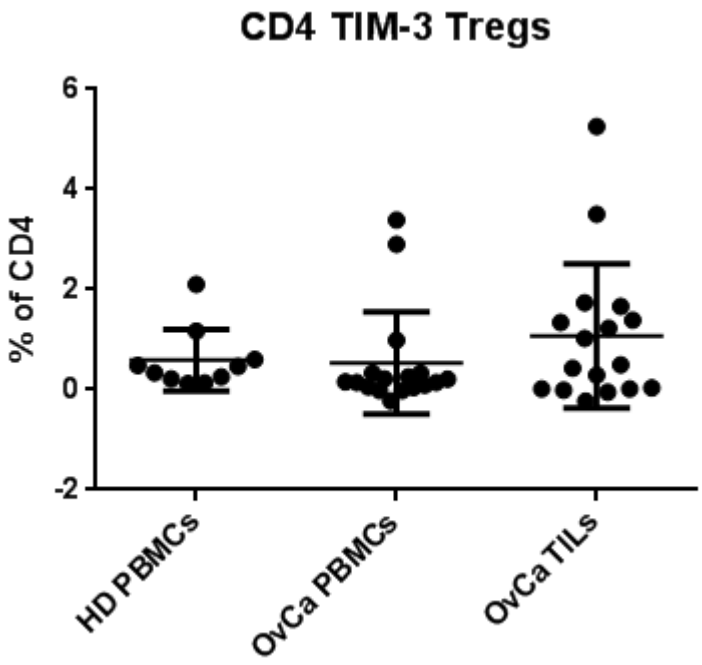

Figure 11 Comparison of CD4+ Tregs expressing TIM-3. Shown are 10 healthy donors (HD) and 17 OvCas. HD did not differ from OvCa PBMCs. TILs trended towards increased amounts but did not differ significantly from PBMCs.

PBMCs from HD were negative for the expression of TIM-3. One sample was an outlier with around 2% of positive cells. There were two outliers in PBMCs of OvCa samples. The other OvCa PBMC samples were negative for the expression of TIM-3. The expression of TIM-3 was more heterogenous in OvCa TILs.

TIM-3 expressing Tregs have been shown to be T cells with the most potent regulatory function and contributing the most to CD8+ CTL exhaustion. The study has shown that over 50% of all Tregs were positive for TIM-3. Further they discussed the use of TIM-3 blocking antibodies in the context of non-small cell lung cancer (NSLC) treatment. NSLC tumor infiltrating Tregs express high amounts of TIM-3 [126]. Regardless TIM-3 was poorly expressed by tumor infiltrating Tregs in OvCa.

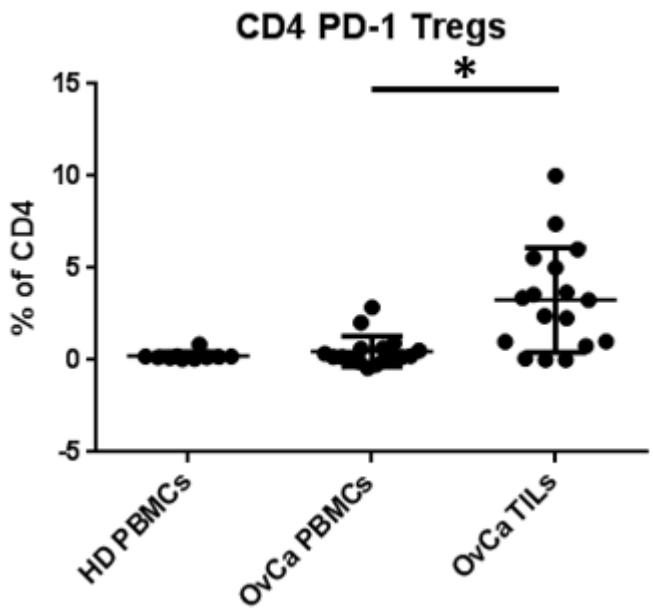

Figure 12 Comparison of CD4+ Tregs expressing PD-1. Shown are 10 healthy donors (HD) and 17 OvCas. There were no detectable differences between HD and OvCa PBMC whereas significantly higher amounts of TILs expressed PD-1.

Over half of tumor-infiltrating Tregs had moderate expression of PD-1 compared to Tregs isolated from PBMCs that did not express PD-1. CD4+CD25+CD127low Tregs from lung cancer patient PBMCs expressed significantly higher amounts of PD-1 than the healthy volunteer control group [127]. PD-1 marked dysfunctional Tregs in malignant gliomas where about 5% of all T cells and Tregs expressed PD-1 which would be comparable to the expression level observed in OvCa [128].

3.2 Coreceptor expression of CD4+ non-regulatory T cells

CD4+ T helper cells play a pivotal role in the mediation of immune responses against infected or tumor cells. Subsequent cells were analyzed for the selected co-receptor expression on PBMCs and TILs.

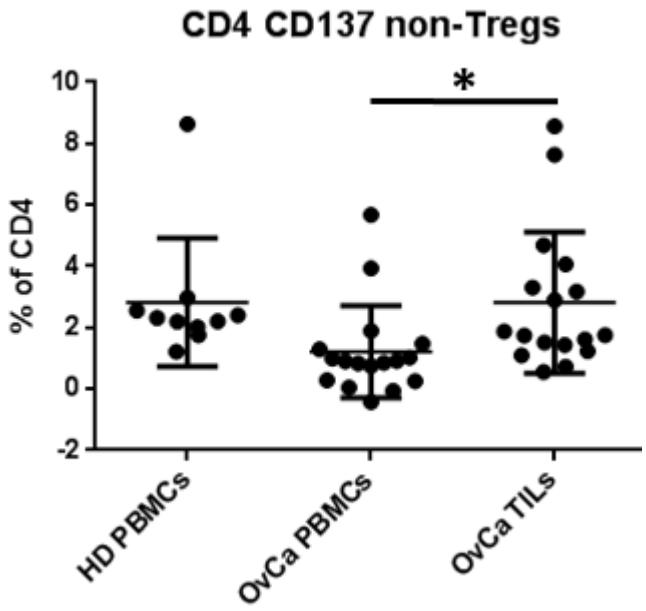

Figure 13 Comparison of CD4+ non-Tregs expressing CD137. Shown are 10 healthy donors (HD) and 17 OvCas. HD did not differ from PBMCs but TILs differed significantly from OvCa PBMCs.

Comparing PBMCs and TILs, there were significant more cells expressing CD137 on TILs than on PBMCs. Five TIL samples showed moderate expression of around 3% to 6% and two samples had about 8% of CD137 positive TILs. Regarding these findings tremendous efforts were made using stimulating agonistic antibody or 4-BB ligand and its variants in cancer immunotherapy. They find use in a broad spectrum of different cancer types [129].

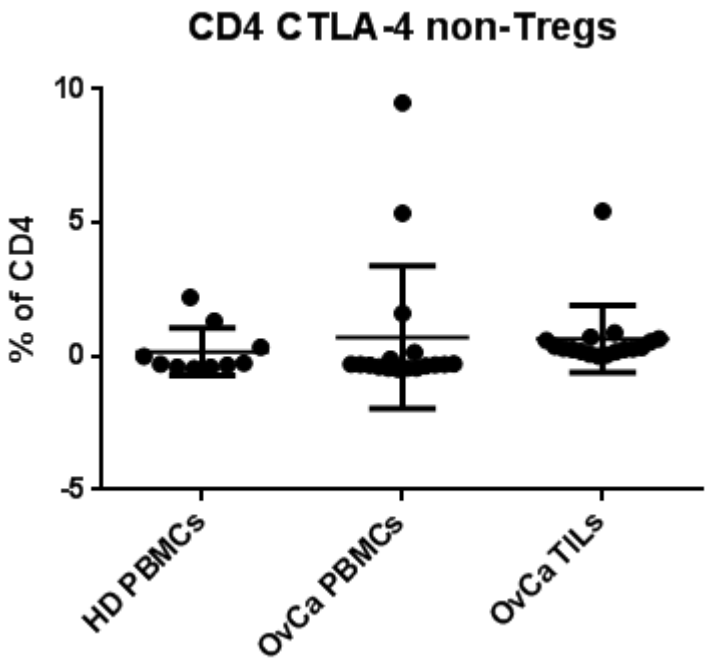

Figure 14 Comparison of CD4+ non-Tregs expressing CTLA-4. Shown are 10 healthy donors (HD) and 17 OvCas. TILs did not differ from PBMCs from HD or OvCa.

Two PBMC samples with 5% and 9% CTLA-4 positive cells were outliers among the group while the rest of the samples remained largely negative. Among the TIL samples only 1 was positive for CTLA-4 (Figure 14). There is no doubt of the success of anti-CTLA-4 blocking antibodies in different tumor types. Thus a quantification of CTLA-4 on T helper cells still remains to be shown. In OvCa however there was only one sample positive in PBMCs and TILs.

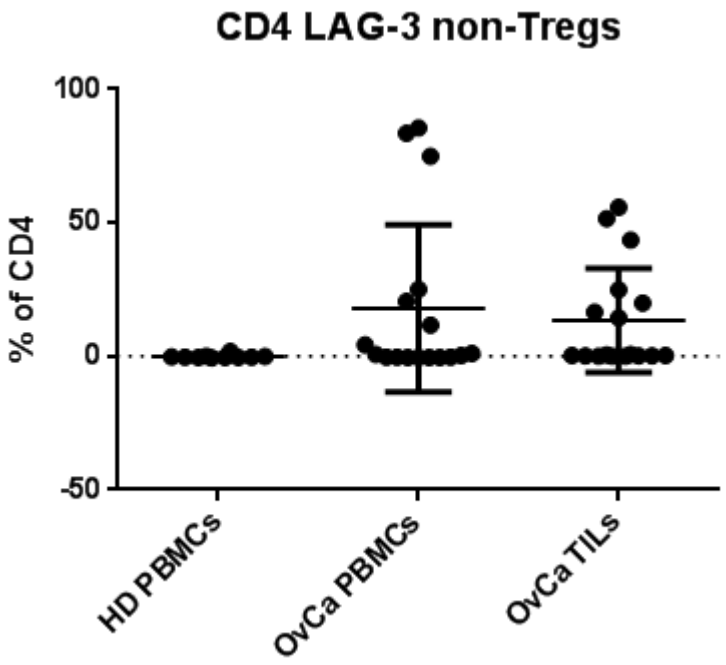

Figure 15 Comparison of CD4+ non-Tregs expressing LAG-3. Shown are 10 healthy donors (HD) and 17 OvCas. HD were negative for expression of LAG-3. PBMCs and TILs were also negative but some outliers were detected. The outliers are most probable due to unspecific binding of antibody.

LAG-3 is known for its regulatory effects on T cell function. Patients analyzed for LAG-3 were largely negative, whereas six samples had high amounts of LAG-3 positive cells. Unfortunately it remains unclear if the positive sample actual true measurements or artefacts caused by the antibody binding nonspecific epitopes.

Preliminary experiments to establish the antibody panel revealed large populations of LAG-3 positive cells among CD4+ and CD8+ T cells on PBMCs of unstimulated healthy donor PBMCs. Titration experiments of LAG-3 antibodies were done in order to find the optimal concentration. To distinguish between a stained antibody artefact and a staining of LAG-3 expression, cells were pretreated for 16 hours with the strong stimulator PHA (10 µg/ml).

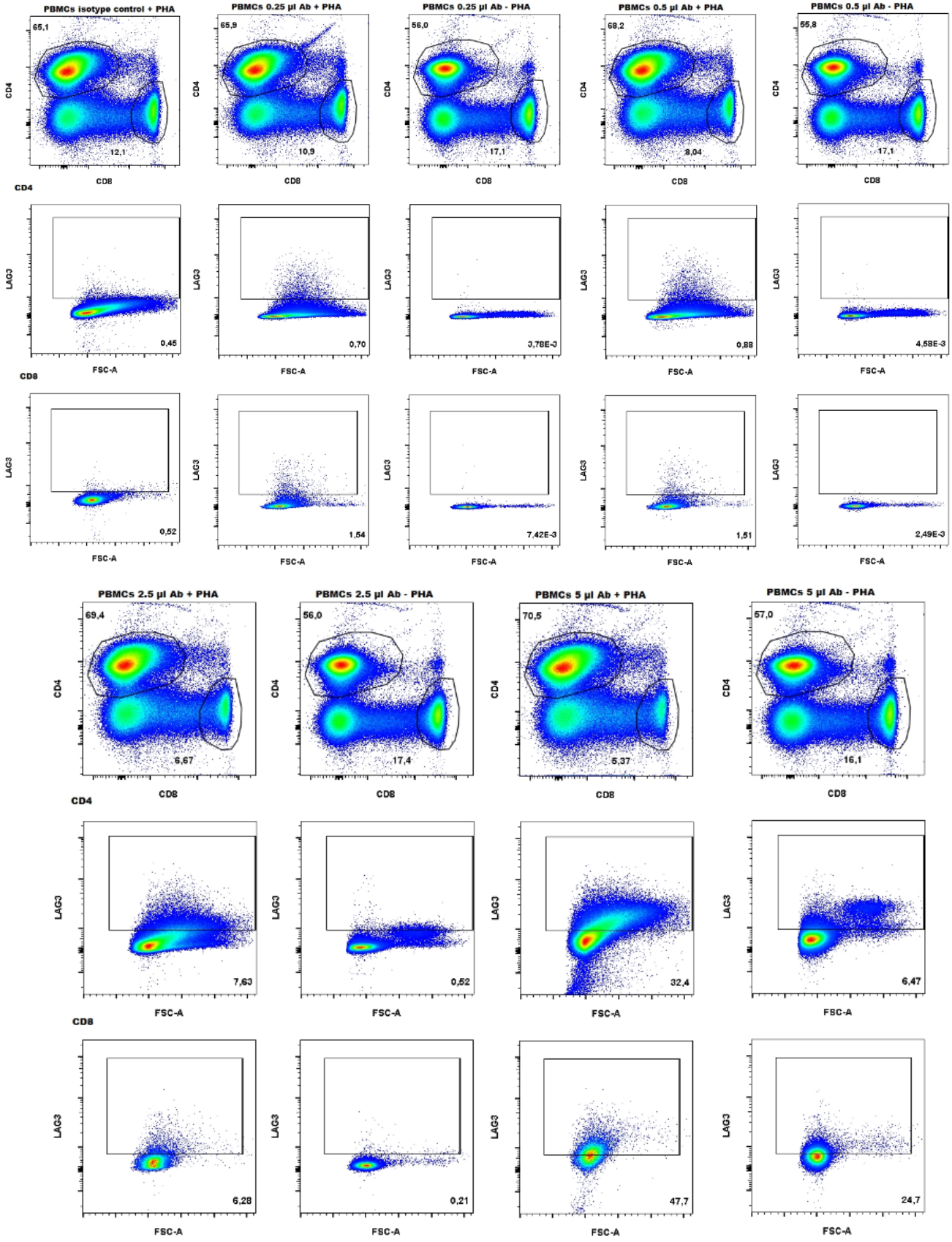

Figure 16 LAG-3 Antibody titration. Cells were stained with CD45 as lymphocyte marker, 7-AAD to assess viability, CD4 Ab and CD8 Ab and then either with FITC-isotype control or LAG-3 staining antibody. The first column contains the isotype control staining. Subsequently 1*10^6 cells were stained with increased

amounts of LAG-3 Ab of 0.25 µl, 0.5 µl, 2.5 µl or 5 µl with or without pretreatment of cells with PHA (PHA treated isotype control). Shown is the gating for CD4 and CD8 followed by the gating for LAG-3. CD4+ LAG-3+ cells are shown in the middle row and CD8+ LAG-3+ cells in the bottom row. The titration experiment unveiled an unspecific binding of LAG-3 Ab by increased LAG-3 populations depending on amount of LAG-3 Ab used.

The titration of LAG-3 staining Ab (Figure 16) unveiled an unspecific binding of the LAG-3 Ab. PHA treatment of cells lead to a stimulation of LAG-3 expression which can be observed throughout all titration steps. If the LAG-3 Ab would bind specifically to LAG-3, populations of LAG-3+ T cells would be equal in size. PHA untreated samples were LAG-3- (population size smaller or equal to isotype control) when stained with 2.5 µl LAG-3 Ab or less. PHA untreated cells stained with 5 µl Ab had 6.47% and 24.7% of positive cells. This effect is also observed in PHA treated cells. Concluding from these experiments 0.5 µl LAG-3 staining Ab per 1*10^6 cells was the chosen concentration because PHA untreated cells were clearly negative and a LAG-3 positive population was observable in PHA stimulated cells.

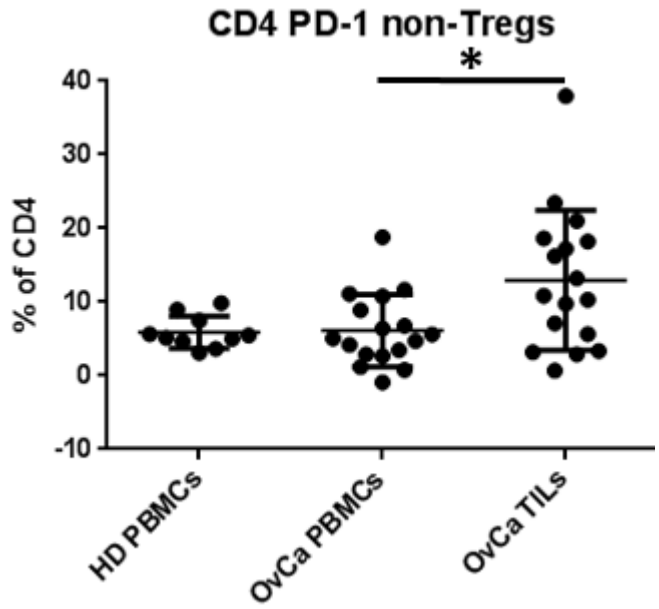

Figure 17 Comparison of CD4+ non-Tregs expressing PD-1. Shown are 10 healthy donors (HD) and 17 OvCas. HD showed moderate expression of PD-1 but did not differ from OvCa PBMCs. PBMCs had significantly lower amounts of cells expressing PD-1 than TILs.

T helper PBMCs were distributed mostly between 2% and 11% of positive cells. One outlier had about 18% of PD-1+ CD4+ T cells in PBMCs with about 17% positive T

cells respectively in the TIL sample. Among the TIL samples only four of them had TIL counts with less than 5% of positive cells. The remaining patients were broadly distributed between 5% and 23% of positive cells. The patient found positive with 38% of PD-1+ CD4+ positive TILs had only 4.7% of positive PBMCs, being even below the average of about 6%. Overall higher amounts of PD-1+ CD4+ non-Tregs were found in TILs compared to the respective PBMCs. A study analyzing PD-1 expression in follicular lymphoma described the influence of PD-1 expression on disease progress. PD-1 expressing cells were categorized upon high or low amounts of cells expressing PD-1. Overall on average 50% of CD4+ T cells were positive in follicular lymphoma patients. But at least 20% of all CD4+ T cells were PD-1+ which is the highest detectable amount of CD4+ non-Tregs in OvCa [130]. In type I diabetes patients PD-1 expression on CD4+ T cells was correlated to different genotypes of diabetes patients. Each of the four analyzed genotypes had around 5% of CD4+ PBMCs. Three patients of the cohort had up to 10% PD-1+ CD4+ T cells [131]. These results are comparable to the findings in OvCa.

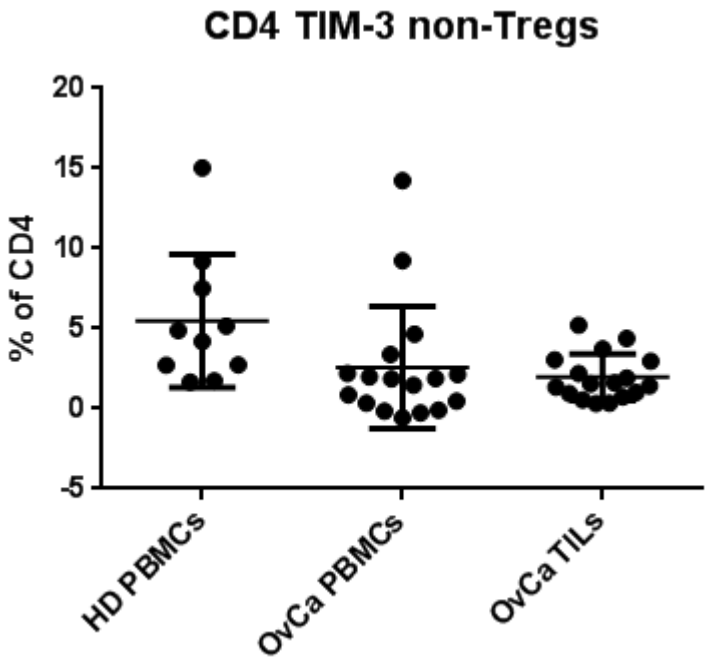

Figure 18 comparison of CD4+ non-Tregs expressing TIM-3. Shown are 10 healthy donors (HD) and 17 OvCas. TIM-3 was negative on TILs and low to absent on OvCa PBMCs but elevated level on HD. Amounts of TIM-3 HD did not differ significantly from OvCa PBMCs.

Two patients had relatively high amounts of TIM-3+ cells whereas the rest of the patients and the TIL sample were largely negative for TIM-3 expressing cells or displayed low numbers. In contrast to our findings it has been reported that a significant higher proportion of CD4+ T cells from OvCa tissue expressed TIM-3 than their respective PBMCs. Patients with high amounts of CD4+TIM-3+ T cells had significantly higher chances of tumor recurrence [132].

3.3 Co-receptor expression of CD8+ T cells

Cytotoxic T cells are often favored by immunologists because of their capability to clear infected or tumorous cells. In the course of development of cancer immunotherapy strategies these cells play pivotal roles. Therefore the OvCa samples were analyzed for CD8+ cytotoxic T cells and the selected markers.

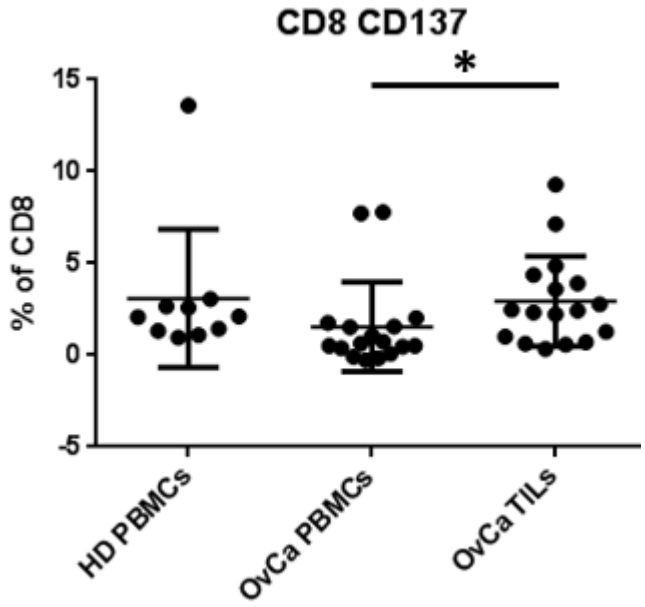

Figure 19 comparison of CD8+ CTL expressing CD137. Shown are 10 healthy donors (HD) and 17 OvCas. HD do not differ from PBMCs but there were significantly higher amounts of TILs compared to PBMCs.

Comparable to the expression of CD4+ non-Tregs the expression of CD137 was relatively low. But comparing PBMCs to TILs showed significant differences between the 2 groups. The two outliers in each group are not related to each other and are from different patients. The Rosenberg lab addressed immune checkpoint inhibitors of CD8+ T cells in metastatic melanoma. It has been shown that adoptive transfer of TILs can lead to tumor regression. TILs of 24 tumors and 21 PBL samples of melanoma

patients were studied and analyzed for the expression of various surface markers. Comparable to our findings in OvCa PBMCs were negative for the expression of CD137. TILs contained significantly higher amounts of up to about 45% of CD137+ CTLs. The average was about 12.5% of positive cells being twice as much as in OvCa [133].

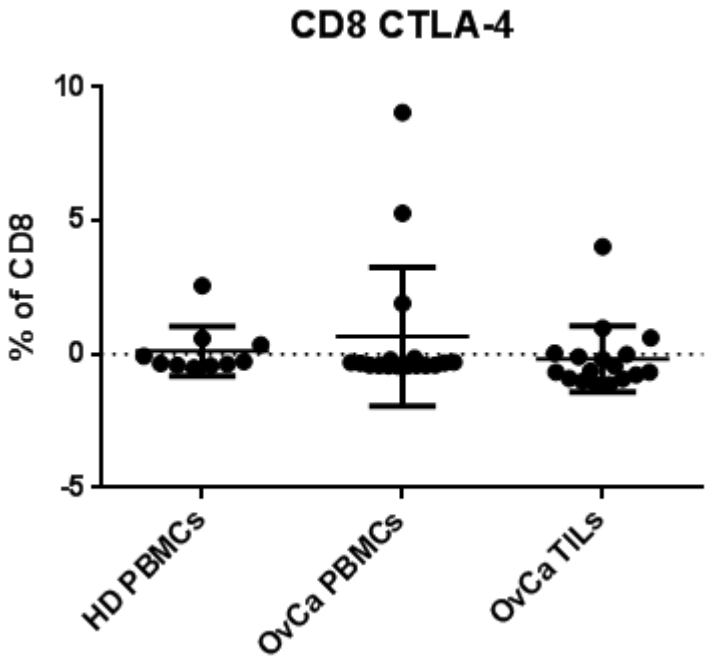

Figure 20 comparison of CD8+ CTL expressing CTLA-4. Shown are 10 healthy donors (HD) and 17 OvCas. Despite two outliers CTLA-4 was not expressed by CTL.

CD8+ T cells remained largely negative for the expression of the co-receptor CTLA-4 regardless if PBMCs or TILs were analyzed. Positive PBMC samples were negative in the respective TIL samples and *vice versa*. Comparable work stimulated PBMCs of healthy donors with the strong activators of T cell gene expression PMA and A23187. Stimulation of T cells lead to an increased expression of CTLA-4 in CD4+ T cells but not in CD8+ T cells [134].

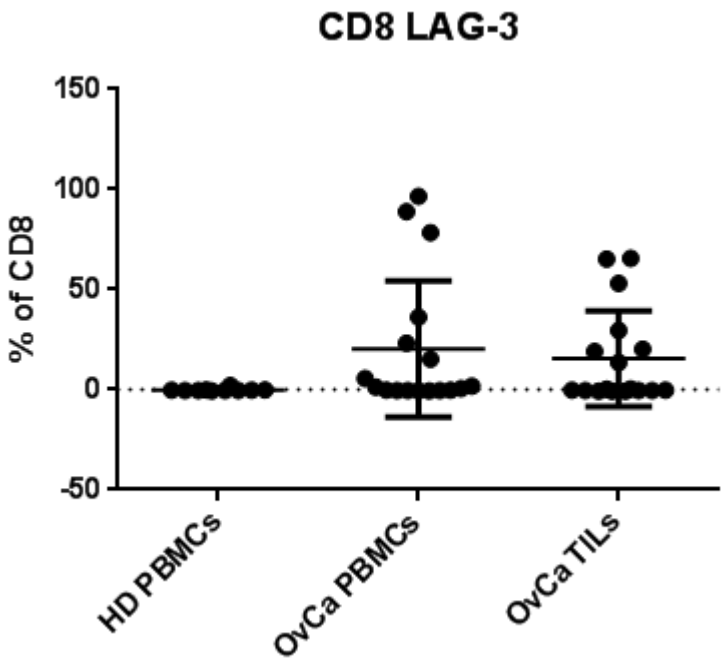

Figure 21 Comparison of CD8+ CTL expressing LAG-3. Shown are 10 healthy donors (HD) and 17 OvCas. Comparable to CD4+ non-Tregs HD, PBMCs and TILs were negative and did not differ from each other, besides the outlier that are most likely due to unspecific binding of antibody.

Samples expressing high amounts of LAG-3 across PBMCs were also positive in TIL samples. The high amounts observed could be related to unspecific binding of the LAG-3 antibody. In the study of the Rosenberg lab LAG-3 was significantly higher expressed in TILs compared to the respective PBMCs. Overall compared to the other immune checkpoint inhibitors its expression was rather moderate. On average 5.7% of TILs expressed LAG-3 [133].

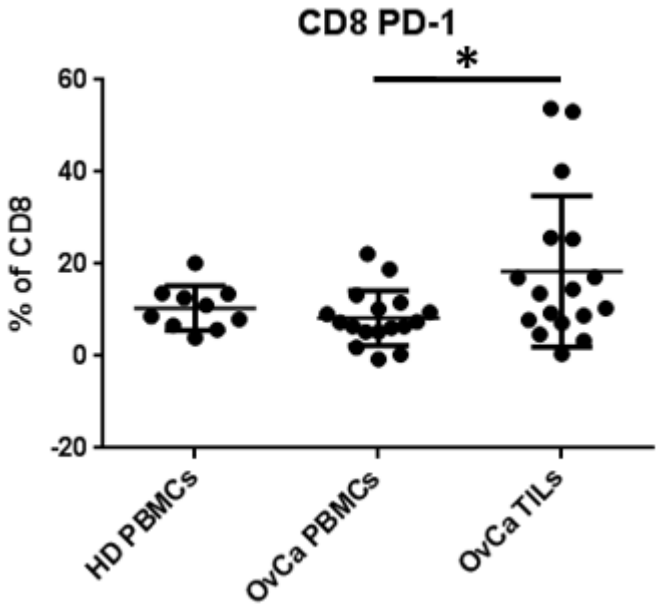

Figure 22 Comparison of CD8+ CTL expressing PD-1. Shown are 10 healthy donors (HD) and 17 OvCas. HD and OvCa PBMCs were comparable to each other and TILs had significantly higher amounts of PD-1 positive cells compared to PBMCs.

The inhibitory co-receptor PD-1 was not only strongly expressed by CD4+ non-Tregs but also on CD8+ T cells. Among PBMCs only 3 samples were negative for the expression of PD-1. 12 out of 17 PBMC samples had between 5% to 13% positive cells. Two patients had 18% and 22% of PD-1+ PBMCs. Among TILs only one patient was negative for the expression of PD-1. 35% of all TIL samples were between 3.4% and 9.4% of positive cells. Ten samples had more than 10% of PD-1+ CD8+ T cells. One of them was around 40% and two even surpassed the 50% mark. In melanoma patients it was shown that PD-1 was expressed on average by about 32% of all TILs while PBLs were mostly below 10% of PD-1+ CD8+ T cells [133]. These results are comparable to the findings in OvCa where numbers were a little lower but the expression pattern seems comparable.

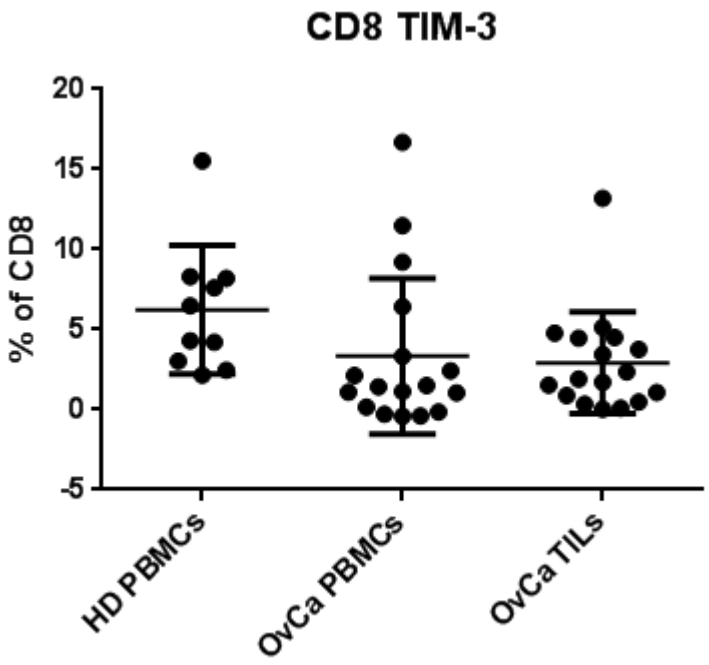

Figure 23 Comparison of CD8+ CTL expressing TIM-3. Shown are 10 healthy donors (HD) and 17 OvCas. All three groups appear heterogeneous but do not differ from each other.

TIM-3 was expressed on comparable amounts of CD8+ cells as it was on CD4+ T cells. Patients that had high amounts of CD4+ TIM-3 positive PBMCs had also higher amounts of CD8+ TIM-3+ PBMCs. Most samples, regardless if PBMCs or TILs had fairly low amounts of TIM-3 positive cells and both groups did not differ from each other significantly. The Rosenberg lab determined about 13% of TIM-3+ CD8+ TILs while PBMCs remained negative for PD-1 expression [133]. Compared to OvCa there were no or very low amounts of TIM-3+ TILs detectable.

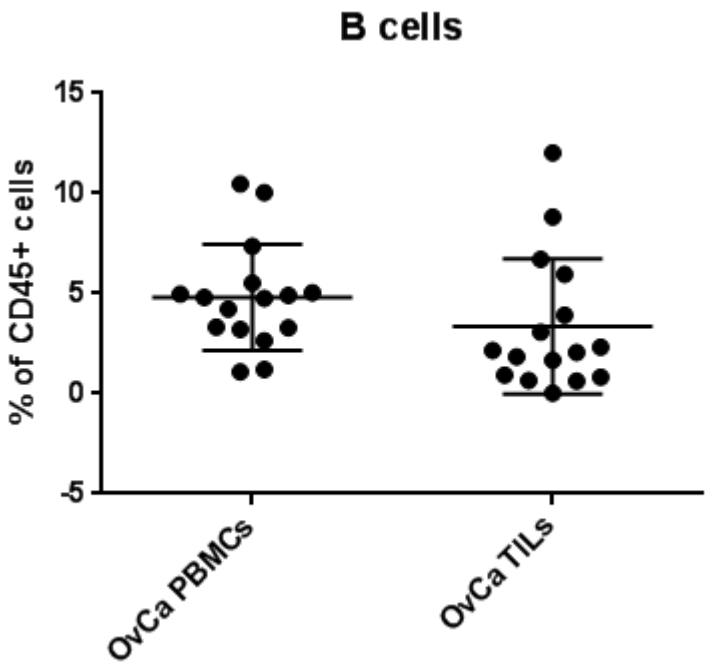

Figure 24 Comparison of frequencies of B cells from OvCa PBMC and TIL samples. Shown are 16 OvCas. Within the group of TILs the amount of infiltrating B cells varied but overall there were no detectable differences between PBMCs and TILs.

Patient samples were analyzed for the infiltration of B cells. While B cells were found on a physiological measure with PBMCs, five samples were negative for tumor-infiltrating B cells. Nine of 16 samples had 2% to 7% of tumor-infiltrating B cells. Two samples had 8% and 12% of B cells among their lymphocytes. B cells from all PBMC samples have shown two distinguishable populations that varied in size. It has been shown that sustained engagement of the B cell receptor to the antigen is required for a sustained B cell activation, proliferation and survival. Upon activation B cells grow in size [135]. In a metastatic melanoma study tumors were subdivided in three histological patterns. The first pattern was not infiltrated by immune cells. The second pattern was characterized by immune cell infiltrates in the blood vessel proximity. The third pattern was distinguished by a diffuse infiltration of immune cells throughout the metastatic tumor. Whereas the histological pattern with the diffuse infiltration of tumor cells represented the group of patients with the least progression and the best survival prognosis. Overall 33% of tumor-infiltrating lymphocytes were B cell lineage cells and the second largest group after T cells with 53% of all tumor infiltrating lymphocytes [52]. In OvCa B cells appear in smaller amounts and are probably of minor importance

for the largest part of OvCas since only two of 16 were positive with around 10% B cells of tumor infiltrating lymphocytes.

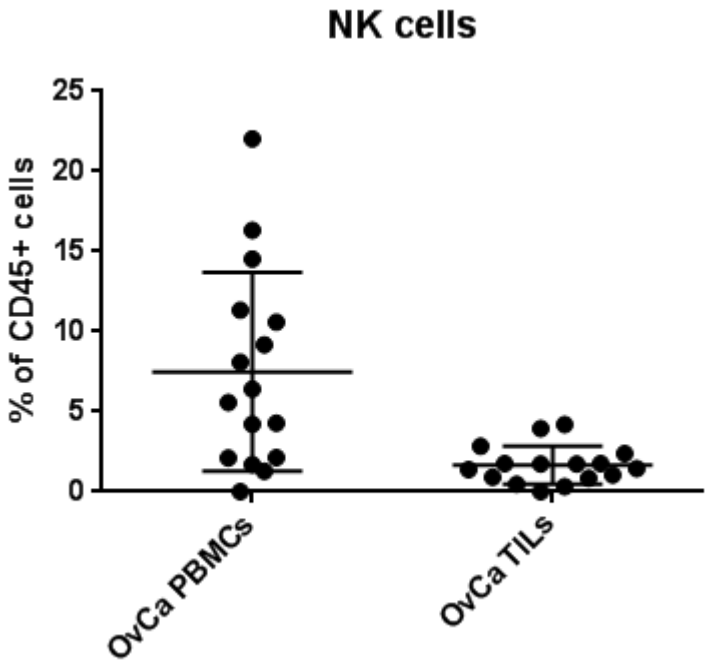

Figure 25 Comparison of frequencies of NK cells from OvCa PBMC and TIL samples. Shown are 16 OvCas. While PBMCs showed for the most part physiological amounts of NK cells, there were no detectable tumor-infiltrating NK cells.

Among patients´ PBMCs there was a heterogeneous distribution of NK cells. In TIL samples NK cells were low abundant or absent. A study histologically analyzing tumor infiltrating lymphocytes in metastatic melanoma described a low presence of tumor infiltrating NK cells [52]. Yet only little is known about the effective function and role of tumor infiltrating NK cells. Despite their poor ability to produce cytokines and cytolytic granules (perforin and granzyme B) over a longer time course, they are able to release a high amount of such within a short amount of time of two to four hours [136, 137]. In 157 colorectal cancer patients, tissue was histologically analyzed for tumor infiltrating NK cells. Patients were monitored for five years and NK cell infiltration was related to overall survival and progression free survival. Additionally NK infiltration was related to tumor stage. The statistical difference was significant comparing cumulative survival of patients with poor or moderate NK infiltration to patients with extensive infiltration favoring the latter. Surprisingly the statistical difference in overall survival between poor/moderate and extensive infiltration was observed between patients diagnosed at

a later stage (stage III or stage IV) and could not be observed in patients with early stage tumors [138]. The same observation was made in gastric cancer. Here 169 patients were divided into two groups according to their grade of infiltration. Patients with highly infiltrated tumors survived significantly longer than patients with poor infiltration [139]. Histological analysis of squamous cell lung cancer revealed there was a significant difference in survival of patients. Patients with less than five tumor infiltrating NK cells were compared to patients with more than five NK cells per field using an image analyzer [140]. These findings indicate that NK cells can be very effective in lower numbers. So despite their poor detection rate in OvCa TILs their role on overall survival and tumor progression should be further addressed.

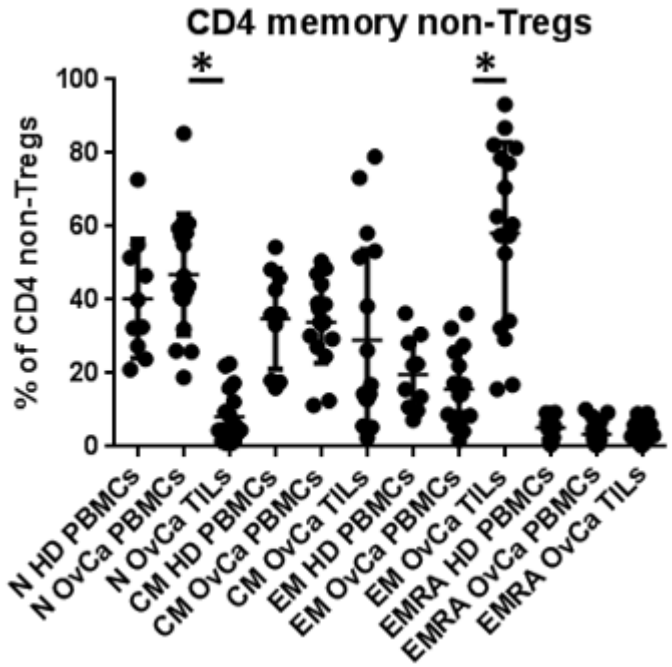

Figure 26 Comparison of memory phenotype of CD4+ non-Tregs. Shown are 10 HD and 17 OvCas. The different groups of naïve (N), central memory (CM), effector memory (EM) and terminally differentiated effector memory (EMRA) T cells are directly compared to each other. Overall HD did not show any difference to the PBMCs group. There is a significant shift of naïve (N) cells towards effector memory (EM) of TILs.

Overall PBMCs from HD did not differ from patients' PBMCs. PBMCs from patients had higher amounts of naïve and central memory T cells and moderate amounts of effector memory T cells. Among TIL samples there were only a few showing low or moderate amounts of naïve T cells. In about one third of all TIL samples patients had more than 50% of CM T cells. Eight of 17 samples were positive for 10% to 27% of

CM. Terminally differentiated EMRA CD4+ non-T cells were only very low abundant in all samples.

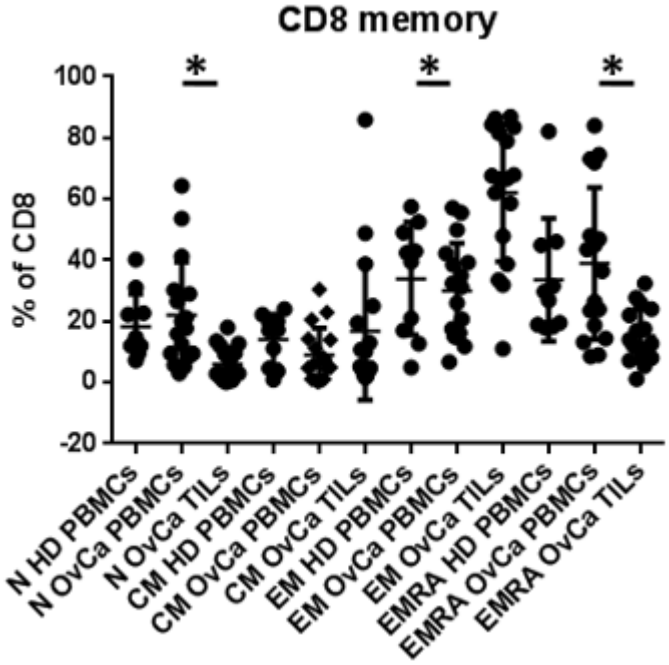

Figure 27 Comparison of memory phenotype of CD8+ CTLs. Shown are 10 HD and 17 OvCa. Overall HD did not show any difference to the PBMCs group. There is a significant shift of naïve (N) cells towards effector memory (EM) of TILs, whereas there are significantly lower amounts of EMRA CTLs in TILs than PBMCs.

HD PBMCs were comparable to PBMCs of patients. Six of 17 patients' PBMC samples have shown below 10% of naïve T cells whereas eight samples had above 20% of naïve CD8+ T cells. In TIL samples none of the samples had more than 18% of positive naïve T cells with four of them surpassing the 10% mark.

3.4 Correlation of flow cytometry and tumor progression data

The data acquired via flow cytometry were correlated to tumor progression. Progression data were available for 14 of the 17 patients analyzed here. Within the first nine months six out of eight patients showed tumor recurrence or progression. One patient was in complete remission 10 months after enrolment another one after 14 months after enrolment. After 14 months one patient showed stable disease and

another one's tumor recurred. The two patients that were enrolled the longest were at complete remission (15 months) or stable disease (17 months).

Table 4 Progression data of OvCa patients analyzed by flow cytometry. The second column shows the time period until tumors progressed. If the patient did not show progression the time duration since when the patient is under complete remission is shown.

OvCa ID	months enrolled until diagnosis	diagnosis
OvCa 1	9	tumor recurrence
OvCa 2	9	complete remission
OvCa 3	10	complete remission
OvCa 4	15	complete remission
OvCa 5	14	complete remission
OvCa 6	17	stable disease
OvCa 7	9	palliative care
OvCa 8	14	tumor recurrence
OvCa 9	5	tumor recurrence
OvCa 10	9	tumor progression
OvCa 11	14	stable disease
OvCa 12	1	supportive care, R2 resection
OvCa 13	6	intestinal obstruction
OvCa 14	6	stable disease

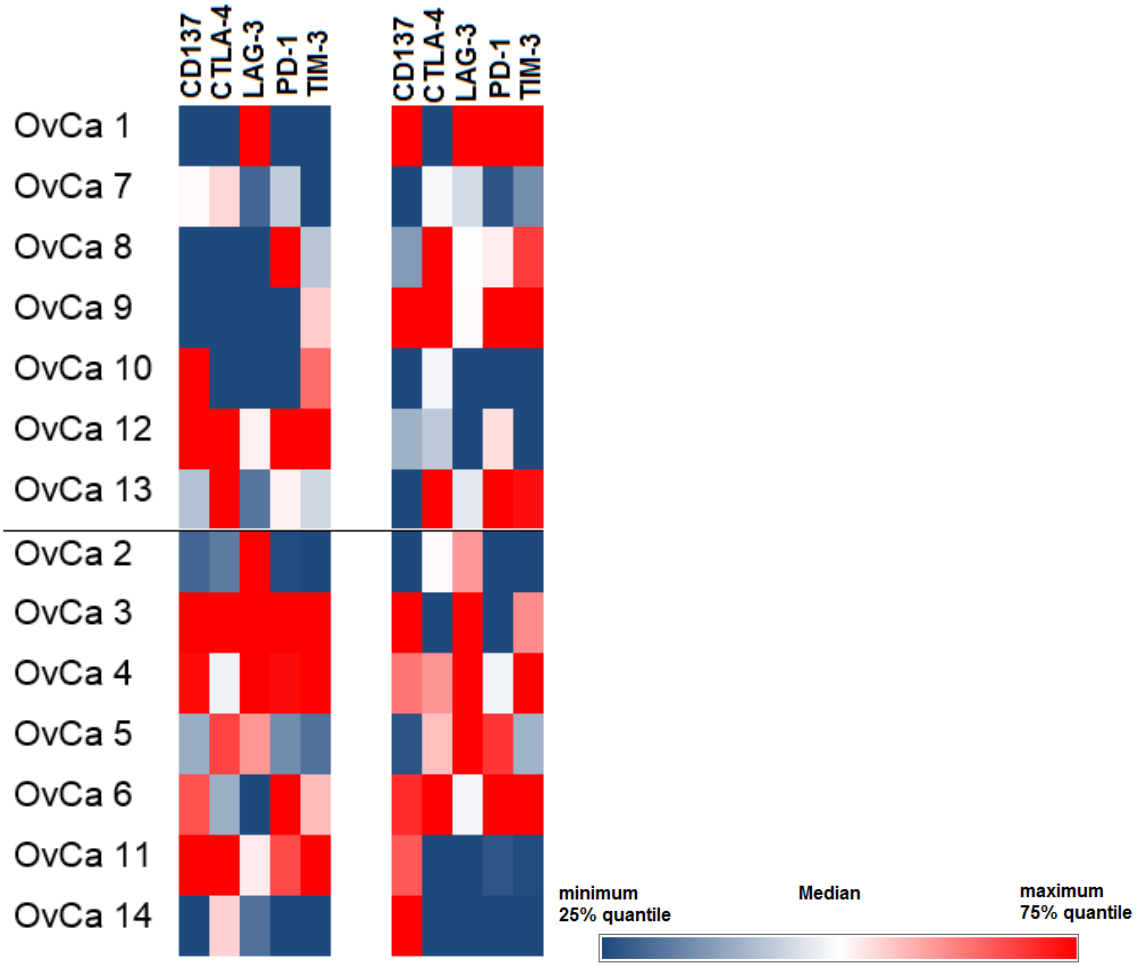

Figure 28 Quartiles for co-receptor expression on CD4+ Tregs of PBMCs (left) and TILs (right). Patients are clustered depending on their disease progression. Patients with malignant progression are above the black bar and patients with no progression are below the black bar (see table 5 for progression details).

Figure 28 depicts the progression free survival data correlated to the frequency of coreceptor+ CD4+ Tregs. The dark blue or dark red coloring indicates that samples are below (dark blue) the 25% quantile or above (dark red) the 75% quantile. This means dark colored samples belonged to the 25% of samples with the lowest/ highest frequencies of positive cells.

PBMC Treg samples of patients with malignant progression (PMP) have 15 dark blue colored fields. Tregs of PBMCs of patients with no progression (PNP) were six times below the 25% quantile. In contrast to this, patients with malignant progression were eight times colored dark red. Tregs of patients with no progression were observed 16 times to have the highest amount of positive cells.

12 samples of tumor-infiltrating Tregs of patients with malignant progression were among the samples containing the highest amounts of positive cells. 9 samples of patients with no progression were colored dark red. Samples of ten patients were colored dark blue when they showed malignant progression and 13 samples when no progression occurred.

Five out of seven CD137 Treg patient samples were colored in a red tone in non-progression patients. Patients with malignant progression were in only two samples above the median. This indicates a minor involvement of CD137 expressed by Tregs in the regulation of tumor recurrence in OvCa patients.

Four out of seven of PD-1 TIL samples of patients with no progression were located in the lower half of patients containing PD-1+ Tregs. One patient with malignant progression was characterized with low amounts of PD-1+ Tregs. Three out of seven PMP had high amounts of PD-1 expressing Tregs. This results suggest a minor involvement of PD-1 expression on tumor infiltrating Tregs. These remaining coreceptors are difficult to evaluate due to the very low abundance of positive Tregs.

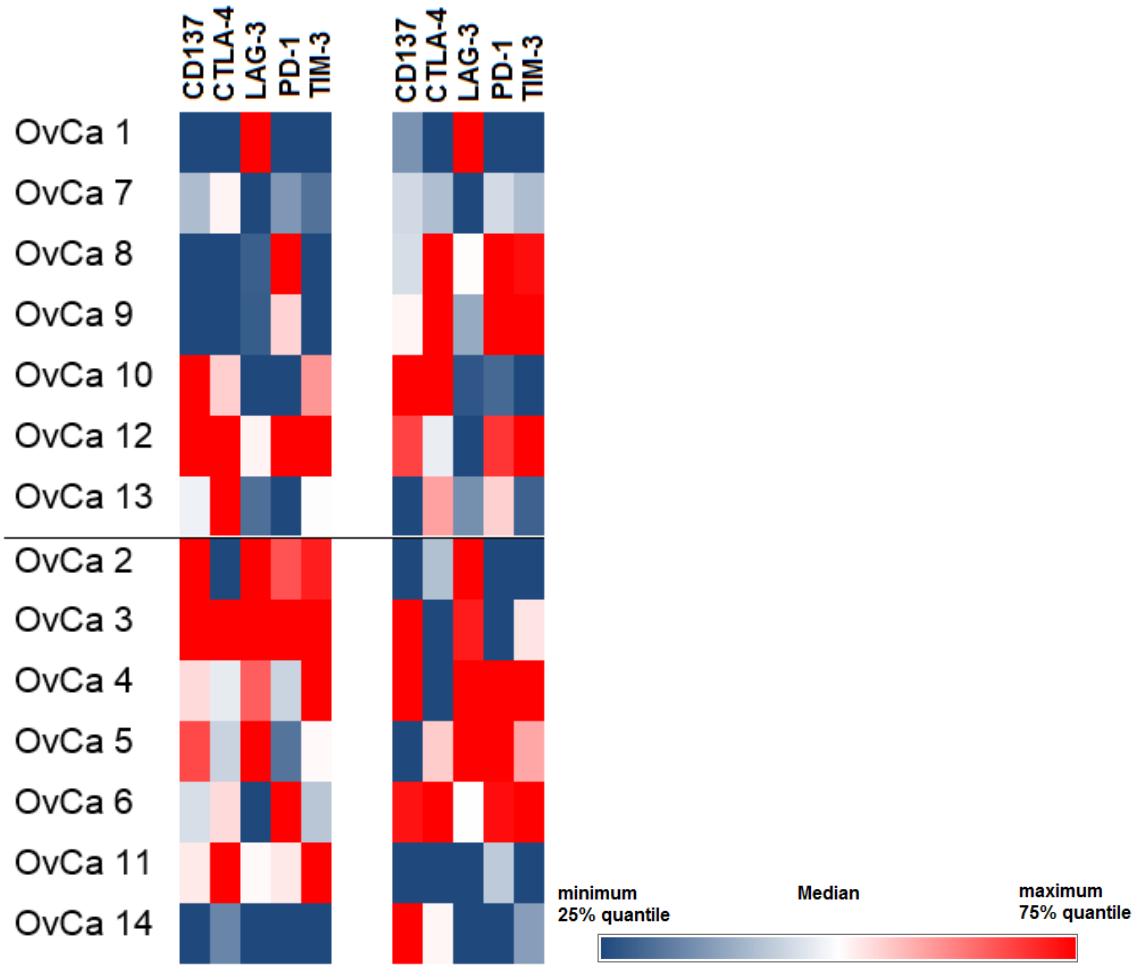

Figure 29 Quartiles for co-receptor expression on CD4+ non-Tregs of PBMCs (left) and TILs (right). Patients are clustered depending on their disease progression, patients with malignant progression are above the black bar and patients with no progression are below the black bar (see table 5 for progression details). The 25% quantile is also referred to as 25% quartile and the 75% quantile as 75% quartile.

Figure 29 correlates the data of disease progression to the flow cytometry results. Correlation was done equally to the heatmap of Figure 28.

Across all CD4 PBMC samples, 14 of PMP samples and six samples of PNP were colored dark blue. 11 PMP samples were above the median with eight of them being colored dark red. 16 PNP samples were above the median in amounts of coreceptor expressing cells.

Among TILs of PMP 12 samples were above the median (10 dark red colored) and 12 below (nine dark blue colored). 13 samples of TILs from PNP were dark red colored and equally as much were dark blue colored.

Four of CD137 TIL samples from PNP were above the 75% quartile and three were below the 25% quartile. On CD137 PMP samples, only two of them were above the median. This indicates a correlation between disease progression and the amount of CD137 CD4+ T cells.
In TIL samples both PMP and PNP contain three samples with high amounts of PD-1+ CD4+ T cells. Three PNP were below the 25% quartile. Three PMP TIL samples were below the median. Thus there was no correlation between tumor progression and PD-1 expression.

Figure 30 is a heatmap correlating the flow cytometry data of CD8+ CTLs and the disease progression data. Overall CD8 PBMC samples of PMP contained 16 dark blue fields and 9 dark red fields. Samples from PBMCs of PNP patients 12 dark red colored field and 7 dark blue colored fields. In TILs of PMP nine receptors were above the 75% quartile and ten below the 25% quartile. TILs of PNP contained ten receptors colored dark blue and 12 colored dark blue.
In PMP OvCa 9 contained more CD137+ CD8+ TILs than over half of all other samples. In contrast to that four samples of PNP were among the 25% of samples containing the highest amounts of positive cells, whereas the remaining three PNP samples were among the lowest 25%.
PD-1 expression on TILs four samples of PMPs had above median amounts of TILs expressing PD-1. In samples of PNPs only two of them were among the samples with the highest amounts of PD-1+ CD8+ TILs. The remaining five samples of PNPs were below median.

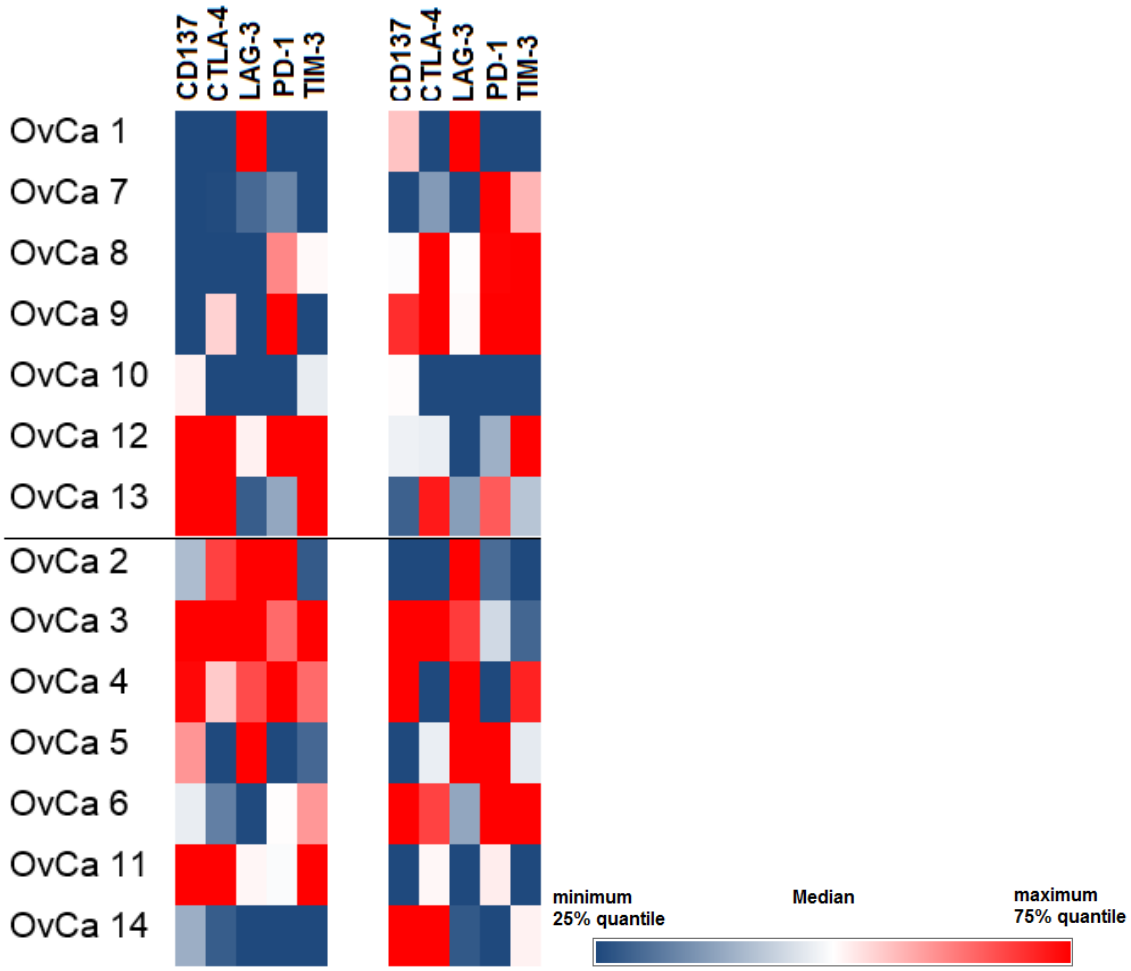

Figure 30 Quartiles for co-receptor expression on CD8+ T cells of PBMCs (left) and TILs (right). Patients are clustered depending on their disease progression, patients with malignant progression are above the black bar and patients with no progression are below the black bar (see table 5 for progression details).

Immune checkpoint receptors were analyzed by flow cytometry using directly labeled monoclonal antibodies. The lymphocytes were distinguished between CD4 and CD8. CD4+ T cells were further distinguished into regulatory T cells and T helper cells. These three T cell subsets were analyzed for the expression of selected immune checkpoint receptors. As an additional control PBMCs of ten healthy donors were obtained and analyzed. PBMCs of healthy donors did not differ from PBMCs from OvCa.

Comparing OvCa TIL and OvCa PBMC samples CD137 and PD-1 were detected in significantly higher amounts compared to PBMCs of the respective patient.

CTLA-4, TIM-3, and LAG-3 had no significant difference between OvCa PBMCs and OvCa TILs.

Subsequently the data obtained from flow cytometry were correlated to disease progression. For this reason flow cytometry data were divided into quartiles and evaluated samples based on which quartile they belong to. CD137 showed a tendency to positively influence progression-free survival in Tregs, T helper cells and CTLs. PD-1 showed a tendency to positively influence progression-free survival on Tregs and CD8+ T cells but seems to have no influence when expressed by CD4+ T helper cells. Whereas a longer period of time monitoring patients might allow a better evaluation of coreceptor expression and the influence on disease progression and overall survival.

3.5 Ovarian cancer ligandomics

As described by Schuster et al. a list of peptides and their respective source proteins was set up for 32 OvCa samples and 22 benign ovaries (OvN). Parts of the results shown here contributed to the work of Schuster et al. (table 8) [121]. Shown are the results either comparing OvCa to OvN or to a benign database containing different benign autopsy tissues. The benign database contains different samples processed by our department.

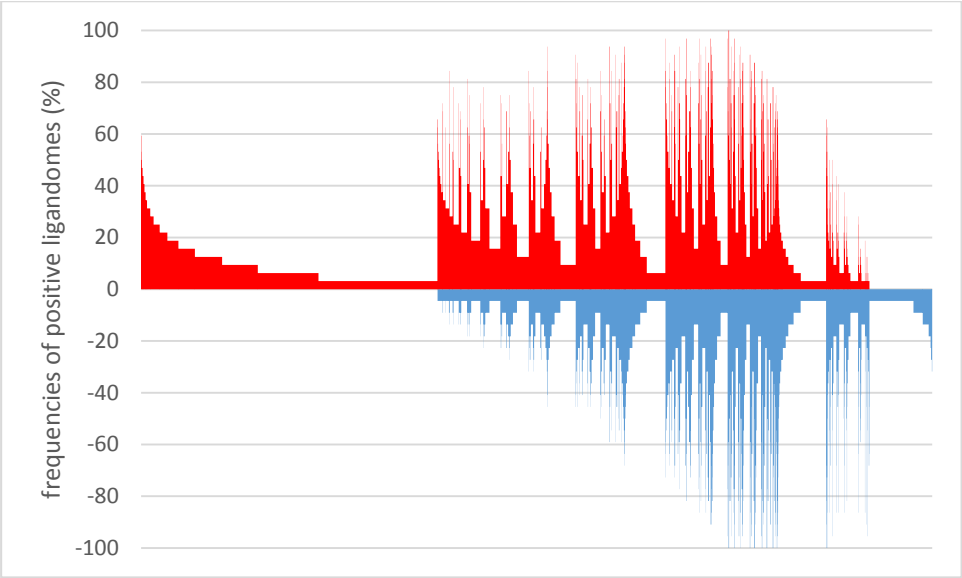

Figure 31 Comparison of frequencies of source proteins of HLA class I ligands from OvCa (red) and OvN (blue). Source proteins found on both tissue types are shown in the middle section of the graph having a red and a blue counterpart. Source proteins of peptides exclusively presented on either tissue are found in the outer rims (far left for OvCa exclusive source proteins and far right for OvN exclusive peptides) of the graph.

A waterfall plot compares the different source proteins represented on OvCa samples (red) and OvN samples (blue) (figure 31). Each peak represents a single source protein. The height of the peak shows the coverage of how many samples represented at least one ligand of that source protein. Source proteins on the far left that are only present in OvCa and have no OvN counterpart are exclusively found in OvCa but not on benign tissue. The other way around peptides found on the far right site that are only depicted in blue but have no red presentation are exclusively found on benign

ovarian tissue. The part in the middle shows source proteins that are represented by HLA class I ligands on both, benign and cancer tissue. In the context of cancer immunotherapy the far left source proteins give rise to peptides that are candidates for peptide-based anti-cancer vaccines.

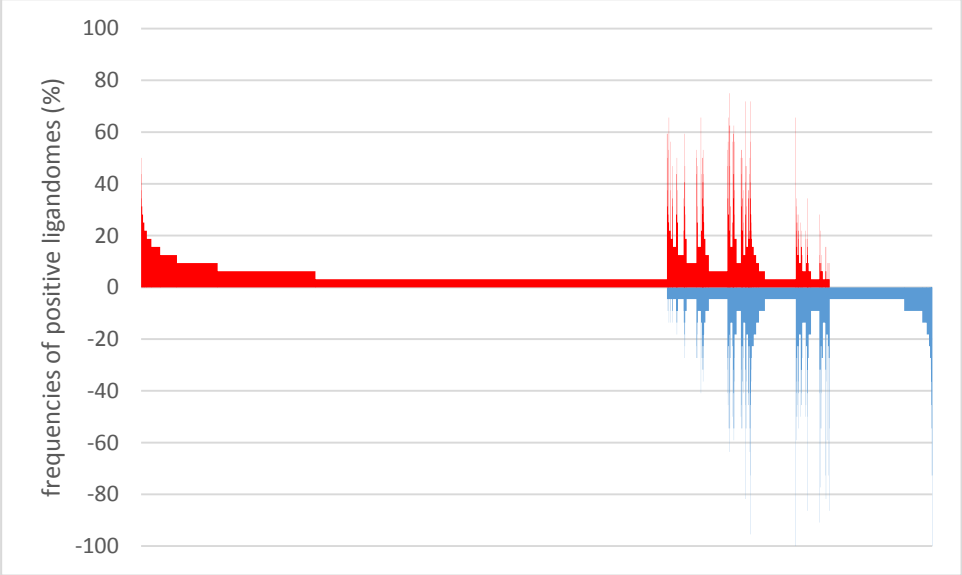

Figure 32 HLA class I presented peptides isolated from benign ovarian tissue (OvN in blue) in comparison to OvCa tissue (red). Comparable to figure 31 the middle section shows the overlap between both tissues meaning peptides that were found on both tissue types. On the far right OvN peptides are exclusively found on benign ovarian tissue.

In Figure 32 the peptides originating from the source proteins depicted in Figure 31 are shown. Each peak represents a single peptide and the height of the peak is the frequency of how many samples presented that peptide. The peptides on the left hand side are exclusively presented on HLA class I of OvCa tissue compared to the benign ovarian tissue. Among them candidates for peptide based anti-cancer vaccines are found.

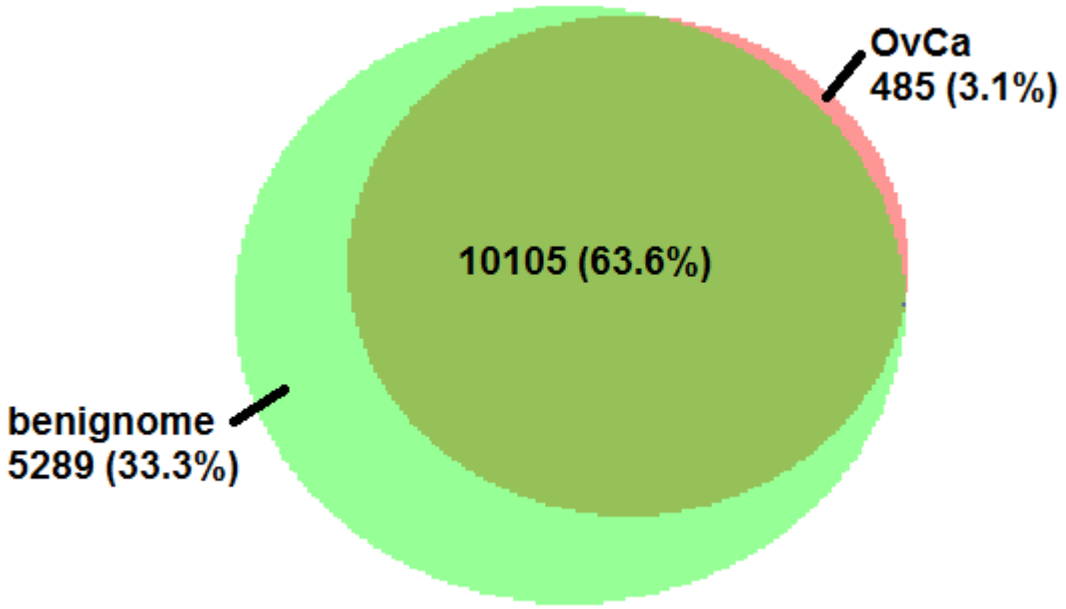

Figure 33 Comparison of source proteins of OvCa and a benignome database. The overlap of the OvCa and the benignome dataset accounts for 63.3% of the source proteins identified. 3.1% of the datasets entered were OvCa exclusively presented source proteins.

The OvCa source proteins were compared to a database containing source proteins of different autopsies of kidney, lung, muscle, small intestine, spleen, bladder, brain, cerebellum, heart, pancreas, skin, stomach, thyroid, adrenal gland, aorta brain, esophagus, liver, testis, bone marrow, tongue, colon and PBMCs. 485 OvCa-unique proteins were identified. These 485 also contain the 56 source proteins described by Schuster et al. to be exclusively represented on HLA class I of OvCa tissue [121].

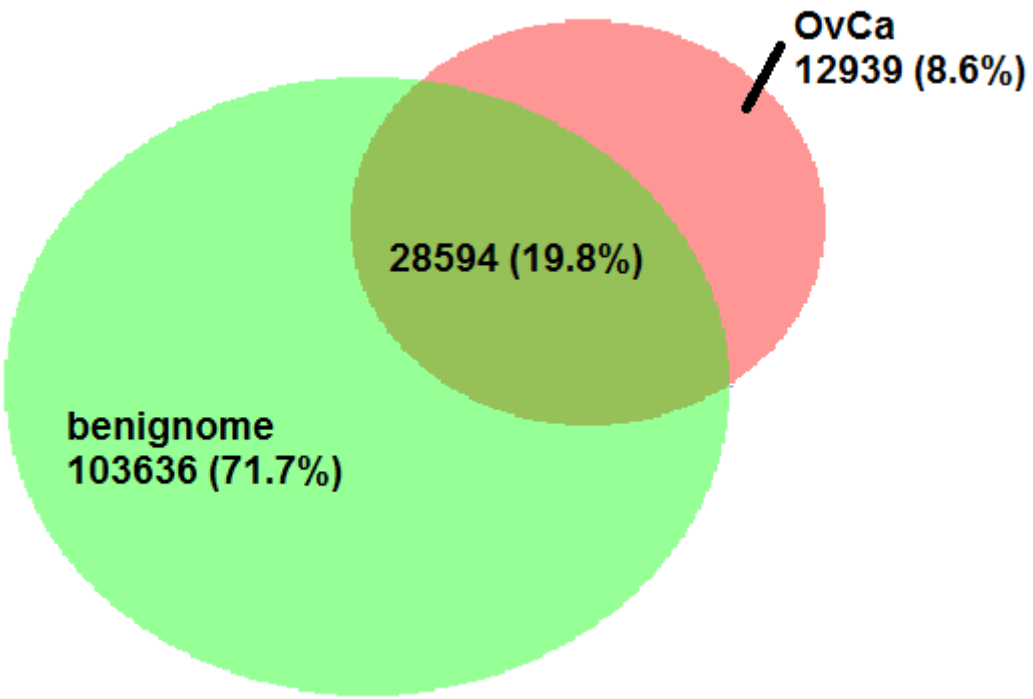

Figure 34 Overlap of OvCa HLA class I peptides and the HLA class I benignome database. 8.6% of the OvCa peptide database was tumor exclusively presented.

To find ligands suitable for peptide based anti-cancer vaccine the amount of HLA class I ligands represented exclusively on OvCa tissue were further narrowed in. Therefore the 56 HLA class I and the 28 HLA class II source proteins described by Schuster et al. were reduced [121]. To reduce the number of target source proteins the frequency of representation on OvCa, their known involvement in the development or progression of OvCa or other tumor entities and the amount of ligands per source protein were taken into account. Under these criteria 13 proteins presented by HLA class I and 4 proteins presented by HLA class II proteins were chosen.

The HLA typing of OvCa samples was acquired from the university hospital. The online tools SYFPEITHI and NetMHC 4.0 utilize the HLA typing to evaluate the binding probability or binding affinity of ligands to the respective HLA type of the sample.

SYFPEITHI is a database that facilitates search for peptides and allows T-cell epitope prediction. The prediction is based on published motifs. It takes amino acids in the anchor, auxiliary anchor positions and frequent amino acids into consideration. The amino acids of peptides are given a specific value. Ideal anchors are scored with 10 points, unusual anchors 6-8 points, auxiliary anchors 4-6 points and preferred residues

are scored with 1-4 points. Amino acids that are having a negative effect on the binding ability score values of -1 to -3 points [141]. Additionally NetMHCpan-3.0 predicted the binding affinity of MHC: peptide binding. NetMHC is a neural network to predict HLA class I epitopes. The methods for prediction of binding to HLA are trained on peptide data containing information about the binding affinity of the peptide to the HLA [142]. Ligands with ≥ 60% of maximum SYFPEITHI score or a binding affinity of ≤ 500 nM on NetMHC were considered probable binders.

The ligands of the 13 HLA class I and the four HLA class II source proteins are listed in the supplemental data (table 9 and table 10). It needs to be mentioned that up to now there is no reliable evaluation tool for HLA class II peptides and their predicted binding.

A large scale study searched for clinically relevant peptide presented by human melanoma tissue. Utilizing MS analysis, the melanoma associated immunopeptidome was surveyed in depth for about 78,000 HLA class I patient presented peptides which is twice as much as we identified in OvCa (> 40900 peptides) [143]. The difference in numbers is related to technical differences in the processing and analysis of tissue. Equally to our procedure HLA class I molecules were immunoaffinity purified using the W6/32 antibody covalently bound to a protein A sepharose matrix. However the antibody used for HLA class II immunoaffinity purification was HB-145. For the LC-MS/MS analysis of HLA peptides, they were eluted with a linear gradient of 2-30% buffer B (80% ACN and 0.5% acetic acid). The flowrate was set to 250 nl/min over 90 min. The column used for elution was 50 cm long and 75 µm in diameter. In contrast the duration of one LC-MS/MS run in our lab lasts 130 min with a linear gradient for 90 min. The peptides were eluted with a linear gradient 2.4-32% ACN and 0.05% formic acid (fa). The applied flow rate was 300 nl/min. The separation column is 25 cm long with an inner diameter of 50 µm.

3.6 Peptide-based therapy development

The first patients under compassionate use setup were treated three days prior to vaccination with cyclophosphamide to reduce the amount of regulatory T cells. On the first day the patient received subcutaneous injection of Ipilimumab at low dose because of its effects on Tregs and its priming supportive effect. Imiquimod was applied on site of vaccination after every vaccination. Each vaccination contained 300 µg of each peptide regardless if HLA class I or HLA class II restricted. The peptides were dissolved in 500 µl DMSO. The patient was vaccinated three times starting day zero, one vaccination a day. Following, vaccination number four occurred on day seven followed by 2 more vaccinations once every week. Two weeks after the sixth vaccination, the patient was vaccinated again, followed by another vaccination on day 49. For the remaining time up to one year duration, the patient received 16 vaccination shots every three weeks. Throughout the course of vaccination blood was collected and used for immunomonitoring purposes. The therapy was prolonged by additional 4 vaccines every 6 weeks. The peptide cocktail was injected intracutanously in order to be processed by professional APCs such as Langerhans cells. Throughout the vaccination the patient received Avastin on a frequent basis in between the peptide vaccination appointments as a standard therapy. Table 2 contains the peptides administered to the first patient (ID: OvCa 115) and the source proteins they are originating from. Table 2 also contains the number of positively tested T cell primings. The peptide SVLADVTTK was synthesized with the wrong sequence. The original sequence was SVLADLVTTK. Therefore the peptide was not further assessed in immunomonitoring. The HLA class II peptide ELGPYTLDRNSLYVNG could not be synthesized efficiently. Thus vaccination and immunomonitoring was done with ELGPYTLDRNSLYVN.

Table 5 Vaccination peptides of OvCa 115, the first patient to be vaccinated in compassionate use treatment. The peptides and their respective source proteins are listed below. HLA restriction and the amount of positive immunogenicity testings is listed respectively. The ten peptides were combined in one cocktail.

vaccination peptides OvCa 115			
	HLA class I		
source protein	peptide sequence	immunogenicity	HLA restriction
MUC16	SVLADVTTK		A*03
IDO1	RSYHLQIVTK	1/1	A*03
EYA2	NVGGLIGTPK	0/1	A*03
MUC16	SPHPVTALL	2/3	B*07
MUC16	SPSKAFASL	3/3	B*07
MUC16	TPGNRAISL	5/5	B*07
MUC16	VPRSAATTL	2/3	B*07
IDO1	NPKAFFSVL	3/5	B*07
	HLA class II		
	longest variant	core peptide	prediction
MSLN	DLPGRFVAESAEVLLPR	FVAESAEVLL	SB to DRB3*0101, WB DRB1*1302
MUC16	ELGPYTLDRNSLYVNG	YTLDRNSLY	SB DRB3*0101

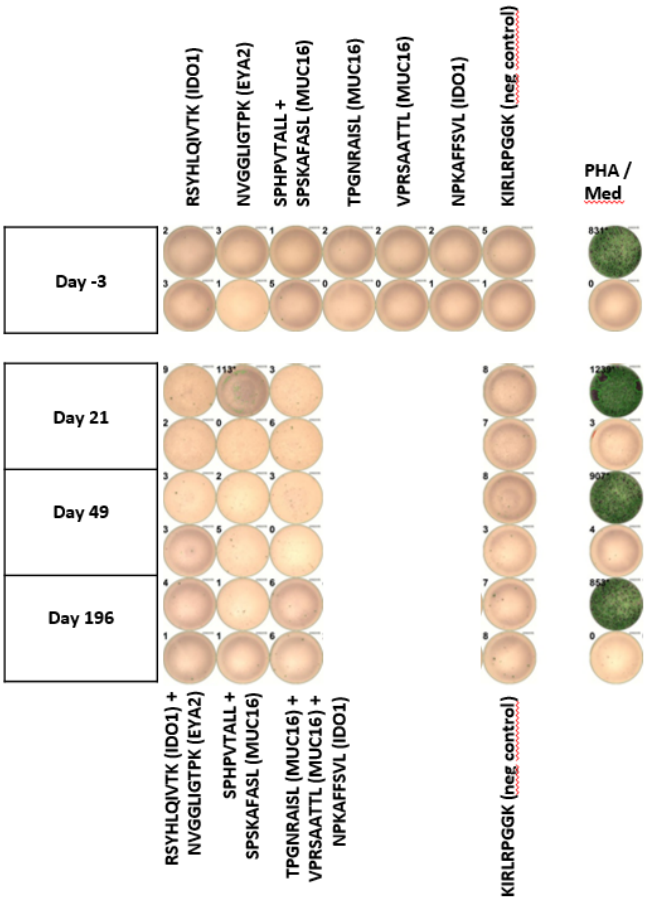

Figure 35 HLA class I mediated reactions at the different time points blood was drained from the patient. PHA control has shown stimulation potential of cells. The numbers in the upper left corner of each well indicates the counted spots respectively.

There were no detectable HLA class I mediated reactions in the ELISpot. Due to a lack of cells after the 12-day stimulation peptide mixes were set up for cells obtained on day 21, 49 and 196. The peptides RSYHLQIVTK and NVGGLIGTPK were combined and analyzed. Likewise the SPHPVTALL and the SPSKAFASL, as well as the TPGNRAISL together with VPRSAATTL and the NPKAFFSVL peptide were combined. The final concentration for each peptide was unchanged at 1 µg/ml. A well was considered to display a positive reaction if a minimum of 15 spots was counted and the count must be three times higher than the count of the negative well (negative peptide or medium control). HLA matched virus peptides were used as negative controls. The virus peptides were either published before or predicted from different viruses. KIRLRPGGK is a HIV peptide that was published before to not induce a detectable immune response [144]. They were tested for their ability to induce HLA class I/II

mediated reactions. They were tested in at least eight healthy donors and did not induce an immune response.

The HLA class II restricted vaccination peptides were combined and analyzed together. A strong immune reaction was observed on day 21. However this reaction was strikingly reduced by day 49 and lost on day 196.

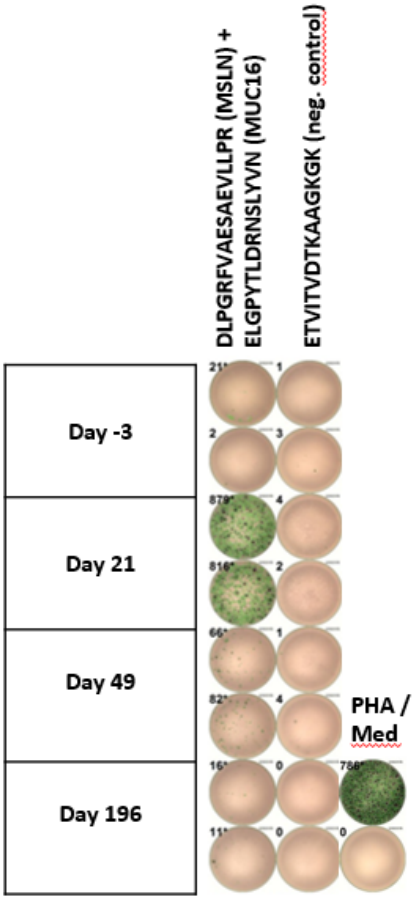

Figure 36 HLA class II immunomonitoring of patient 1. The two vaccination peptides were analyzed together within the same well due to low availability of PBMCs.

Subsequently in the second round of immunomonitoring Figure (37/38), due to low cell counts after 12-day stimulation vaccination peptides were mixed similarly as described above (Figure 35/36). PHA stimulated control was positive. HLA-class I peptides failed to induce a response of memory T cells.

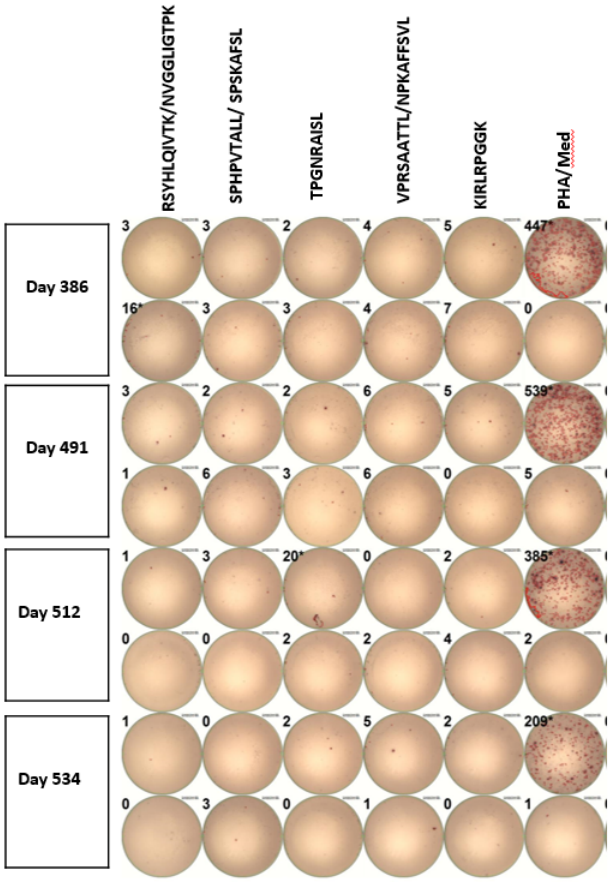

Figure 37 Immunomonitoring of OvCa 115 at later time points between 386 and 534 days of vaccination. PHA control induced T cell responses but HLA class I vaccination peptides failed to do so.

The 12-day stimulation for HLA-class II restricted vaccination peptides did not show an immune reaction either (Figure 38). Also here the reaction from day 21 could not be recovered.

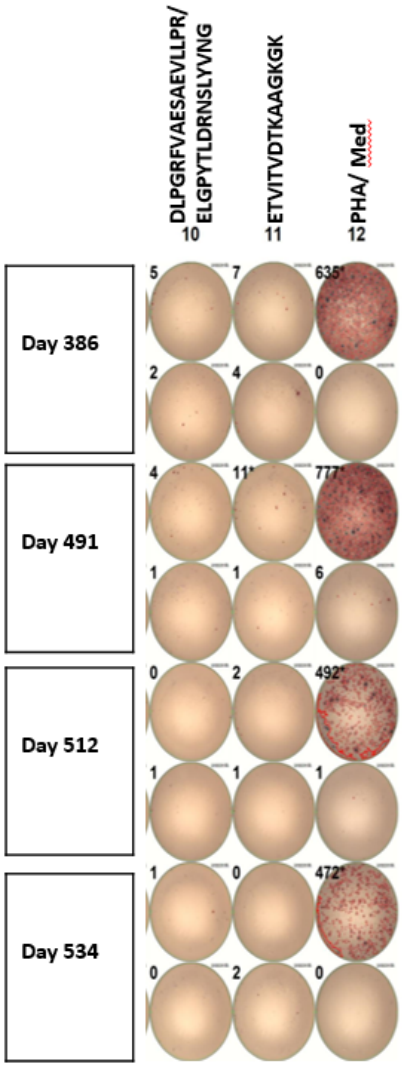

Figure 38 HLA class II mediated reaction of OvCa 115. The analyzed PBMCs were obtained 386-534 days after first vaccination. There were no detectable HLA class II mediated reactions.

A second patient (OvCa 100) was analyzed under the same protocol as the first one. The cocktail was composed of six HLA class I peptides and two HLA class II peptides from the warehouse. From preliminary work from our lab ExomeSeq data were available. The peptides were determined and chosen by Dr. Heiko Schuster.

Table 6 List of vaccination peptides of OvCa 100. It consists of six HLA class I peptides and two HLA class II peptides from the warehouse. Two peptides were predicted from exome sequencing (ExomeSeq) containing a point mutation at the indicated position.

vaccination peptides OvCa 100			
	HLA class I		
source protein	peptide sequence	immunogenicity	HLA restriction
MUC16	KMISAIPTL	4/6	A*02
MUC16	SPHPVTALL	1/2	B*07
MUC16	SPSKAFASL	2/2	B*07
MUC16	TPGNRAISL	2/2	B*07
IDO1	NPKAFFSVL	3/5	B*07
DDR1	FLAEDALNTV	n/a	A*02

	HLA class II		
	longest variant	core peptide	prediction
MSLN	DLPGRFVAESAEVLLPR	FVAESAEVLL	SB to DRB3*0101, WB DRB1*1302
MUC16	ELGPYTLDRNSLYVNG	YTLDRNSLY	SB DRB3*0101

predicted from ExomeSeq		position of mutation (uniprot)	
MUC16	SLTHELSSRV	p.T2285S	A*02
PLEKHG2	PGGGAPASSRGSWSS	p.A1303S	HLA class II

Each vaccination peptide was tested separately. At day 21 an immune reaction was detectable by ELISpot against the MUC16 peptide SPSKAFASL with about 150 counted spots. At day 49 up to 700 spots were counted showing an even stronger immune reaction to this peptide. Other wells of vaccination peptides of day 49 were not accounted as positive since negative because of on average 15 spots of the wells of the YLLPAIVHI negative control.

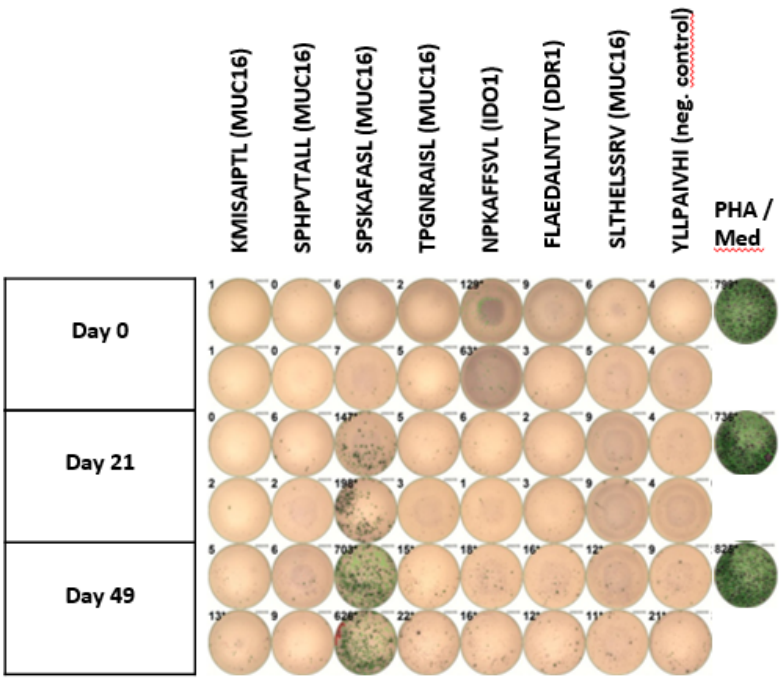

Figure 39 Immunomonitoring of HLA class I mediated T cell responses in OvCa 100. The SPSKAFASL peptide showed an immune response 21 days after the first vaccination.

Two HLA-class II peptides, DLPGRFVAESAEVLLPR (MSLN) and ELGPYTLDRNSLYVN (MUC16) have induced positive wells at day 21. Both reactions were strong with about 500 and 700 counted spots. The reaction of DLPGRFVAESAEVLLPR (MSLN) at day 49 was clearly reduced with about 300 detected spots. On the other hand the reaction of ELGPYTLDRNSLYVN (MUC16) was completely lost by day 49.

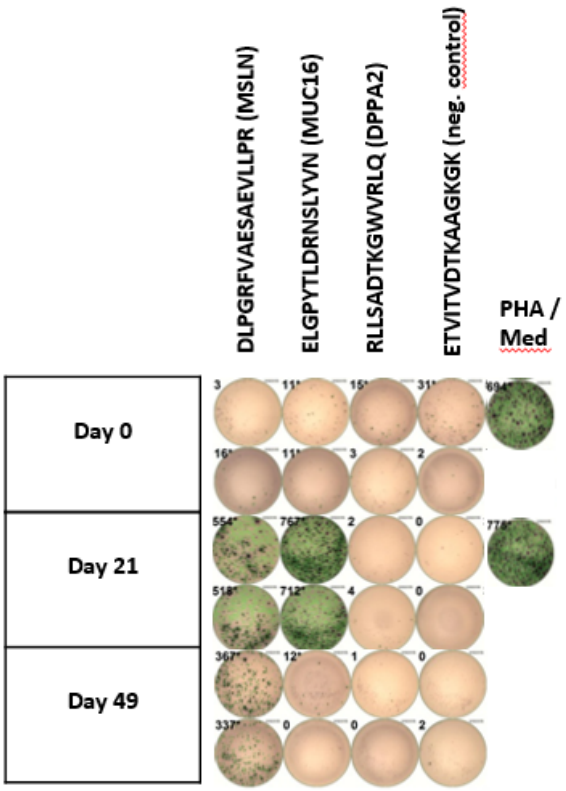

Figure 40 HLA class II restricted vaccination peptide immunomonitoring of OvCa 100. The MSLN peptide induced a strong response that was weaker on day 49. The reaction against the MUC16 peptide was clearly detectable on day 21 but vanished completely by day 49.

The patient discontinued the treatment due to disease progression but reentered 403 days after first vaccination. Besides the positive reaction against PHA there were no detectable reactions in any of the tested HLA-class I peptide tested wells.

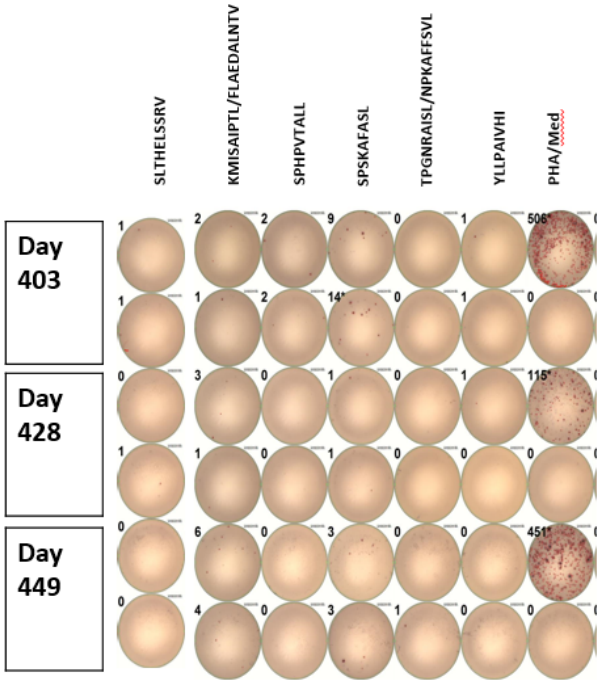

Figure 41 HLA class I peptides immunomonitoring of OvCa 100. She continued vaccination procedure at a later time point (403 days after first vaccination). There were no detectable HLA class I mediated reactions. Reactions that were visible on day 21 could not be recovered on later time points of vaccination.

The early HLA-class II mediated reaction shown in Figure 40 could not be recovered (Figure 42). Analyzed wells were negative throughout all peptides.

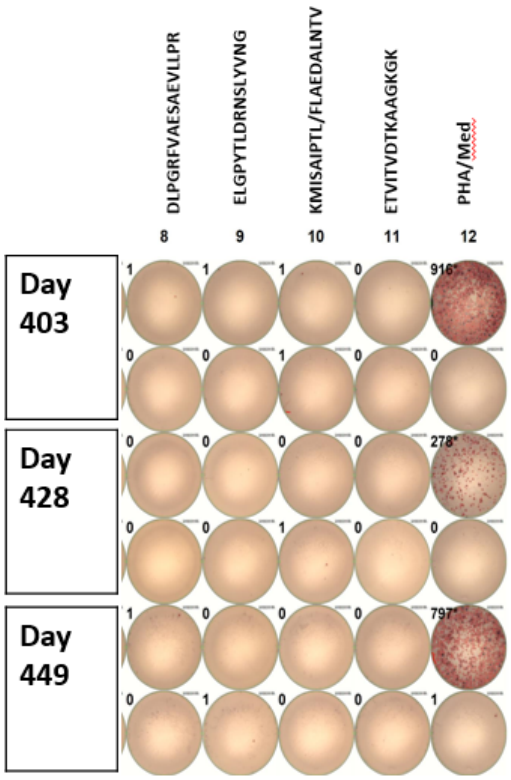

Figure 42 HLA class II peptide immunomonitoring of patient 2 after continued vaccination. Similar to HLA class I immune reactions detectable during early days of vaccination were not recovered in later stages of vaccination.

In order to improve performance of the peptide-based anti-cancer vaccine the treatment protocol was altered. For this purpose the 500 µl of peptide cocktail were emulsified in 1 ml Montanide ISA-720™, a plant oil based adjuvant. Since Montanide™ ISA-720™ has a depot effect on the vaccinated peptides the amount of injections was reduced and vaccination was applied subcutanously. Again three days prior to vaccination low dose cyclophosphamide was given in order to reduce regulatory T cells. The first four vaccinations were given every three weeks and following injections were given every 8 weeks. The subcutanous application is more patient friendly and easier to inject. Ipilimumab was removed from the setting due to no visible effect. Imiquimod was still applied epicutanously.

Table 7 List of vaccination peptides for OvCa 134. Five HLA class I restricted peptides and three HLA class II restricted peptides were chosen.

vaccination peptides OvCa 134			
	HLA class I		
source protein	sequence	immunogenicity	HLA restriction
MUC16	ERSPVIQTL	n.t.	B*39 (B*27)
MUC16	ITETSAVLY	1/2	A*01
CRABP2	NVMLRKIAV	0/1	B*08
CRABP1/2	RTTEINFKV	1/2	A*02
CTAGE5	VGREKKLAL	n.t.	B*08

	HLA class II		
	sequence	core peptide	prediction
MSLN	DLPGRFVAESAEVLLPR	FVAESAEVLL	SB to DRB3*0101, WB DRB1*1302
MUC16	ELGPYTLDRNSLYVN	YTLDRNSLY	SB DRB3*0101
DPPA2	RLLSADTKGWVRLQ	LSADTKGWV	SB to DRB3*0101, WB DRB1*1302

The third patient (OvCa 134) had weak T-cell responses to ERSPVIQTL. Nevertheless the reaction seemed to be preexisting since it was detectable at day 0. The immune reaction prevailed until day 63. All wells containing PBMCs isolated on day 21 had a background reaction that was visible in well treated with vaccination peptides as well in wells treated with negative control peptide or of the medium control. A possible explanation for this can be that a high percentage of cells may have underwent cell death in freezing/ thawing process.

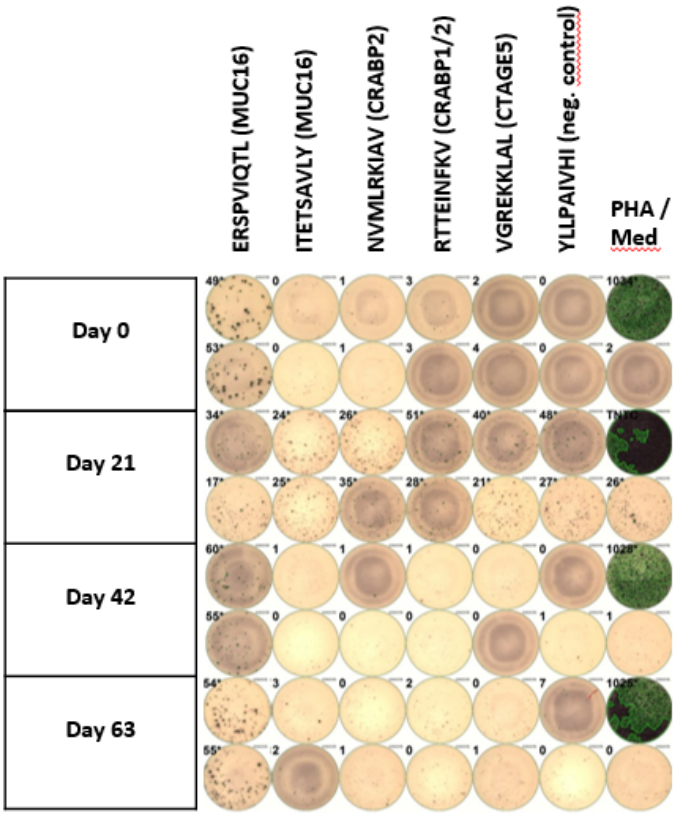

Figure 43 Immunomonitoring of HLA class I mediated reactions of OvCa 134. A pre-existing response was detected against the MUC16 ERSPVIQTL peptide.

In the case of HLA-class II reaction the patient had a vaccine-induced reaction starting on day 21 in the DLPGRFVAESAEVLLPR (MSLN) treated wells. A weak pre-existing reaction against the ELGPYTLDRNSLYVN (MUC16) peptide was detectable before the first vaccine was administered. Furthermore there was a very strong reaction detectable starting day 21 against the RLLSADTKGWVRLQ (DPPA2) peptide.

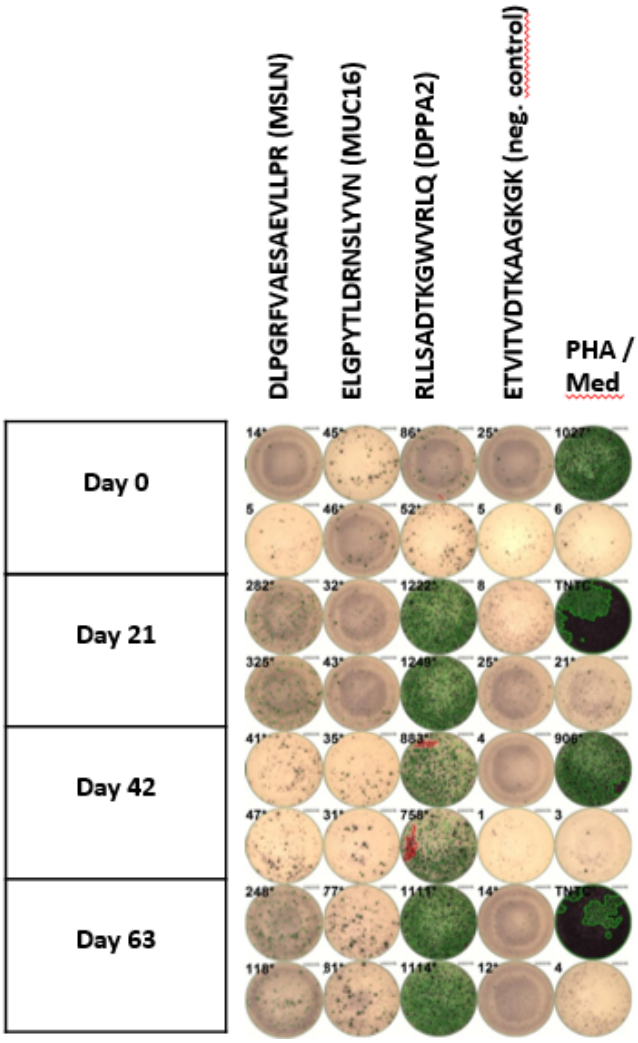

Figure 44 HLA class II mediated reactions of patient OvCa 134. The DPPA2 peptide induced a strong induction of immune response by day 21 which persisted until day 63. The MSLN peptide stimulated reactive T cells on day 21 and day 63 but weaker on day 42 indicating a restimulation of cells.

It remains unknown if the weaker reaction on day 42 is due to homoestatic downregulation of T cells or if stimulated cells at day 21 infiltrated the peripheral tissue and therefore where not detectable within PBMCs.

A study conducted by the Wu lab was published in the course of this year. The study was designed for melanoma patients. Utilizing whole exome sequencing of benign and tumor tissue, somatic mutations were identified. RNA sequencing confirmed the expression of mutated alleles. Subsequently peptides were predicted to bind autologous HLA-A or HLA-B molecules. Peptides were synthesized as long peptides (15-30 amino acids long). Hiltonol, a known TLR3 antagonist, was used as an adjuvants. Patients were vaccinated with 13-20 peptides. Patients received seven

vaccinations all in all, of which five were administered within the first four weeks of treatment, one at week 12 and one at week 20. The readout of the study was done via *ex vivo* ELISpot. They were capable of showing a strong induction of T cell responses, whereas clinical response was detectable in only two out of six patients. Thus the remaining four patients had no tumor recurrence for at least 21 months after vaccination [145].

Comparable to our findings in OvCa the antigenic landscape of multiple myeloma was assessed by mass spectrometry in our department. The HLA ligandome of PBMCs from multiple myeloma patients and multiple myeloma cell lines was analyzed. PBMCs from healthy donors and MM patients were pulsed with MM-associated peptides. In the course of the study pre-existing, peptide-specific T cell responses were characterized exclusively in myeloma patients indicating the pathophysiological relevance of the identified peptides [146].

The aims of this thesis were to characterize the expression of immune checkpoint inhibitors CD137, CTLA-4, LAG-3, PD-1 and TIM-3 of CD4+ Tregs, non-Tregs and CTL in PBMCs and TILS of OvCa tissue. PD-1 was significantly higher expressed on TILs than on PBMCs or PBMCs of healthy donors. The author of this thesis contributed further MS analysis of OvCa and OvN tissue deepening the understanding of the OvCa ligandome and finding peptides suitable for therapeutic treatment of OvCa patients. These peptides have been administered in compassionate use treatment of three patients. Via ELISpot immune reactions against vaccinated peptides were monitored.

4. References

1. Ng, J.S., Low, J.J., and Ilancheran, A., *Epithelial ovarian cancer.* Best Pract Res Clin Obstet Gynaecol, 2012. **26**(3): p. 337-45.
2. World Health Organization, *Cancer Country Profiles, Germany*. 2014; Available from: http://who.int/cancer/country-profiles/deu_en.pdf.
3. American Cancer Society, *Cancer Facts & Figures*. 2017; Available from: https://www.cancer.org/cancer/ovarian-cancer/about/key-statistics.html.
4. Heintz, A.P., Odicino, F., Maisonneuve, P., Beller, U., Benedet, J.L., Creasman, W.T., Ngan, H.Y., and Pecorelli, S., *Carcinoma of the ovary.* Int J Gynaecol Obstet, 2003. **83 Suppl 1**: p. 135-66.
5. Timor-Tritsch, L.E., Lerner, J.P., Monteagudo, A., and Santos, R., *Transvaginal ultrasonographic characterization of ovarian masses by means of color flow-directed Doppler measurements and a morphologic scoring system.* Am J Obstet Gynecol, 1993. **168**(3 Pt 1): p. 909-13.
6. Bristow, R.E., Tomacruz, R.S., Armstrong, D.K., Trimble, E.L., and Montz, F.J., *Survival effect of maximal cytoreductive surgery for advanced ovarian carcinoma during the platinum era: a meta-analysis.* J Clin Oncol, 2002. **20**(5): p. 1248-59.
7. Johnston, C., *ICON2: randomised trial of single-agent carboplatin against three-drug combination of CAP (cyclophosphamide, doxorubicin, and cisplatin) in women with ovarian cancer.* The Lancet, 1998. **352**(9140): p. 1571-1576.
8. Hato, S.V., Khong, A., de Vries, I.J., and Lesterhuis, W.J., *Molecular pathways: the immunogenic effects of platinum-based chemotherapeutics.* Clin Cancer Res, 2014. **20**(11): p. 2831-7.
9. Todd, R.C. and Lippard, S.J., *Inhibition of transcription by platinum antitumor compounds.* Metallomics, 2009. **1**(4): p. 280-91.
10. Trimble, E.L., Adams, J.D., Vena, D., Hawkins, M.J., Friedman, M.A., Fisherman, J.S., Christian, M.C., Canetta, R., Onetto, N., Hayn, R., and et al., *Paclitaxel for platinum-refractory ovarian cancer: results from the first 1,000 patients registered to National Cancer Institute Treatment Referral Center 9103.* J Clin Oncol, 1993. **11**(12): p. 2405-10.
11. Weaver, B.A., *How Taxol/paclitaxel kills cancer cells.* Mol Biol Cell, 2014. **25**(18): p. 2677-81.
12. American Cancer Society, *Lifetime Risk of Developing or Dying From Cancer*. 2016; Available from: https://www.cancer.org/cancer/cancer-basics/lifetime-probability-of-developing-or-dying-from-cancer.html.
13. Risch, H.A., Marrett, L.D., and Howe, G.R., *Parity, contraception, infertility, and the risk of epithelial ovarian cancer.* Am J Epidemiol, 1994. **140**(7): p. 585-97.
14. Mink, P.J., Folsom, A.R., Sellers, T.A., and Kushi, L.H., *Physical activity, waist-to-hip ratio, and other risk factors for ovarian cancer: a follow-up study of older women.* Epidemiology, 1996. **7**(1): p. 38-45.
15. Schildkraut, J.M., Alberg, A.J., Bandera, E.V., Barnholtz-Sloan, J., Bondy, M., Cote, M.L., Funkhouser, E., Peters, E., Schwartz, A.G., Terry, P., Wallace, K., Akushevich, L., Wang, F., Crankshaw, S., and Moorman, P.G., *A multi-center population-based case-control study of ovarian cancer in African-American women: the African American Cancer Epidemiology Study (AACES).* BMC Cancer, 2014. **14**: p. 688.
16. Shah, D.K. *T-cell development in the thymus*. Available from: https://www.immunology.org/public-information/bitesized-immunology/immune-development/t-cell-development-in-thymus.
17. Egerton, M., Scollay, R., and Shortman, K., *Kinetics of mature T-cell development in the thymus.* Proc Natl Acad Sci U S A, 1990. **87**(7): p. 2579-82.
18. Shah, D.K., *T-cell development in the thymus.* British Society for Immunology.
19. Halpern, A.C. and Schuchter, L.M., *Prognostic models in melanoma.* Semin Oncol, 1997. **24**(1 Suppl 4): p. S2-7.

20. Marrogi, A.J., Munshi, A., Merogi, A.J., Ohadike, Y., El-Habashi, A., Marrogi, O.L., and Freeman, S.M., *Study of tumor infiltrating lymphocytes and transforming growth factor-beta as prognostic factors in breast carcinoma.* Int J Cancer, 1997. **74**(5): p. 492-501.
21. Nakano, O., Sato, M., Naito, Y., Suzuki, K., Orikasa, S., Aizawa, M., Suzuki, Y., Shintaku, I., Nagura, H., and Ohtani, H., *Proliferative activity of intratumoral CD8(+) T-lymphocytes as a prognostic factor in human renal cell carcinoma: clinicopathologic demonstration of antitumor immunity.* Cancer Res, 2001. **61**(13): p. 5132-6.
22. Naito, Y., Saito, K., Shiiba, K., Ohuchi, A., Saigenji, K., Nagura, H., and Ohtani, H., *CD8+ T cells infiltrated within cancer cell nests as a prognostic factor in human colorectal cancer.* Cancer Res, 1998. **58**(16): p. 3491-4.
23. Schumacher, K., Haensch, W., Roefzaad, C., and Schlag, P.M., *Prognostic significance of activated CD8(+) T cell infiltrations within esophageal carcinomas.* Cancer Res, 2001. **61**(10): p. 3932-6.
24. Zhang, L., Conejo-Garcia, J.R., Katsaros, D., Gimotty, P.A., Massobrio, M., Regnani, G., Makrigiannakis, A., Gray, H., Schlienger, K., Liebman, M.N., Rubin, S.C., and Coukos, G., *Intratumoral T cells, recurrence, and survival in epithelial ovarian cancer.* N Engl J Med, 2003. **348**(3): p. 203-13.
25. Caux, C., Vanbervliet, B., Massacrier, C., Azuma, M., Okumura, K., Lanier, L.L., and Banchereau, J., *B70/B7-2 is identical to CD86 and is the major functional ligand for CD28 expressed on human dendritic cells.* J Exp Med, 1994. **180**(5): p. 1841-7.
26. Thaiss, C.A., Semmling, V., Franken, L., Wagner, H., and Kurts, C., *Chemokines: a new dendritic cell signal for T cell activation.* Front Immunol, 2011. **2**: p. 31.
27. Linsley, P.S. and Ledbetter, J.A., *The role of the CD28 receptor during T cell responses to antigen.* Annu Rev Immunol, 1993. **11**: p. 191-212.
28. Berke, G., *The CTL's kiss of death.* Cell, 1995. **81**(1): p. 9-12.
29. Pardoll, D.M., *The blockade of immune checkpoints in cancer immunotherapy.* Nat Rev Cancer, 2012. **12**(4): p. 252-64.
30. Couzin-Frankel, J., *Breakthrough of the year 2013. Cancer immunotherapy.* Science, 2013. **342**(6165): p. 1432-3.
31. Li, S.Y. and Liu, Y., *Immunotherapy of melanoma with the immune costimulatory monoclonal antibodies targeting CD137.* Clin Pharmacol, 2013. **5**(Suppl 1): p. 47-53.
32. Melero, I., Shuford, W.W., Newby, S.A., Aruffo, A., Ledbetter, J.A., Hellstrom, K.E., Mittler, R.S., and Chen, L., *Monoclonal antibodies against the 4-1BB T-cell activation molecule eradicate established tumors.* Nat Med, 1997. **3**(6): p. 682-5.
33. Ju, S.A., Lee, S.C., Kwon, T.H., Heo, S.K., Park, S.M., Paek, H.N., Suh, J.H., Cho, H.R., Kwon, B., Kwon, B.S., and Kim, B.S., *Immunity to melanoma mediated by 4-1BB is associated with enhanced activity of tumour-infiltrating lymphocytes.* Immunol Cell Biol, 2005. **83**(4): p. 344-51.
34. Wu, C., Guo, H., Wang, Y., Gao, Y., Zhu, Z., and Du, Z., *Extracellular domain of human 4-1BBL enhanced the function of cytotoxic T-lymphocyte induced by dendritic cell.* Cell Immunol, 2011. **271**(1): p. 118-23.
35. Ito, F., Li, Q., Shreiner, A.B., Okuyama, R., Jure-Kunkel, M.N., Teitz-Tennenbaum, S., and Chang, A.E., *Anti-CD137 monoclonal antibody administration augments the antitumor efficacy of dendritic cell-based vaccines.* Cancer Res, 2004. **64**(22): p. 8411-9.
36. Guo, Z., Cheng, D., Xia, Z., Luan, M., Wu, L., Wang, G., and Zhang, S., *Combined TIM-3 blockade and CD137 activation affords the long-term protection in a murine model of ovarian cancer.* J Transl Med, 2013. **11**: p. 215.
37. Yonezawa, A., Dutt, S., Chester, C., Kim, J., and Kohrt, H.E., *Boosting Cancer Immunotherapy with Anti-CD137 Antibody Therapy.* Clin Cancer Res, 2015. **21**(14): p. 3113-20.
38. Hodi, F.S., O'Day, S.J., McDermott, D.F., Weber, R.W., Sosman, J.A., Haanen, J.B., Gonzalez, R., Robert, C., Schadendorf, D., Hassel, J.C., Akerley, W., van den Eertwegh, A.J., Lutzky, J., Lorigan, P., Vaubel, J.M., Linette, G.P., Hogg, D., Ottensmeier, C.H., Lebbe, C., Peschel, C.,

Quirt, I., Clark, J.I., Wolchok, J.D., Weber, J.S., Tian, J., Yellin, M.J., Nichol, G.M., Hoos, A., and Urba, W.J., *Improved survival with ipilimumab in patients with metastatic melanoma.* N Engl J Med, 2010. **363**(8): p. 711-23.

39. Linsley, P.S., Greene, J.L., Brady, W., Bajorath, J., Ledbetter, J.A., and Peach, R., *Human B7-1 (CD80) and B7-2 (CD86) bind with similar avidities but distinct kinetics to CD28 and CTLA-4 receptors.* Immunity, 1994. **1**(9): p. 793-801.
40. Tivol, E.A., Borriello, F., Schweitzer, A.N., Lynch, W.P., Bluestone, J.A., and Sharpe, A.H., *Loss of CTLA-4 leads to massive lymphoproliferation and fatal multiorgan tissue destruction, revealing a critical negative regulatory role of CTLA-4.* Immunity, 1995. **3**(5): p. 541-7.
41. Peggs, K.S., Quezada, S.A., Chambers, C.A., Korman, A.J., and Allison, J.P., *Blockade of CTLA-4 on both effector and regulatory T cell compartments contributes to the antitumor activity of anti-CTLA-4 antibodies.* J Exp Med, 2009. **206**(8): p. 1717-25.
42. Thaventhiran, T.S., S. Yeang, HXA. Al-Huseini, L. Hamdam, J. and Sathish, J. G., *T cell Co-inhibitory Receptors: Functions and Signalling Mechanisms.* J Clin Cell Immunol 2012. **S12:004**.
43. Lipson, E.J., Forde, P.M., Hammers, H.J., Emens, L.A., Taube, J.M., and Topalian, S.L., *Antagonists of PD-1 and PD-L1 in Cancer Treatment.* Semin Oncol, 2015. **42**(4): p. 587-600.
44. Topalian, S.L., Hodi, F.S., Brahmer, J.R., Gettinger, S.N., Smith, D.C., McDermott, D.F., Powderly, J.D., Carvajal, R.D., Sosman, J.A., Atkins, M.B., Leming, P.D., Spigel, D.R., Antonia, S.J., Horn, L., Drake, C.G., Pardoll, D.M., Chen, L., Sharfman, W.H., Anders, R.A., Taube, J.M., McMiller, T.L., Xu, H., Korman, A.J., Jure-Kunkel, M., Agrawal, S., McDonald, D., Kollia, G.D., Gupta, A., Wigginton, J.M., and Sznol, M., *Safety, activity, and immune correlates of anti-PD-1 antibody in cancer.* N Engl J Med, 2012. **366**(26): p. 2443-54.
45. Okazaki, T., Okazaki, I.M., Wang, J., Sugiura, D., Nakaki, F., Yoshida, T., Kato, Y., Fagarasan, S., Muramatsu, M., Eto, T., Hioki, K., and Honjo, T., *PD-1 and LAG-3 inhibitory co-receptors act synergistically to prevent autoimmunity in mice.* J Exp Med, 2011. **208**(2): p. 395-407.
46. Bruniquel, D., Borie, N., and Triebel, F., *Genomic organization of the human LAG-3/CD4 locus.* Immunogenetics, 1997. **47**(1): p. 96-8.
47. Workman, C.J., Cauley, L.S., Kim, I.J., Blackman, M.A., Woodland, D.L., and Vignali, D.A., *Lymphocyte activation gene-3 (CD223) regulates the size of the expanding T cell population following antigen activation in vivo.* J Immunol, 2004. **172**(9): p. 5450-5.
48. Workman, C.J. and Vignali, D.A., *Negative regulation of T cell homeostasis by lymphocyte activation gene-3 (CD223).* J Immunol, 2005. **174**(2): p. 688-95.
49. Monney, L., Sabatos, C.A., Gaglia, J.L., Ryu, A., Waldner, H., Chernova, T., Manning, S., Greenfield, E.A., Coyle, A.J., Sobel, R.A., Freeman, G.J., and Kuchroo, V.K., *Th1-specific cell surface protein Tim-3 regulates macrophage activation and severity of an autoimmune disease.* Nature, 2002. **415**(6871): p. 536-41.
50. Gorosito Serran, M., Fiocca Vernengo, F., Beccaria, C.G., Acosta Rodriguez, E.V., Montes, C.L., and Gruppi, A., *The regulatory role of B cells in autoimmunity, infections and cancer: Perspectives beyond IL10 production.* FEBS Lett, 2015. **589**(22): p. 3362-9.
51. Schmidt, M., Bohm, D., von Torne, C., Steiner, E., Puhl, A., Pilch, H., Lehr, H.A., Hengstler, J.G., Kolbl, H., and Gehrmann, M., *The humoral immune system has a key prognostic impact in node-negative breast cancer.* Cancer Res, 2008. **68**(13): p. 5405-13.
52. Erdag, G., Schaefer, J.T., Smolkin, M.E., Deacon, D.H., Shea, S.M., Dengel, L.T., Patterson, J.W., and Slingluff, C.L., Jr., *Immunotype and immunohistologic characteristics of tumor-infiltrating immune cells are associated with clinical outcome in metastatic melanoma.* Cancer Res, 2012. **72**(5): p. 1070-80.
53. Nielsen, J.S., Sahota, R.A., Milne, K., Kost, S.E., Nesslinger, N.J., Watson, P.H., and Nelson, B.H., *CD20+ tumor-infiltrating lymphocytes have an atypical CD27- memory phenotype and together with CD8+ T cells promote favorable prognosis in ovarian cancer.* Clin Cancer Res, 2012. **18**(12): p. 3281-92.

54. Flores-Borja, F., Bosma, A., Ng, D., Reddy, V., Ehrenstein, M.R., Isenberg, D.A., and Mauri, C., *CD19+CD24hiCD38hi B cells maintain regulatory T cells while limiting TH1 and TH17 differentiation.* Sci Transl Med, 2013. **5**(173): p. 173ra23.
55. Kessel, A., Haj, T., Peri, R., Snir, A., Melamed, D., Sabo, E., and Toubi, E., *Human CD19(+)CD25(high) B regulatory cells suppress proliferation of CD4(+) T cells and enhance Foxp3 and CTLA-4 expression in T-regulatory cells.* Autoimmun Rev, 2012. **11**(9): p. 670-7.
56. Diefenbach, A., Jensen, E.R., Jamieson, A.M., and Raulet, D.H., *Rae1 and H60 ligands of the NKG2D receptor stimulate tumour immunity.* Nature, 2001. **413**(6852): p. 165-71.
57. Seaman, W.E., Sleisenger, M., Eriksson, E., and Koo, G.C., *Depletion of natural killer cells in mice by monoclonal antibody to NK-1.1. Reduction in host defense against malignancy without loss of cellular or humoral immunity.* J Immunol, 1987. **138**(12): p. 4539-44.
58. Hayakawa, Y., Kelly, J.M., Westwood, J.A., Darcy, P.K., Diefenbach, A., Raulet, D., and Smyth, M.J., *Cutting edge: tumor rejection mediated by NKG2D receptor-ligand interaction is dependent upon perforin.* J Immunol, 2002. **169**(10): p. 5377-81.
59. Lee, R.K., Spielman, J., Zhao, D.Y., Olsen, K.J., and Podack, E.R., *Perforin, Fas ligand, and tumor necrosis factor are the major cytotoxic molecules used by lymphokine-activated killer cells.* J Immunol, 1996. **157**(5): p. 1919-25.
60. Johnsen, A.C., Haux, J., Steinkjer, B., Nonstad, U., Egeberg, K., Sundan, A., Ashkenazi, A., and Espevik, T., *Regulation of APO-2 ligand/trail expression in NK cells-involvement in NK cell-mediated cytotoxicity.* Cytokine, 1999. **11**(9): p. 664-72.
61. Marcus, A., Gowen, B.G., Thompson, T.W., Iannello, A., Ardolino, M., Deng, W., Wang, L., Shifrin, N., and Raulet, D.H., *Recognition of tumors by the innate immune system and natural killer cells.* Adv Immunol, 2014. **122**: p. 91-128.
62. Janeway C. A. Jr. Travers P., W.M., *Immunobiology: The Immune System in Health and Disease.* . Vol. 5th Edition. 2001, New York: Garland Science.
63. O'Brien, T.J., Beard, J.B., Underwood, L.J., Dennis, R.A., Santin, A.D., and York, L., *The CA 125 gene: an extracellular superstructure dominated by repeat sequences.* Tumour Biol, 2001. **22**(6): p. 348-66.
64. Das, S. and Batra, S.K., *Understanding the Unique Attributes of MUC16 (CA125): Potential Implications in Targeted Therapy.* Cancer Res, 2015. **75**(22): p. 4669-74.
65. Streppel, M.M., Vincent, A., Mukherjee, R., Campbell, N.R., Chen, S.H., Konstantopoulos, K., Goggins, M.G., Van Seuningen, I., Maitra, A., and Montgomery, E.A., *Mucin 16 (cancer antigen 125) expression in human tissues and cell lines and correlation with clinical outcome in adenocarcinomas of the pancreas, esophagus, stomach, and colon.* Hum Pathol, 2012. **43**(10): p. 1755-63.
66. Kim, N., Hong, Y., Kwon, D., and Yoon, S., *Somatic mutaome profile in human cancer tissues.* Genomics Inform, 2013. **11**(4): p. 239-44.
67. Di Fronzo, G., Cappelletti, V., Miodini, P., Bertario, L., and Ravasi, G., *Role of cellular retinoic acid binding protein (cRABP) in patients with large bowel cancer.* Cancer Detect Prev, 1987. **10**(5-6): p. 327-33.
68. Vreeland, A.C., Levi, L., Zhang, W., Berry, D.C., and Noy, N., *Cellular retinoic acid-binding protein 2 inhibits tumor growth by two distinct mechanisms.* J Biol Chem, 2014. **289**(49): p. 34065-73.
69. Vacchelli, E., Aranda, F., Eggermont, A., Sautes-Fridman, C., Tartour, E., Kennedy, E.P., Platten, M., Zitvogel, L., Kroemer, G., and Galluzzi, L., *Trial watch: IDO inhibitors in cancer therapy.* Oncoimmunology, 2014. **3**(10): p. e957994.
70. Platten, M., Wick, W., and Van den Eynde, B.J., *Tryptophan catabolism in cancer: beyond IDO and tryptophan depletion.* Cancer Res, 2012. **72**(21): p. 5435-40.
71. Motrescu, E.R., Blaise, S., Etique, N., Messaddeq, N., Chenard, M.P., Stoll, I., Tomasetto, C., and Rio, M.C., *Matrix metalloproteinase-11/stromelysin-3 exhibits collagenolytic function against collagen VI under normal and malignant conditions.* Oncogene, 2008. **27**(49): p. 6347-55.

72. Wang, X., Duan, W., Li, X., Liu, J., Li, D., Ye, L., Qian, L., Yang, A., Xu, Q., Liu, H., Fu, Q., Wu, E., Ma, Q., and Shen, X., *PTTG regulates the metabolic switch of ovarian cancer cells via the c-myc pathway.* Oncotarget, 2015. **6**(38): p. 40959-69.
73. El-Naggar, S.M., Malik, M.T., and Kakar, S.S., *Small interfering RNA against PTTG: a novel therapy for ovarian cancer.* Int J Oncol, 2007. **31**(1): p. 137-43.
74. Li, Y., Zhou, L.P., Ma, P., Sui, C.G., Meng, F.D., Tian, X., Fu, L.Y., and Jiang, Y.H., *Relationship of PTTG expression with tumor invasiveness and microvessel density of pituitary adenomas: a meta-analysis.* Genet Test Mol Biomarkers, 2014. **18**(4): p. 279-85.
75. Zhou, C., Tong, Y., Wawrowsky, K., and Melmed, S., *PTTG acts as a STAT3 target gene for colorectal cancer cell growth and motility.* Oncogene, 2014. **33**(7): p. 851-61.
76. Farabaugh, S.M., Micalizzi, D.S., Jedlicka, P., Zhao, R., and Ford, H.L., *Eya2 is required to mediate the pro-metastatic functions of Six1 via the induction of TGF-beta signaling, epithelial-mesenchymal transition, and cancer stem cell properties.* Oncogene, 2012. **31**(5): p. 552-62.
77. Barrow, H., Rhodes, J.M., and Yu, L.G., *The role of galectins in colorectal cancer progression.* Int J Cancer, 2011. **129**(1): p. 1-8.
78. Rorive, S., Belot, N., Decaestecker, C., Lefranc, F., Gordower, L., Micik, S., Maurage, C.A., Kaltner, H., Ruchoux, M.M., Danguy, A., Gabius, H.J., Salmon, I., Kiss, R., and Camby, I., *Galectin-1 is highly expressed in human gliomas with relevance for modulation of invasion of tumor astrocytes into the brain parenchyma.* Glia, 2001. **33**(3): p. 241-55.
79. Dalotto-Moreno, T., Croci, D.O., Cerliani, J.P., Martinez-Allo, V.C., Dergan-Dylon, S., Mendez-Huergo, S.P., Stupirski, J.C., Mazal, D., Osinaga, E., Toscano, M.A., Sundblad, V., Rabinovich, G.A., and Salatino, M., *Targeting galectin-1 overcomes breast cancer-associated immunosuppression and prevents metastatic disease.* Cancer Res, 2013. **73**(3): p. 1107-17.
80. Szoke, T., Kayser, K., Baumhakel, J.D., Trojan, I., Furak, J., Tiszlavicz, L., Horvath, A., Szluha, K., Gabius, H.J., and Andre, S., *Prognostic significance of endogenous adhesion/growth-regulatory lectins in lung cancer.* Oncology, 2005. **69**(2): p. 167-74.
81. Saussez, S., Camby, I., Toubeau, G., and Kiss, R., *Galectins as modulators of tumor progression in head and neck squamous cell carcinomas.* Head Neck, 2007. **29**(9): p. 874-84.
82. Chow, S.N., Chen, R.J., Chen, C.H., Chang, T.C., Chen, L.C., Lee, W.J., Shen, J., and Chow, L.P., *Analysis of protein profiles in human epithelial ovarian cancer tissues by proteomic technology.* Eur J Gynaecol Oncol, 2010. **31**(1): p. 55-62.
83. Laderach, D.J., Gentilini, L.D., Giribaldi, L., Delgado, V.C., Nugnes, L., Croci, D.O., Al Nakouzi, N., Sacca, P., Casas, G., Mazza, O., Shipp, M.A., Vazquez, E., Chauchereau, A., Kutok, J.L., Rodig, S.J., Elola, M.T., Compagno, D., and Rabinovich, G.A., *A unique galectin signature in human prostate cancer progression suggests galectin-1 as a key target for treatment of advanced disease.* Cancer Res, 2013. **73**(1): p. 86-96.
84. Shen, K.H., Li, C.F., Chien, L.H., Huang, C.H., Su, C.C., Liao, A.C., and Wu, T.F., *Role of galectin-1 in urinary bladder urothelial carcinoma cell invasion through the JNK pathway.* Cancer Sci, 2016. **107**(10): p. 1390-1398.
85. Necela, B.M., Crozier, J.A., Andorfer, C.A., Lewis-Tuffin, L., Kachergus, J.M., Geiger, X.J., Kalari, K.R., Serie, D.J., Sun, Z., Moreno-Aspitia, A., O'Shannessy, D.J., Maltzman, J.D., McCullough, A.E., Pockaj, B.A., Cunliffe, H.E., Ballman, K.V., Thompson, E.A., and Perez, E.A., *Folate receptor-alpha (FOLR1) expression and function in triple negative tumors.* PLoS One, 2015. **10**(3): p. e0122209.
86. Emami, N. and Diamandis, E.P., *Utility of kallikrein-related peptidases (KLKs) as cancer biomarkers.* Clin Chem, 2008. **54**(10): p. 1600-7.
87. Cheng, Z., Guo, J., Chen, L., Luo, N., Yang, W., and Qu, X., *Overexpression of TMEM158 contributes to ovarian carcinogenesis.* J Exp Clin Cancer Res, 2015. **34**: p. 75.
88. Shimizu, A., Hirono, S., Tani, M., Kawai, M., Okada, K., Miyazawa, M., Kitahata, Y., Nakamura, Y., Noda, T., Yokoyama, S., and Yamaue, H., *Coexpression of MUC16 and mesothelin is related*

to the invasion process in pancreatic ductal adenocarcinoma. Cancer Sci, 2012. **103**(4): p. 739-46.
89. Khong, H. and Overwijk, W.W., *Adjuvants for peptide-based cancer vaccines.* J Immunother Cancer, 2016. **4**: p. 56.
90. Melief, C.J. and van der Burg, S.H., *Immunotherapy of established (pre)malignant disease by synthetic long peptide vaccines.* Nat Rev Cancer, 2008. **8**(5): p. 351-60.
91. Reinhardt, R.L., Bullard, D.C., Weaver, C.T., and Jenkins, M.K., *Preferential accumulation of antigen-specific effector CD4 T cells at an antigen injection site involves CD62E-dependent migration but not local proliferation.* J Exp Med, 2003. **197**(6): p. 751-62.
92. Lindblad, E.B. and Schonberg, N.E., *Aluminum adjuvants: preparation, application, dosage, and formulation with antigen.* Methods Mol Biol, 2010. **626**: p. 41-58.
93. He, P., Zou, Y., and Hu, Z., *Advances in aluminum hydroxide-based adjuvant research and its mechanism.* Hum Vaccin Immunother, 2015. **11**(2): p. 477-88.
94. Medzhitov, R., Preston-Hurlburt, P., and Janeway, C.A., Jr., *A human homologue of the Drosophila Toll protein signals activation of adaptive immunity.* Nature, 1997. **388**(6640): p. 394-7.
95. Kanneganti, T.D., Lamkanfi, M., and Nunez, G., *Intracellular NOD-like receptors in host defense and disease.* Immunity, 2007. **27**(4): p. 549-59.
96. Loo, Y.M. and Gale, M., Jr., *Immune signaling by RIG-I-like receptors.* Immunity, 2011. **34**(5): p. 680-92.
97. Geijtenbeek, T.B. and Gringhuis, S.I., *Signalling through C-type lectin receptors: shaping immune responses.* Nat Rev Immunol, 2009. **9**(7): p. 465-79.
98. Hertz, C.J., Kiertscher, S.M., Godowski, P.J., Bouis, D.A., Norgard, M.V., Roth, M.D., and Modlin, R.L., *Microbial lipopeptides stimulate dendritic cell maturation via Toll-like receptor 2.* J Immunol, 2001. **166**(4): p. 2444-50.
99. Chua, B.Y., Zeng, W., Lau, Y.F., and Jackson, D.C., *Comparison of lipopeptide-based immunocontraceptive vaccines containing different lipid groups.* Vaccine, 2007. **25**(1): p. 92-101.
100. Borsutzky, S., Kretschmer, K., Becker, P.D., Muhlradt, P.F., Kirschning, C.J., Weiss, S., and Guzman, C.A., *The mucosal adjuvant macrophage-activating lipopeptide-2 directly stimulates B lymphocytes via the TLR2 without the need of accessory cells.* J Immunol, 2005. **174**(10): p. 6308-13.
101. Yang, R.B., Mark, M.R., Gray, A., Huang, A., Xie, M.H., Zhang, M., Goddard, A., Wood, W.I., Gurney, A.L., and Godowski, P.J., *Toll-like receptor-2 mediates lipopolysaccharide-induced cellular signalling.* Nature, 1998. **395**(6699): p. 284-8.
102. Steinhagen, F., Kinjo, T., Bode, C., and Klinman, D.M., *TLR-based immune adjuvants.* Vaccine, 2011. **29**(17): p. 3341-55.
103. Kawai, T. and Akira, S., *TLR signaling.* Cell Death Differ, 2006. **13**(5): p. 816-25.
104. Alexopoulou, L., Holt, A.C., Medzhitov, R., and Flavell, R.A., *Recognition of double-stranded RNA and activation of NF-kappaB by Toll-like receptor 3.* Nature, 2001. **413**(6857): p. 732-8.
105. Netea, M.G., Van der Meer, J.W., Sutmuller, R.P., Adema, G.J., and Kullberg, B.J., *From the Th1/Th2 paradigm towards a Toll-like receptor/T-helper bias.* Antimicrob Agents Chemother, 2005. **49**(10): p. 3991-6.
106. Sosman, J.A., Unger, J.M., Liu, P.Y., Flaherty, L.E., Park, M.S., Kempf, R.A., Thompson, J.A., Terasaki, P.I., Sondak, V.K., and Southwest Oncology, G., *Adjuvant immunotherapy of resected, intermediate-thickness, node-negative melanoma with an allogeneic tumor vaccine: impact of HLA class I antigen expression on outcome.* J Clin Oncol, 2002. **20**(8): p. 2067-75.
107. Atanackovic, D., Altorki, N.K., Stockert, E., Williamson, B., Jungbluth, A.A., Ritter, E., Santiago, D., Ferrara, C.A., Matsuo, M., Selvakumar, A., Dupont, B., Chen, Y.T., Hoffman, E.W., Ritter, G., Old, L.J., and Gnjatic, S., *Vaccine-induced CD4+ T cell responses to MAGE-3 protein in lung cancer patients.* J Immunol, 2004. **172**(5): p. 3289-96.

108. North, S.A., Graham, K., Bodnar, D., and Venner, P., *A pilot study of the liposomal MUC1 vaccine BLP25 in prostate specific antigen failures after radical prostatectomy.* J Urol, 2006. **176**(1): p. 91-5.
109. Adams, S., O'Neill, D.W., Nonaka, D., Hardin, E., Chiriboga, L., Siu, K., Cruz, C.M., Angiulli, A., Angiulli, F., Ritter, E., Holman, R.M., Shapiro, R.L., Berman, R.S., Berner, N., Shao, Y., Manches, O., Pan, L., Venhaus, R.R., Hoffman, E.W., Jungbluth, A., Gnjatic, S., Old, L., Pavlick, A.C., and Bhardwaj, N., *Immunization of malignant melanoma patients with full-length NY-ESO-1 protein using TLR7 agonist imiquimod as vaccine adjuvant.* J Immunol, 2008. **181**(1): p. 776-84.
110. Feyerabend, S., Stevanovic, S., Gouttefangeas, C., Wernet, D., Hennenlotter, J., Bedke, J., Dietz, K., Pascolo, S., Kuczyk, M., Rammensee, H.G., and Stenzl, A., *Novel multi-peptide vaccination in Hla-A2+ hormone sensitive patients with biochemical relapse of prostate cancer.* Prostate, 2009. **69**(9): p. 917-27.
111. Smith, B.D., Kasamon, Y.L., Kowalski, J., Gocke, C., Murphy, K., Miller, C.B., Garrett-Mayer, E., Tsai, H.L., Qin, L., Chia, C., Biedrzycki, B., Harding, T.C., Tu, G.H., Jones, R., Hege, K., and Levitsky, H.I., *K562/GM-CSF immunotherapy reduces tumor burden in chronic myeloid leukemia patients with residual disease on imatinib mesylate.* Clin Cancer Res, 2010. **16**(1): p. 338-47.
112. Daayana, S., Elkord, E., Winters, U., Pawlita, M., Roden, R., Stern, P.L., and Kitchener, H.C., *Phase II trial of imiquimod and HPV therapeutic vaccination in patients with vulval intraepithelial neoplasia.* Br J Cancer, 2010. **102**(7): p. 1129-36.
113. Lazoura, E. and Apostolopoulos, V., *Rational Peptide-based vaccine design for cancer immunotherapeutic applications.* Curr Med Chem, 2005. **12**(6): p. 629-39.
114. Buhrman, J.D., Jordan, K.R., Munson, D.J., Moore, B.L., Kappler, J.W., and Slansky, J.E., *Improving antigenic peptide vaccines for cancer immunotherapy using a dominant tumor-specific T cell receptor.* J Biol Chem, 2013. **288**(46): p. 33213-25.
115. Disis, M.L., Gooley, T.A., Rinn, K., Davis, D., Piepkorn, M., Cheever, M.A., Knutson, K.L., and Schiffman, K., *Generation of T-cell immunity to the HER-2/neu protein after active immunization with HER-2/neu peptide-based vaccines.* J Clin Oncol, 2002. **20**(11): p. 2624-32.
116. Aucouturier, J., Dupuis, L., Deville, S., Ascarateil, S., and Ganne, V., *Montanide ISA 720 and 51: a new generation of water in oil emulsions as adjuvants for human vaccines.* Expert Rev Vaccines, 2002. **1**(1): p. 111-8.
117. Bollinger, J.N., *Metabolic fate of mineral oil adjuvants using 14C-labeled tracers. I. Mineral oil.* J Pharm Sci, 1970. **59**(8): p. 1084-8.
118. Barnstable, C.J., Bodmer, W.F., Brown, G., Galfre, G., Milstein, C., Williams, A.F., and Ziegler, A., *Production of monoclonal antibodies to group A erythrocytes, HLA and other human cell surface antigens-new tools for genetic analysis.* Cell, 1978. **14**(1): p. 9-20.
119. Lampson, L.A. and Levy, R., *Two populations of Ia-like molecules on a human B cell line.* J Immunol, 1980. **125**(1): p. 293-9.
120. Maeda, H. and Hirata, R., *Separation of four class II molecules from DR2 and DRw6 homozygous B lymphoid cell lines.* Immunogenetics, 1984. **20**(6): p. 639-47.
121. Schuster, H., Peper, J.K., Bösmüller, H.-C., Röhle, K., Backert, L., Bilich, T., Ney, B., Löffler, M.W., Kowalewski, D.J., Trautwein, N., Rabsteyn, A., Engler, T., Braun, S., Haen, S.P., Walz, J.S., Schmid-Horch, B., Brucker, S., Wallwiener, D., Kohlbacher, O., Fend, F., Rammensee, H.-G., Stevanovic, S., Staebler, A., Wagner, P. , *The immunopeptidomic landscape of ovarian carcinomas.* PNAS, 2017. **in press**.
122. Goldstein, M.J., Kohrt, H.E., Houot, R., Varghese, B., Lin, J.T., Swanson, E., and Levy, R., *Adoptive cell therapy for lymphoma with CD4 T cells depleted of CD137-expressing regulatory T cells.* Cancer Res, 2012. **72**(5): p. 1239-47.
123. Tai, X., Van Laethem, F., Pobezinsky, L., Guinter, T., Sharrow, S.O., Adams, A., Granger, L., Kruhlak, M., Lindsten, T., Thompson, C.B., Feigenbaum, L., and Singer, A., *Basis of CTLA-4 function in regulatory and conventional CD4(+) T cells.* Blood, 2012. **119**(22): p. 5155-63.

124. Duraiswamy, J., Kaluza, K.M., Freeman, G.J., and Coukos, G., *Dual blockade of PD-1 and CTLA-4 combined with tumor vaccine effectively restores T-cell rejection function in tumors.* Cancer Res, 2013. **73**(12): p. 3591-603.
125. Okamura, T., Sumitomo, S., Morita, K., Iwasaki, Y., Inoue, M., Nakachi, S., Komai, T., Shoda, H., Miyazaki, J., Fujio, K., and Yamamoto, K., *TGF-beta3-expressing CD4+CD25(-)LAG3+ regulatory T cells control humoral immune responses.* Nat Commun, 2015. **6**: p. 6329.
126. Sakuishi, K., Ngiow, S.F., Sullivan, J.M., Teng, M.W., Kuchroo, V.K., Smyth, M.J., and Anderson, A.C., *TIM3+FOXP3+ regulatory T cells are tissue-specific promoters of T-cell dysfunction in cancer.* Oncoimmunology, 2013. **2**(4): p. e23849.
127. Zhong, A., Pan, X., and Shi, M., *Expression of PD-1 by CD4(+)CD25(+)CD127(low) Treg cells in the peripheral blood of lung cancer patients.* Onco Targets Ther, 2015. **8**: p. 1831-3.
128. Lowther, D.E., Goods, B.A., Lucca, L.E., Lerner, B.A., Raddassi, K., van Dijk, D., Hernandez, A.L., Duan, X., Gunel, M., Coric, V., Krishnaswamy, S., Love, J.C., and Hafler, D.A., *PD-1 marks dysfunctional regulatory T cells in malignant gliomas.* JCI Insight, 2016. **1**(5).
129. Vinay, D.S. and Kwon, B.S., *Immunotherapy of cancer with 4-1BB.* Mol Cancer Ther, 2012. **11**(5): p. 1062-70.
130. Yang, Z.Z., Grote, D.M., Ziesmer, S.C., Xiu, B., Novak, A.J., and Ansell, S.M., *PD-1 expression defines two distinct T-cell sub-populations in follicular lymphoma that differentially impact patient survival.* Blood Cancer J, 2015. **5**: p. e281.
131. Fujisawa, R., Haseda, F., Tsutsumi, C., Hiromine, Y., Noso, S., Kawabata, Y., Mitsui, S., Terasaki, J., Ikegami, H., Imagawa, A., and Hanafusa, T., *Low programmed cell death-1 (PD-1) expression in peripheral CD4(+) T cells in Japanese patients with autoimmune type 1 diabetes.* Clin Exp Immunol, 2015. **180**(3): p. 452-7.
132. Xu, Y., Zhang, H., Huang, Y., Rui, X., and Zheng, F., *Role of TIM-3 in ovarian cancer.* Clin Transl Oncol, 2017. **19**(9): p. 1079-1083.
133. Gros, A., Robbins, P.F., Yao, X., Li, Y.F., Turcotte, S., Tran, E., Wunderlich, J.R., Mixon, A., Farid, S., Dudley, M.E., Hanada, K., Almeida, J.R., Darko, S., Douek, D.C., Yang, J.C., and Rosenberg, S.A., *PD-1 identifies the patient-specific CD8(+) tumor-reactive repertoire infiltrating human tumors.* J Clin Invest, 2014. **124**(5): p. 2246-59.
134. Chan, D.V., Gibson, H.M., Aufiero, B.M., Wilson, A.J., Hafner, M.S., Mi, Q.S., and Wong, H.K., *Differential CTLA-4 expression in human CD4+ versus CD8+ T cells is associated with increased NFAT1 and inhibition of CD4+ proliferation.* Genes Immun, 2014. **15**(1): p. 25-32.
135. Donahue, A.C. and Fruman, D.A., *Proliferation and survival of activated B cells requires sustained antigen receptor engagement and phosphoinositide 3-kinase activation.* J Immunol, 2003. **170**(12): p. 5851-60.
136. De Maria, A., Bozzano, F., Cantoni, C., and Moretta, L., *Revisiting human natural killer cell subset function revealed cytolytic CD56(dim)CD16+ NK cells as rapid producers of abundant IFN-gamma on activation.* Proc Natl Acad Sci U S A, 2011. **108**(2): p. 728-32.
137. Fauriat, C., Long, E.O., Ljunggren, H.G., and Bryceson, Y.T., *Regulation of human NK-cell cytokine and chemokine production by target cell recognition.* Blood, 2010. **115**(11): p. 2167-76.
138. Coca, S., Perez-Piqueras, J., Martinez, D., Colmenarejo, A., Saez, M.A., Vallejo, C., Martos, J.A., and Moreno, M., *The prognostic significance of intratumoral natural killer cells in patients with colorectal carcinoma.* Cancer, 1997. **79**(12): p. 2320-8.
139. Ishigami, S., Natsugoe, S., Tokuda, K., Nakajo, A., Xiangming, C., Iwashige, H., Aridome, K., Hokita, S., and Aikou, T., *Clinical impact of intratumoral natural killer cell and dendritic cell infiltration in gastric cancer.* Cancer Lett, 2000. **159**(1): p. 103-8.
140. Villegas, F.R., Coca, S., Villarrubia, V.G., Jimenez, R., Chillon, M.J., Jareno, J., Zuil, M., and Callol, L., *Prognostic significance of tumor infiltrating natural killer cells subset CD57 in patients with squamous cell lung cancer.* Lung Cancer, 2002. **35**(1): p. 23-8.
141. Rammensee, H.G.B., J. Emmerich, N. N. Bachor, O. A. Stevanovic, S., *SYFPEITHI: database for MHC ligands and peptide motifs.* Immunogenetics, 1999. **50**: p. 213-219.

142. Nielsen, M. and Andreatta, M., *NetMHCpan-3.0; improved prediction of binding to MHC class I molecules integrating information from multiple receptor and peptide length datasets.* Genome Med, 2016. **8**(1): p. 33.
143. Bassani-Sternberg, M., Braunlein, E., Klar, R., Engleitner, T., Sinitcyn, P., Audehm, S., Straub, M., Weber, J., Slotta-Huspenina, J., Specht, K., Martignoni, M.E., Werner, A., Hein, R., D, H.B., Peschel, C., Rad, R., Cox, J., Mann, M., and Krackhardt, A.M., *Direct identification of clinically relevant neoepitopes presented on native human melanoma tissue by mass spectrometry.* Nat Commun, 2016. **7**: p. 13404.
144. Zarling, A.L., Johnson, J.G., Hoffman, R.W., and Lee, D.R., *Induction of primary human CD8+ T lymphocyte responses in vitro using dendritic cells.* J Immunol, 1999. **162**(9): p. 5197-204.
145. Ott, P.A., Hu, Z., Keskin, D.B., Shukla, S.A., Sun, J., Bozym, D.J., Zhang, W., Luoma, A., Giobbie-Hurder, A., Peter, L., Chen, C., Olive, O., Carter, T.A., Li, S., Lieb, D.J., Eisenhaure, T., Gjini, E., Stevens, J., Lane, W.J., Javeri, I., Nellaiappan, K., Salazar, A.M., Daley, H., Seaman, M., Buchbinder, E.I., Yoon, C.H., Harden, M., Lennon, N., Gabriel, S., Rodig, S.J., Barouch, D.H., Aster, J.C., Getz, G., Wucherpfennig, K., Neuberg, D., Ritz, J., Lander, E.S., Fritsch, E.F., Hacohen, N., and Wu, C.J., *An immunogenic personal neoantigen vaccine for patients with melanoma.* Nature, 2017. **547**(7662): p. 217-221.
146. Walz, S., Stickel, J.S., Kowalewski, D.J., Schuster, H., Weisel, K., Backert, L., Kahn, S., Nelde, A., Stroh, T., Handel, M., Kohlbacher, O., Kanz, L., Salih, H.R., Rammensee, H.G., and Stevanovic, S., *The antigenic landscape of multiple myeloma: mass spectrometry (re)defines targets for T-cell-based immunotherapy.* Blood, 2015. **126**(10): p. 1203-13.

5. Supplemental data

5.1 Gating strategy of co-inhibitory and co-stimulatory receptors.

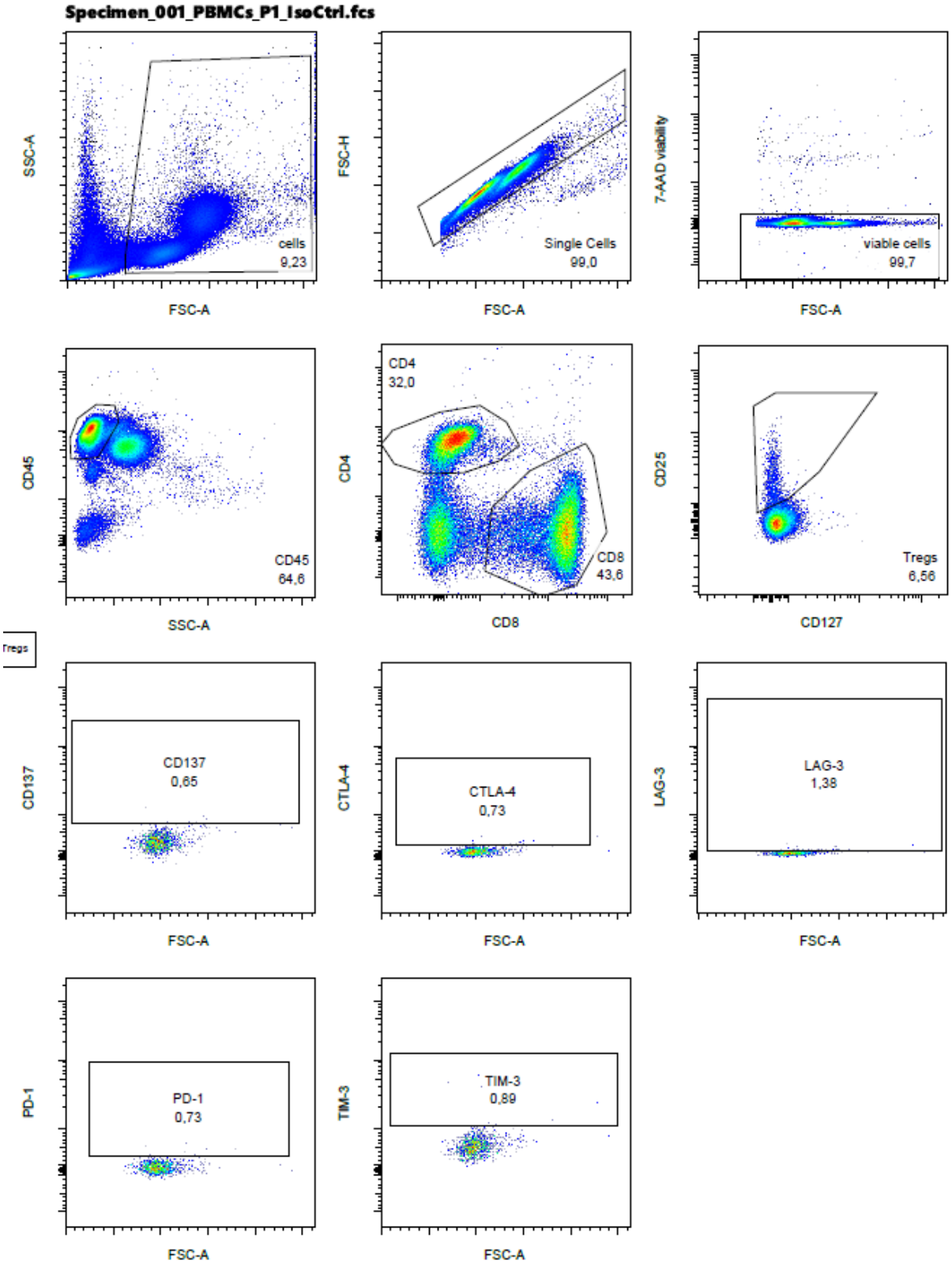

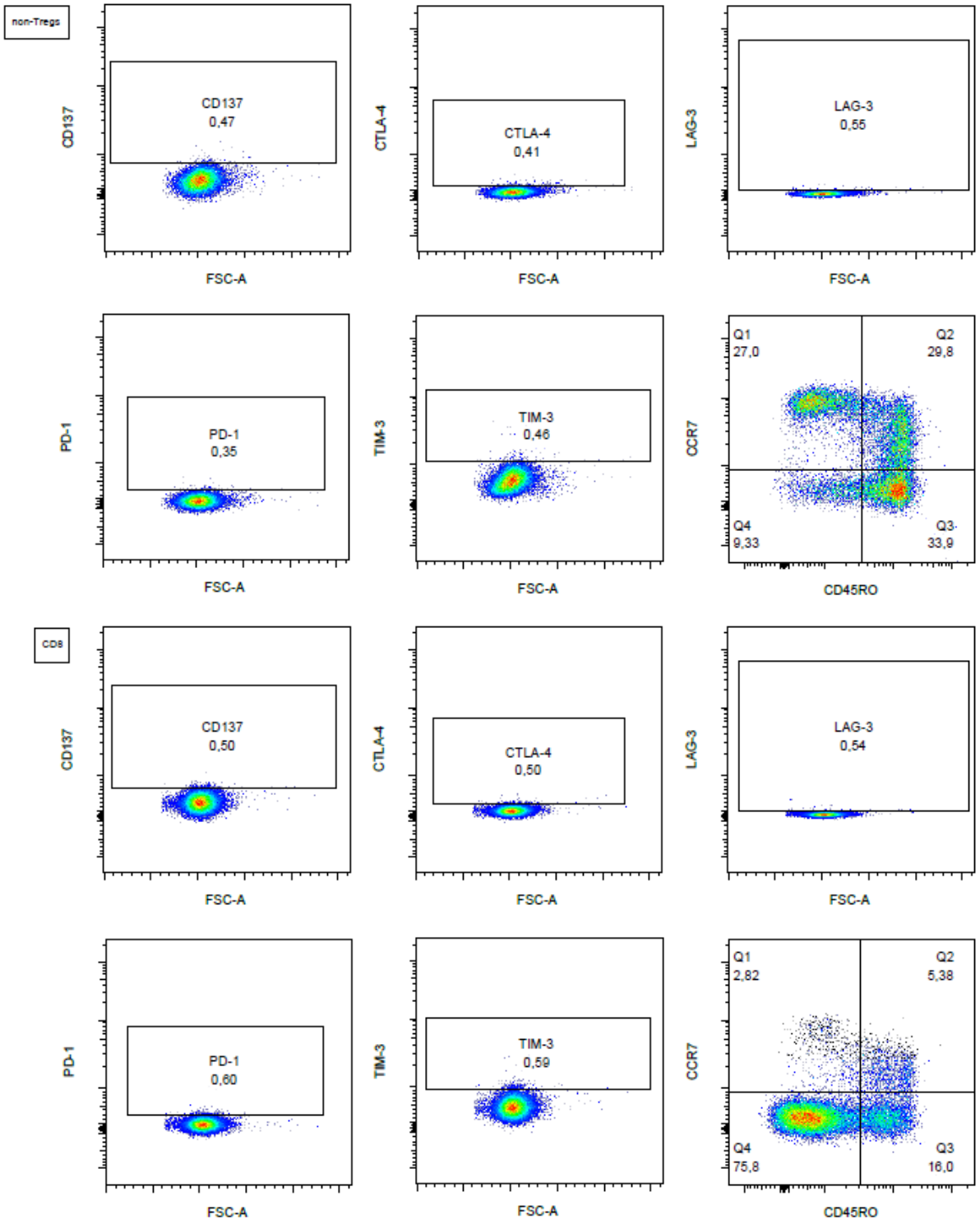

Figure 45 Gating strategy for the PBMC isotype control. In the first pictures the gate is set on cells to distinguish them from debris. The second picture shows the single cell gate followed by the viability staining with 7-AAD (negative staining). The lymphocyte gate was set on CD45 and side scatter (SSC) to distinguish lymphocytes from monocytes. Originating from the CD4+ cells, cells were gated for their expression of CD25/CD127 to determine the amount of Tregs (CD25+ $CD127^{low}$). The memory phenotype was assessed via CCR7 and CD45RO.

Q1 is characterized as naïve T cells, followed clockwise by central memory (Q2), effector memory (Q3) and EMRA (Q4).

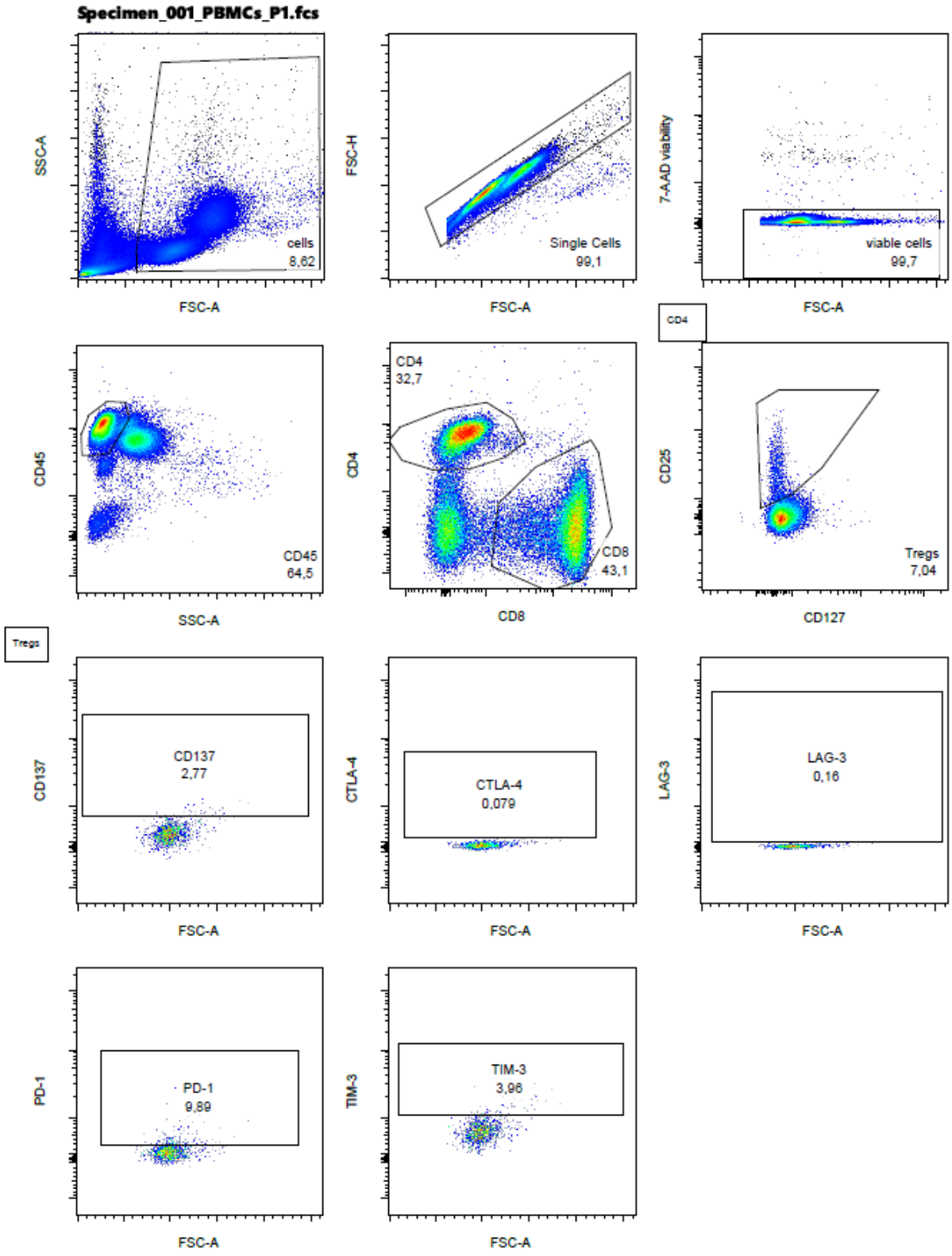

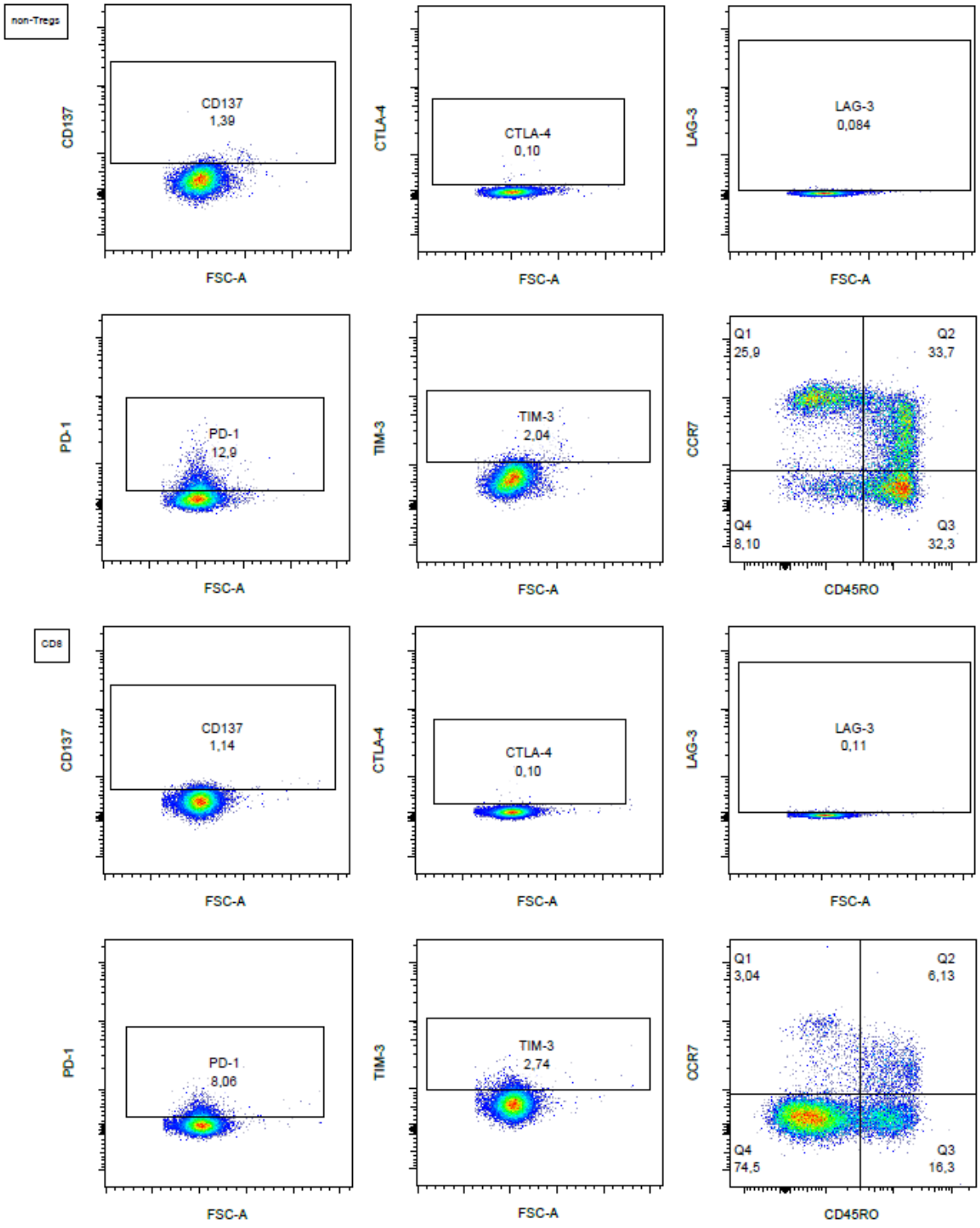

Figure 46 Gating strategy for PBMCs oriented on the isotype control staining of PBMCs from Figure 45.

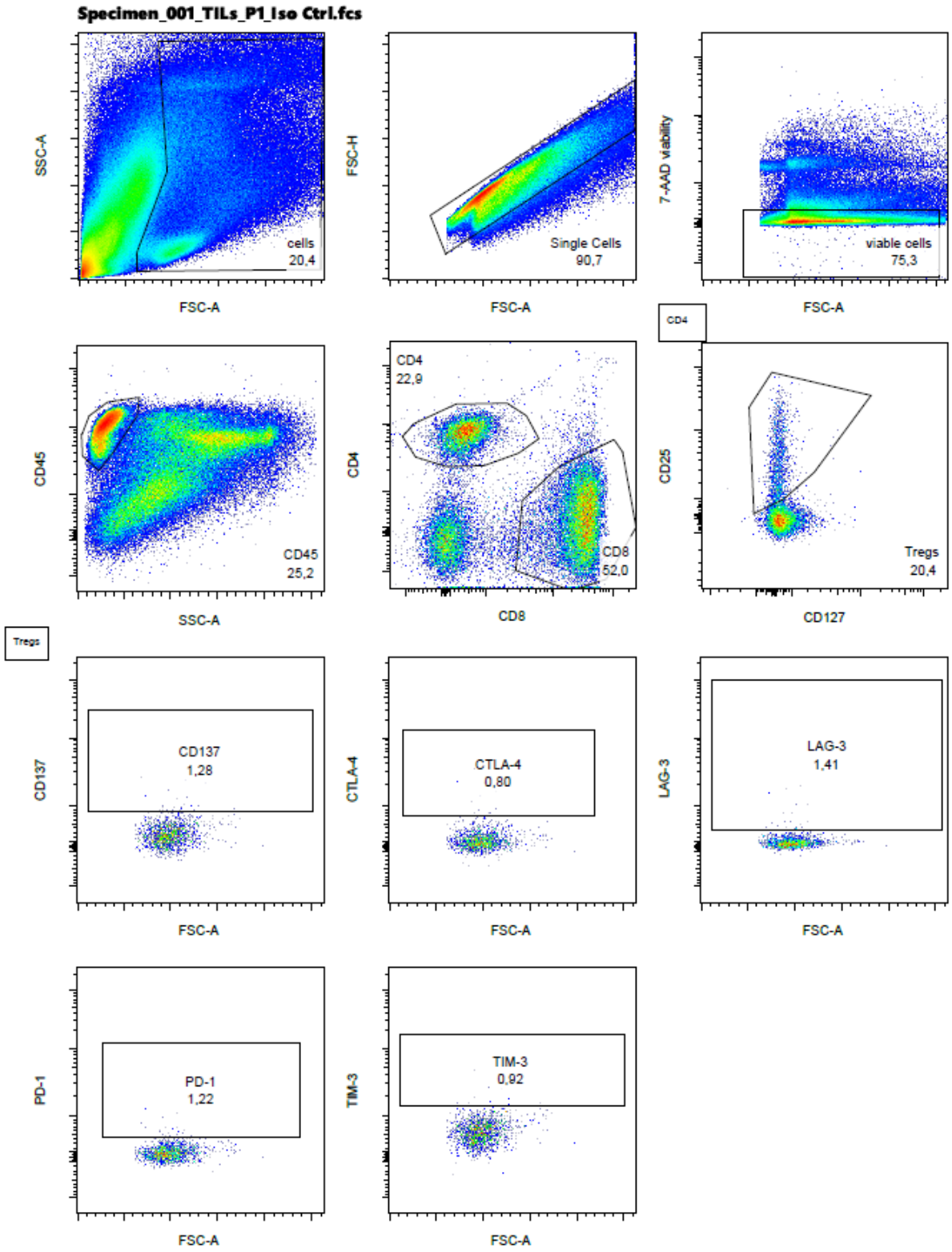
Specimen_001_TILs_P1_Iso Ctrl.fcs
SSC-A
FSC-A
cells
20,4
FSC-H
Single Cells
90,7
7-AAD viability
viable cells
75,3
CD45
SSC-A
CD45
25,2
CD4
22,9
CD8
52,0
CD8
CD4
CD25
CD127
Tregs
20,4
Tregs
CD137
CD137
1,28
CTLA-4
CTLA-4
0,80
LAG-3
LAG-3
1,41
PD-1
PD-1
1,22
TIM-3
TIM-3
0,92

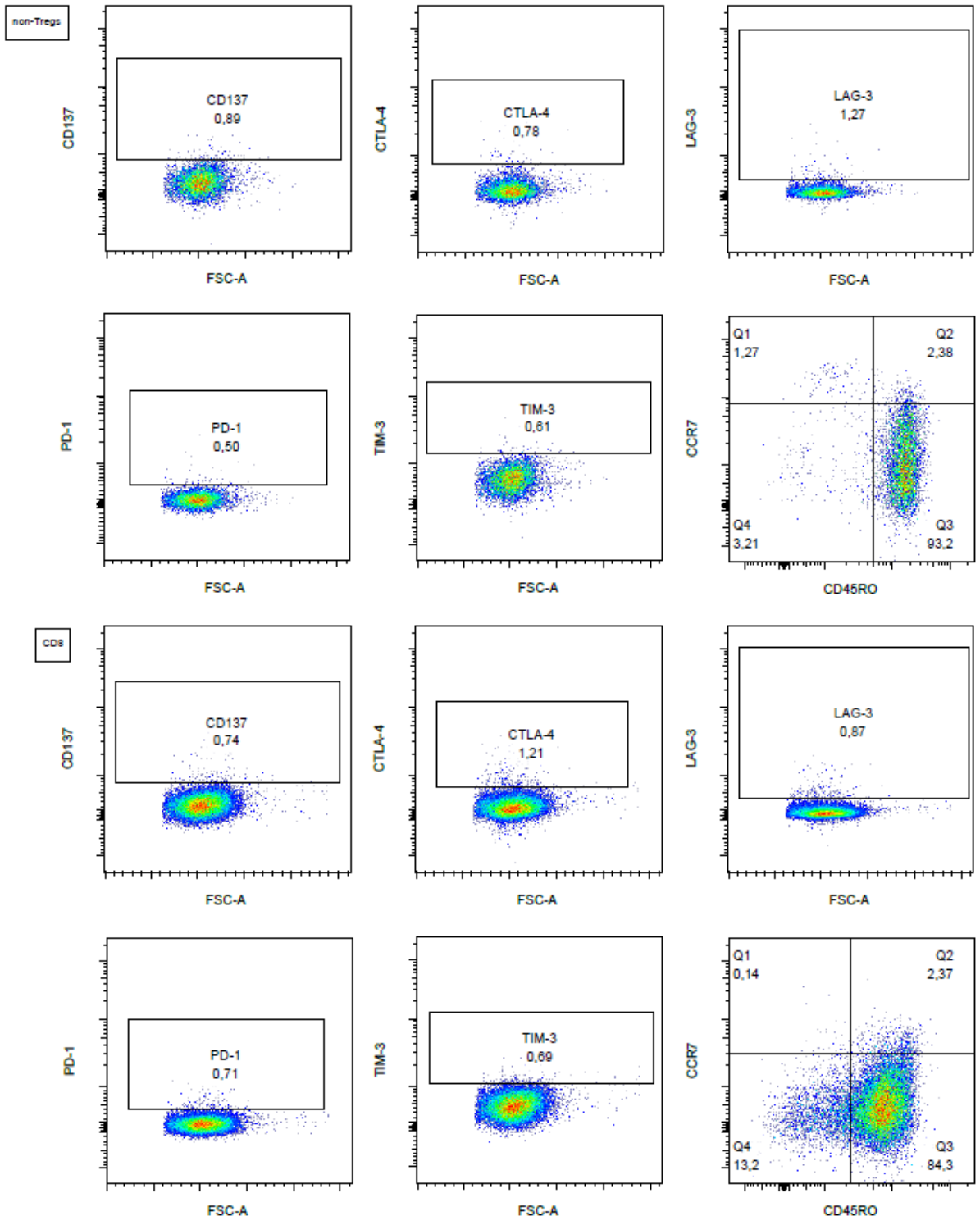

Figure 47 Isotype control staining for TILs to determine unspecific background staining.

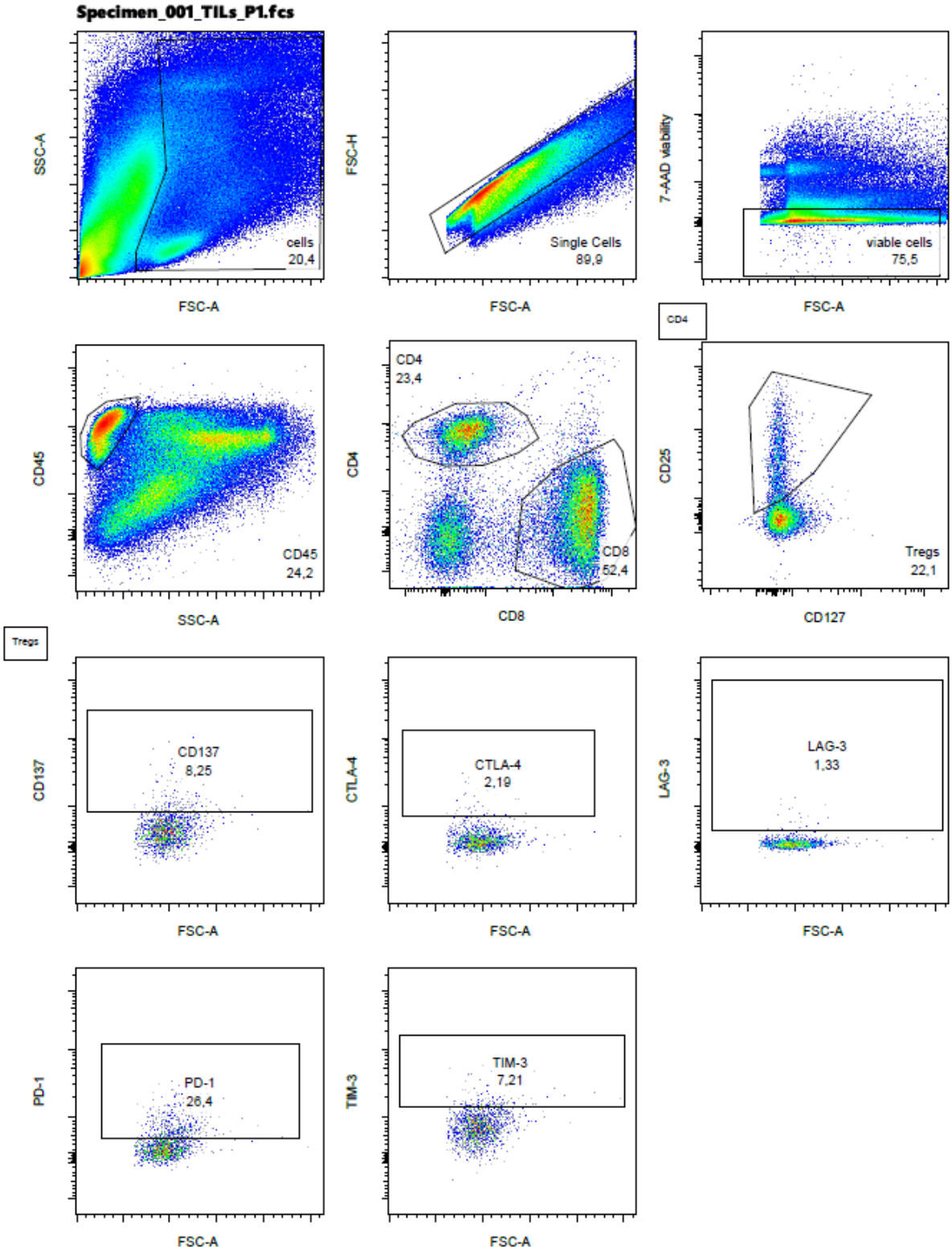
Specimen_001_TILs_P1.fcs
SSC-A
FSC-A
cells
20,4
FSC-H
FSC-A
Single Cells
89,9
7-AAD viability
FSC-A
viable cells
75,5
CD45
SSC-A
CD45
24,2
CD4
CD8
CD4
23,4
CD8
52,4
CD4
CD25
CD127
Tregs
22,1
Tregs
CD137
FSC-A
CD137
8,25
CTLA-4
FSC-A
CTLA-4
2,19
LAG-3
FSC-A
LAG-3
1,33
PD-1
FSC-A
PD-1
26,4
TIM-3
FSC-A
TIM-3
7,21

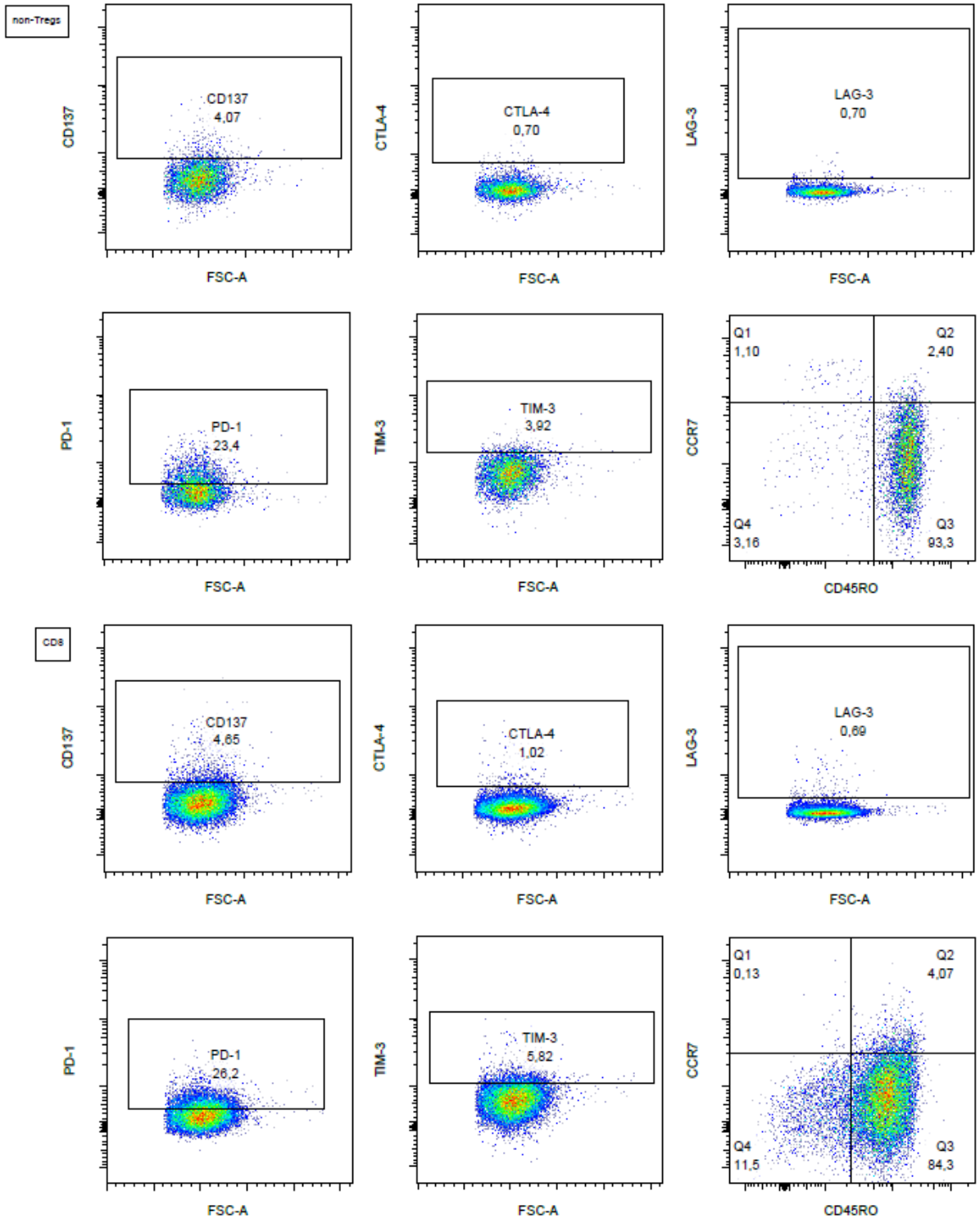

Figure 48 TIL staining for panel 1 oriented on isotype control stained TILs.

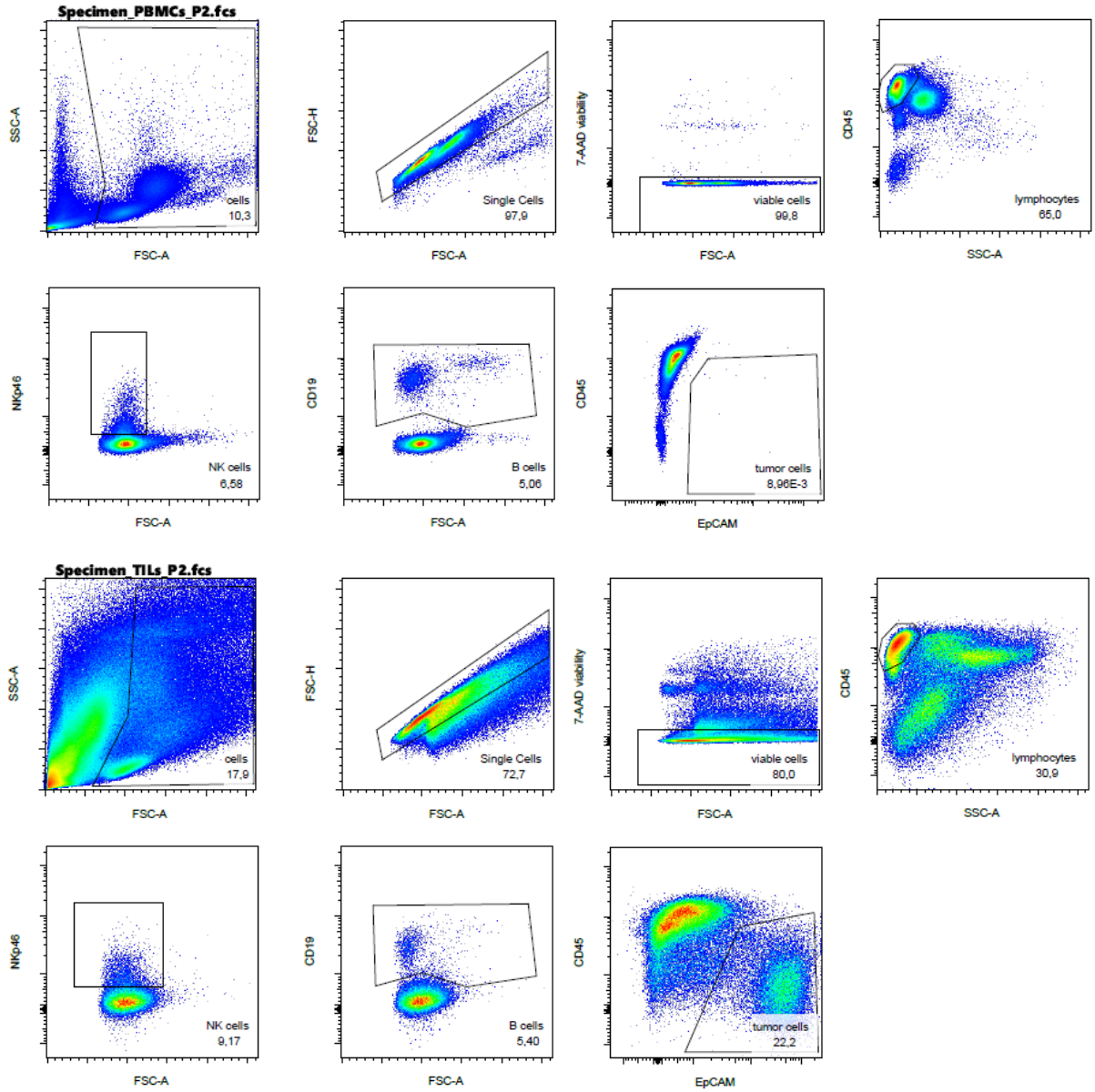

Figure 49 Gating strategy of the second panel, staining for NK cells (NKp46), B cells (CD19) and tumor cells (CD45- EpCAM+). In PBMCs the CD19 gate contains two small populations differing in size. B cells increase in size upon activation [135].

5.2 Ligand list of HLA class I binders for selected tumor exclusive source proteins

Table 8 sample IDs of HLA ligandome analyzed OvCas (left column) and OvN (right column). The list below contains all samples processed by the author of this thesis. Samples contributed to the work of Schuster et al. are highlighted in red [121].

sample ID	sample ID
OvCa 99	OvN 26
OvCa 100	OvN 27
OvCa 103	OvN 28
OvCa 104	OvN 29
OvCa 105	OvN 31
OvCa 107	OvN 33
OvCa 109	OvN 36
OvCa 110	OvN 38
OvCa 111	OvN 39
OvCa 114	OvN 40
OvCa 116	OvN 41
OvCa 118	OvN 43
OvCa 120	OvN 45
OvCa 121	OvN 46
OvCa 126	OvN 47
OvCa 128	OvN 48
OvCa 130	OvN 49
OvCa 131	OvN 50
OvCa 134	OvN 51
OvCa 135	OvN 52
OvCa 136	OvN 56
OvCa 137	OvN 57
OvCa 140	
OvCa 141	
OvCa 142	
OvCa 144	
OvCa 148	
OvCa 150	
OvCa 154	
OvCa 157	
OvCa 162	
OvCa 167	

Table 9 Peptide sequences for each derived from the 13 proteins that were considered for peptide-based immunotherapy of OvCa patients. Table organized for proteins and uniprot accession ID. The amount of OvCas the peptide was isolated from is another parameter to evaluate the relevance of the peptide for warehouse. These peptide sequences were all presented on OvCa tumor tissue processed by the author of this thesis. Sequences might overlap with preliminary work.

protein	accession	sequence	# of OvCa IDs
MUC16	Q8WXI7	AEITITTQTGY	1
		AESIPTVSF	4
		AETILTFHAF	1
		AHSKITTAM	1
		DALTPLVTI	3
		DALVLKTV	2
		DPYKATSAV	3
		EAYSSTSSW	1
		EPETTTSFITY	1
		ERSPVIQTL	2
		ETILTFHAF	3
		ETTASLVSR	1
		EVISSRGTSM	1
		EVPSGATTEVSR	2
		EVYPELGTQGR	1
		FAVPTGISM	3
		FESHSTVSA	1
		FPFVTGSTEM	1
		FPHSEETTTM	1
		FPHSEITTL	1
		FPHSEMTTV	2
		FQRQGQTAL	1
		FSTDTSIVL	1
		GEPATTVSL	1
		GHESHSPAL	1
		GSDTSSKSL	1
		GVATRVDAI	1
		HESEATASW	1
		HETETRTTW	3
		HFPEKTTHSF	1

		HLTEVYPEL	1
		HQFITSTNTF	2
		IEHSTQAQDTL	1
		IITEVITRL	1
		IPGPAQSTI	1
		IPRVFTSSI	4
		IQIEPTSSL	1
		ISDEVVTRL	4
		ISVPAKTSL	1
		ITETSAVLY	2
		ITRLPTSSI	1
		KMISAIPTL	4
		KTFPASTVF	2
		LPHSEITTL	1
		LPTSESLVSF	1
		LYVDGFTHW	1
		MPNLPSTTSL	1
		NLSSITHER	1
		PGGTRQSL	1
		PLLVLFTI	1
		QAKTHSTL	1
		QFITSTNTF	2
		QRFPHSEM	1
		QSTPYVNSV	1
		RETSTSEETSL	1
		RETSTSQKI	1
		RPLFQKSSM	2
		RVFTSSIKTK	1
		RVRSTISSL	3
		SAFESHSTV	3
		SAIETSAVL	2
		SAIPFSmTL	1
		SATERSASL	1
		SEPDTTASW	3
		SEQRTSPSL	1
		SESVTSRTSY	1
		SETPVGASI	1
		SEVPLPMAI	1
		SGDQGITSL	1

		SIKTKSAEM	1
		SPAGEAHSL	2
		SPAMTSTSF	1
		SPFSAEEANSL	2
		SPGATSRGTL	1
		SPHPVSTTF	2
		SPHPVTALL	4
		SPHPVTALLTL	3
		SPLFQRSSL	1
		SPMATTSTL	1
		SPMTSLLTSGL	1
		SPQNLRNTL	4
		SPQSMSNTL	1
		SPRFKTGL	1
		SPRLNTQGNTAL	4
		SPRTEASSAVL	2
		SPSEAITRL	2
		SPSKAFASL	7
		SPSPVSSTL	2
		SPSSPMSTF	1
		SPSSPTPKV	1
		SQGFSHSQM	3
		SRTEISSSR	1
		SRTEVASSR	1
		SRTEVISSR	2
		SSETTKIKR	1
		STETSTVLY	1
		STIPALHEI	1
		STSQEIHSATK	1
		STTFPTLTK	1
		SVLADLVTTK	1
		SVLTSSLVK	1
		SVSGVKTTF	2
		SVSSETTKIKR	2
		SVTESTHHL	1
		TAGPTTHQF	4
		TAKTPDATF	1
		TEARATSDSW	1
		TEFPLFSAA	1

		TETEAIHVF	6
		TEVSRTEAI	1
		THSAMTHGF	1
		THSTASQGF	1
		THSTISQGF	1
		TPGGTRQSL	4
		TPGLRETSI	2
		TPGNRAISL	6
		TPKLRETSI	1
		TSDFPTITV	1
		TSGPVTEKY	1
		TSHERLTTL	1
		TSIFSGQSL	1
		TSMPRSSAM	1
		TSRSVDEAY	1
		TTALKTTSR	1
		TTYEGSITV	1
		TVAKTTTTF	2
		TYSEKTTLF	3
		VPRSAATTL	2
		VPTPVFPTM	1
		VSKTTGMEF	1
		YPDPSKASSAM	4
		VLQGLLRSL	1
CRABP1/2	P29373;P29762	FYIKTSTTV	1
		MLRKIAVAA	1
		NAMLRKVAV	1
		NVMLRKIAV	3
		RTTEINFKV	8
		VAAASKPAV	1
IDO1	P14902	LELPPILVY	2
		NPKAFFSVL	6
		NPSVREFVL	1
		RSYHLQIVTK	7
		RYMPPAHRNF	4
		TLLKALLEI	3
MMP11	P24347	APAAWLRSA	3
		APAAWLRSAA	3
		APRPASSL	3

		FPRLVGPDF	1
		GRADIMIDF	1
		GRWEKTDLTY	1
		HEFGHVLGL	1
		LLQPPPLLAR	1
		LPSPVDAAF	2
		RPASSLRP	2
		VRFPVHAAL	1
		VRFPVHAALVW	1
		VWSDVTPLTF	7
		YTFRYPLSL	3
PTTG1/2	O95997	DAYPEIEKF	1
		FPFNPLDF	2
		FPFNPLDFE	1
		SPSSILSTL	3
EYA2	O00167	AELEALTDLW	2
		ETIIIFHSL	3
		NEIERVFVW	8
		NVGGLIGTPK	10
		RVKEMYNTY	2
		SVFPIENIY	1
LGALS1	P09382	APDAKSFVL	1
		AVFPFQPGSV	1
		EVAPDAKSF	2
		FPFQPGSV	2
		FPNRLNLEA	1
		GEVAPDAKSFVL	1
		LPDGYEFKF	1
		YEFKFPNRL	3
FOLR1	P15328	NPNEEVARF	2
		NPNEEVARFY	2
KLK10	O43240	RALAKLLPL	7
		VLVDQSWVL	3
TMEM158	Q8WZ71	GRAFFAAAF	2
		KPIESTLVA	1

5.3 List of HLA class II restricted peptides for selected tumor exclusive source proteins

Table 10 HLA class II eluted peptides of the tumor-exclusive ligandome. Three different proteins are shown with mesothelin (MSLN), MUC16 and DPPA2.

protein	accession	sequence	# of OvCa IDs
MSLN	Q13421	AEVLLPRLV	1
		AIPFTYEQLDVLKHKLDE	1
		ALGGLACDLPGRFVAES	1
		ALRGLLPVLGQPI	1
		ALRGLLPVLGQPII	1
		ALRGLLPVLGQPIIR	3
		ALRGLLPVLGQPIIRS	1
		ALRGLLPVLGQPIIRSIPQ	1
		ALRGLLPVLGQPIIRSIPQG	1
		ALRGLLPVLGQPIIRSIPQGIVA	1
		APERQRLLPAALA	1
		AVLPLTVAEVQKLLGPHVEG	2
		AVRPQDLDTCDPR	2
		DALRGLLPVLGQPIIR	1
		DALRGLLPVLGQPIIRS	2
		DALRGLLPVLGQPIIRSIP	1
		DALRGLLPVLGQPIIRSIPQ	3
		DALRGLLPVLGQPIIRSIPQG	2
		DALRGLLPVLGQPIIRSIPQGIVA	2
		DLPGRFVAESA	1
		DLPGRFVAESAEVL	1
		DLPGRFVAESAEVLL	3
		DLPGRFVAESAEVLLP	4
		DLPGRFVAESAEVLLPR	11
		EADVRALGG	1
		ERHRPVRDWILRQRQ	1
		ERVRELAVALAQKNVK	1
		EVQKLLGPHVEG	1
		EVSGLSTER	1
		FLKMSPEDIRK	1
		FMKLRTDAVLPL	1
		FmKLRTDAVLPLT	2
		FMKLRTDAVLPLTVA	1
		FVKIQSFLG	1
		FVKIQSFLGG	1
		FVKIQSFLGGAPT	2
		GGIPNGYLVL	1
		GIVAAWRQRSSRDPS	1

		GLLPVLGQPIIR	1
		GLLPVLGQPIIRSIPQGIVA	3
		GLLPVLGQPIIRSIPQGIVAA	1
		GLLPVLGQPIIRSIPQGIVAAWRQ	2
		GLSTERVRELAVALAQ	1
		GLSTERVRELAVALAQKN	1
		GQPIIRSIPQGIV	1
		GQPIIRSIPQGIVA	4
		GSLLSEADVRA	1
		GSLLSEADVRALG	2
		GSLLSEADVRALGG	2
		GSLLSEADVRALGGL	3
		GVRGSLLSEADVRAL	1
		GVRGSLLSEADVRALG	1
		GVRGSLLSEADVRALGG	3
		GVRGSLLSEADVRALGGL	3
		GVRGSLLSEADVRALGGLA	3
		IPFTYEQLDVLKHKLD	1
		IPFTYEQLDVLKHKLDE	2
		IPFTYEQLDVLKHKLDELYPQ	1
		IPQGIVAAWRQRSSR	1
		IPQGIVAAWRQRSSRDPS	2
		IWAVRPQDLDTCDPR	1
		LGLQGGIPNGYLVL	1
		LGQPIIRSIPQGIVA	4
		LGQPIIRSIPQGIVAA	1
		LKALLEVNKGHEMSPQ	1
		LLPVLGQPIIRSIPQGIVA	1
		LLPVLGQPIIRSIPQGIVAA	1
		LLSEADVRALG	1
		LLSEADVRALGG	1
		LPGRFVAESAEVL	1
		LPGRFVAESAEVLL	3
		LPGRFVAESAEVLLP	5
		LPGRFVAESAEVLLPR	10
		LPLTVAEVQKLLGPHVEG	1
		LPLTVAEVQKLLGPHVEGLK	1
		LPVLGQPIIRSIPQGIVA	5
		LPVLGQPIIRSIPQGIVAA	1
		LPVLGQPIIRSIPQGIVAAW	1
		LPVLGQPIIRSIPQGIVAAWRQ	1
		LQGGIPNGYLVL	2
		LQGGIPNGYLVLDL	1
		LRGLLPVLGQPI	1
		LRGLLPVLGQPIIR	2

		LRGLLPVLGQPIIRS	1
		LRGLLPVLGQPIIRSIPQ	1
		LRGLLPVLGQPIIRSIPQG	1
		LRGLLPVLGQPIIRSIPQGIVA	1
		LRGLLPVLGQPIIRSIPQGIVAA	1
		LRTDAVLPLTVAEVQKLLGPHVEG	1
		LSEADVRALGG	1
		LSTERVRELAVALAQ	1
		LSTERVRELAVALAQK	1
		LSTERVRELAVALAQKN	2
		LSTERVRELAVALAQKNVK	1
		LTVAEVQKLLG	1
		LTVAEVQKLLGPHVEG	1
		LTVAEVQKLLGPHVEGL	1
		LTVAEVQKLLGPHVEGLK	1
		LTVAEVQKLLGPHVEGLKA	1
		LTVAEVQKLLGPHVEGLKAE	1
		LTVAEVQKLLGPHVEGLKAEE	2
		LTVAEVQKLLGPHVEGLKAEER	1
		LTVAEVQKLLGPHVEGLKAEERHRP	1
		MDALRGLLPVLGQPIIRSIPQGIVA	1
		PGRFVAESAEVLLPRL	1
		PVLGQPIIRSIPQGIVA	4
		PVLGQPIIRSIPQGIVAAW	1
		QPIIRSIPQGIVA	1
		RELAVALAQKNVKLSTE	1
		RGLLPVLGQPI	1
		RGLLPVLGQPIIR	1
		RGLLPVLGQPIIRSIPQGIVA	1
		RGLLPVLGQPIIRSIPQGIVAAWRQ	1
		RGSLLSEADVRALG	2
		RGSLLSEADVRALGG	2
		RTDAVLPLTVAEVQKLLGPHVEG	1
		RVRELAVALAQKNVK	1
		SEADVRALGG	1
		SLLSEADVRALG	1
		SPRQLLGFPCAEVSG	1
		TERVRELAVALAQKN	1
		TFMKLRTDAVLPLTVA	1
		TLGLGLQGGIPNGYLV	1
		TVAEVQKLLGPHVEG	3
		TVAEVQKLLGPHVEGL	1
		TVAEVQKLLGPHVEGLK	2
		VAEVQKLLGPHVE	1
		VAEVQKLLGPHVEG	6

		VAEVQKLLGPHVEGL	1
		VAEVQKLLGPHVEGLK	1
		VLDLSMQEA	1
		VLGQPIIRSIPQGIVA	2
		VLPLTVAEVQKLLGPHVEG	1
		VLPLTVAEVQKLLGPHVEGLK	1
		VLPLTVAEVQKLLGPHVEGLKAEE	1
		VPPSSIWAVRPQDLDTCDPR	3
		VQKLLGPHVEG	3
		VRELAVALAQKNVK	1
		VRGSLLSEADVRA	1
		VRGSLLSEADVRALG	6
		VRGSLLSEADVRALGG	4
		VRGSLLSEADVRALGGL	3
		VRGSLLSEADVRALGGLA	2
		VSTMDALRGLLPVLGQPIIR	1
		VSTMDALRGLLPVLGQPIIRSIPQ	1
		VSTMDALRGLLPVLGQPIIRSIPQG	1
		VTSLETLKALLEVNK	1
		WGVRGSLLS	1
		WGVRGSLLSEADVR	1
		WGVRGSLLSEADVRA	1
		WGVRGSLLSEADVRAL	1
		WGVRGSLLSEADVRALG	2
		WGVRGSLLSEADVRALGG	2
		WGVRGSLLSEADVRALGGL	3
		WGVRGSLLSEADVRALGGLA	3
MUC16	Q8WXI7	ATTEVSRTEAISFSR	1
		ATTPSWVETHSIVIQGFPH	1
		DKAFTAATTEVSR	1
		EELGPYTLDRNSLYVNG	1
		EITITTQTGYSLATSQVTLP	1
		ELGPYTLDRDSLYVN	1
		ELGPYTLDRNSL	1
		ELGPYTLDRNSLYV	1
		ELGPYTLDRNSLYVN	2
		ELGPYTLDRNSLYVNG	2
		ETILTFHAF	1
		FDKAFTAATTEVSR	2
		FDKAFTAATTEVSRTE	1
		GIKELGPYTLDRN	1
		GIKELGPYTLDRNSL	1
		GIKELGPYTLDRNSLYVNG	1
		GLLKPLFKSTSVGPL	1
		GPYTLDRNSLYVN	1

		GPYTLDRNSLYVNG	2
		GSRKFNTMESVLQGLL	1
		IELGPYLLDRGSLYVNG	1
		INNLRYMADMGQPG	2
		ISTRTVSWFSTSPV	1
		LAQSMRSSDSPSEAIT	1
		LGFYVLDRDSLFIN	1
		LGPYLLDRGSLYV	1
		LGPYLLDRGSLYVN	1
		LGPYLLDRGSLYVNG	1
		LGPYTLDRNSL	1
		LGPYTLDRNSLY	1
		LGPYTLDRNSLYV	2
		LGPYTLDRNSLYVN	4
		LGPYTLDRNSLYVNG	3
		LKPLFKSTSVGPL	1
		LKPLFKSTSVGPLY	1
		LKPLFKSTSVGPLYS	1
		LKPLFKSTSVGPLYSG	1
		LLKPLFKSTSVGPL	1
		LRPVFKNTSVGPL	1
		LVTSSRAVTST	1
		NLQYSPDmGKGSATFNSTE	1
		QLGFYVLDRDSLFIN	1
		QVTLPLGTSMTFLSGT	1
		RTGSRKFNTMESVLQGLL	1
		SASLPTPGQSLNTIPDSDAS	1
		SDPYKATSAVVITS	1
		SDPYKATSAVVITST	1
		SRKFNTMESVLQG	1
		SRKFNTMESVLQGLL	1
		SSGYKSQSSVLADS	1
		STETITRLSTFPFVT	1
		STETITRLSTFPFVTG	1
		STQRVTTSMIMDTVE	1
		SVPDILSTSW	1
		THGIKELGPYTLDRN	1
		TLDRNSLYVN	1
		TLDRNSLYVNG	1
		TPSWVETHSIVIQG	1
		TPSWVETHSIVIQGFP	1
		TPSWVETHSIVIQGFPH	2
		TRKIIKFPTSPI	1
		TSTVYWATTGTPSSFP	1
		TTPSWVETHSIVIQGFP	1

		TTPSWVETHSIVIQGFPH	2
		TTSVPSVVSGFTTLK	1
		WELSQLTNSVTELGPYTLDRD	1
		WPSPPFVKETSPPSSPL	1
		WVETHSIVIQGFPH	1
DPPA2	Q7Z7J5	RLLSADTKGWVRLQ	1

Table 11 HLA typing of patients treated with multipeptide vaccine cocktails.

patient number	patient ID	HLA typing
1	OvCa 115	A*03:01:01:01;B*07:02:01;C*07:02:01:03, DRB1*13:05:01, DRB1*15:01:01:01, DRB3, DRB5, DQB1*03:01:01:02, DQB1*06:03:01, DQ7
2	OvCa 100	A*02:01:01:01;B*07:02:01;B*41:02:01;C*07:02:01:01;C*17:01:01:01; DRB1*13:03:01, DRB1*15:01:01:01, DRB3*01:01:02:01, DRB5*01:01:01, DQB1*03:01:01, DQB1*06:02:01, DQA1*01:02:01, DQA1*05:01:01, DPB1*03:01:01 DPB1*05:01:01
3	OvCa134	A*01:01;A*02:01;B*08:01;B*39:01;C*07:01;C*12:03, DQB1*02:01, DQB1*03:01, DRB1*03:01, DRB1*12:01, DQA1*05:01, DRB3,

Table 12 warehouse of OvCa exclusive peptides that can be used for peptide-based anti-cancer vaccines. Peptides are organized based on their HLA restriction. Additionally immunogenicity assessed by aAPC priming, the amount of OvCas the peptide was represented on and the OvCa IDs are shown. OvCas with an ID of 99 or higher are contributed by the author of the thesis.

HLA	sequenz	protein	Immuno. (aAPC)	N OvCas found on	OvCa IDs found on
A*01	ITETSAVLY	MUC16	**1 / 2**	3	OvCa 111 OvCa 134 OvCa 65
A*02	TLLKALLEI	IDO1		4	OvCa 99 OvCa 132 OvCa 137 OvCa 140
A*02	RTTEINFKV	CRABP1/2	**1 / 2**	18	OvCa 103 OvCa 13 OvCa 16 OvCa 59 OvCa 60 OvCa 65 OvCa 70 OvCa 81 OvCa 99 OvCa 107 OvCa 120 OvCa 126 OvCa 137 OvCa 138 OvCa 142 OvCa 132 OvCa 150 OvCa 151
A*02	VLVDQSWVL	KLK10		5	OvCa 81 OvCa 126 OvCa 142 OvCa 151 OvCa 162
A*02 (auch B*08)	RALAKLLPL	KLK10	**2 / 2**	12	OvCa 104 OvCa 111 OvCa 114 OvCa 64 OvCa 72 OvCa 84 OvCa 9 OvCa 107 OvCa 126 OvCa 148 OvCa 150 OvCa 151
A*02	IITEVITRL	MUC16	**3 / 10**	1	OvCa 126
A*02	KMISAIPTL	MUC16	**4 / 6**	6	OvCa 81 PC2011-14 OvCa 103 OvCa 107 OvCa 126 OvCa 162
A*03	KTKGPLKQK	PTTG1	**0 / 1**	3	OvCa 23 OvCa 53 OvCa 72
A*03 (auch A*11)	AVTSGVATK	TMEM158		4	OvCa 10 OvCa 54 OvCa 59 PC2011-14
A*03	NVGGLIGTPK	EYA2	**0 / 2**	17	OvCa 104 OvCa 58 OvCa 69 OvCa 72 OvCa 82 OvCa 116 OvCa 120 OvCa 121 OvCa 128 OvCa 135 OvCa 136 OvCa 148 OvCa 150 OvCa 151 OvCa 157 OvCa 162 OvCa 167
A*03 (auch A*11)	RSYHLQIVTK	IDO1	**2 / 2**	13	OvCa 10 OvCa 104 OvCa 54 OvCa 59 OvCa 66 OvCa 116 OvCa 121 OvCa 135 OvCa 148 OvCa 151 OvCa 157 OvCa 162 OvCa 167
A*11 (auch A*03)	AVTSGVATK	TMEM158			
A*11	STSQEIHSATK	MUC16	**2 / 6**	2	OvCa 167 PC2011-14
A*11 (auch A*03)	RSYHLQIVTK	IDO1	**1 / 1**		
A*24	VWSDVTPLTF	MMP11	**0 / 1**	10	OvCa 103 OvCa 111 OvCa 65 OvCa 99 OvCa 118 OvCa 121 OvCa 130 OvCa 135 OvCa 153 OvCa 155

A*24	TYSEKTTLF	MUC16	**3 / 3**	8	OvCa 12 OvCa 41 OvCa 60 OvCa 65 OvCa 103 OvCa 121 OvCa 130 OvCa 153
A*24	QFITSTNTF	MUC16	**2 / 3**	4	OvCa 60 OvCa 118 OvCa 121 OvCa 153
A*24	RYMPPAHRNF	IDO1	**5 / 5**	4	OvCa 103 OvCa 99 OvCa 121 OvCa 130
A*25 (auch A*30)	RVKEMYNTY	EYA2		4	OvCa 59 OvCa 80 OvCa 137 OvCa 157
A*25	EVITSSRTTI	MUC16	**1 / 1**	1	OvCa 141
A*25	EVISSRGTSM	MUC16	**1 / 3**	6	OvCa 105 OvCa 111 OvCa 48 OvCa 60 OvCa 64 OvCa 80
A*25	EVTSSGRTSI	MUC16	**2 / 3**	2	OvCa 107 OvCa 111
A*25	ETILTFHAF	MUC16	**2 / 2**	5	OvCa 105 OvCa 111 OvCa 48 OvCa 64 OvCa 80
A*25	EVAPDAKSF	LGALS	**1 / 1**	9	OvCa 39 OvCa 48 OvCa 57 OvCa 60 OvCa 80 OvCa 107 OvCa 132 OvCa 141 OvCa 153
A*30 (auch A*25)	RVKEMYNTY	EYA2		4	OvCa 59 OvCa 80 OvCa 137 OvCa 157
A*68	EVPSGATTEVSR	CA125		2	OvCa 105 OvCa 110
A*68	EVPTGTTAEVSR	CA125		2	OvCa 105 OvCa 110
B*07	APRPASSL	MMP11		3	OvCa 107 OvCa 126 OvCa 136
B*07	NPKAFFSVL	IDO1	**3 / 5**	12	OvCa 9 OvCa 107 OvCa 116 OvCa 136 OvCa 148 OvCa 151 OvCa 154 OvCa 167 OvCa 104 OvCa 109 OvCa 13 OvCa 135
B*07 (auch B*35)	TPGNRAISL	MUC16	**6 / 6**	8	OvCa 104 OvCa 107 OvCa 109 OvCa 111 OvCa 126 OvCa 148 OvCa 151 OvCa 167
B*07	SPHPVTALL	MUC16	**2 / 3**	8	OvCa 72 OvCa 84 OvCa 9 OvCa 104 OvCa 107 OvCa 126 OvCa 148 OvCa 151
B*07	SPSKAFASL	MUC16	**3 / 3**	15	OvCa 23 OvCa 39 OvCa 69 OvCa 72 OvCa 84 OvCa 9 OvCa 104 OvCa 107 OvCa 109 OvCa 111 OvCa 126 OvCa 148 OvCa 151 OvCa 154 OvCa 167
B*08 (auch A*02)	RALAKLLPL	KLK10	**0 / 1**	12	OvCa 104 OvCa 111 OvCa 114 OvCa 64 OvCa 72 OvCa 84 OvCa 9 OvCa 107 OvCa 126 OvCa 148 OvCa 150 OvCa 151
B*08	NVMLRKIAV	CRABP1	**0 / 1**	5	OvCa 102 OvCa 107 OvCa 111 OvCa 134 OvCa 64
B*13	AVTNVRTSI	MUC16		3	OvCa 132 OvCa 137 OvCa 140
B*15	SQGFSHSQM	MUC16	**5 / 6**	3	OvCa 131 OvCa 157 OvCa 162
B*15	FQRQGQTAL	MUC16	**1 / 6**	1	OvCa 48
B*18 (auch B*40)	YEFKFPNRL	LGALS		5	OvCa 153 OvCa 109 OvCa 116 OvCa 142 OvCa 151
B*18	LELPPILVY	IDO1		2	OvCa 116 OvCa 128
B*18	NEIWTHSY	FOLR1		3	OvCa 105 OvCa 74 OvCa 116

B*18 (auch B*44)	TETEAIHVF	MUC16	**1 / 1**	8	OvCa 41 OvCa 80 OvCa 111 OvCa 114 OvCa 116 OvCa 128 OvCa 142 OvCa 157
B*27	GRAFFAAAF	TMEM158		2	OvCa 103 OvCa 128
B*27	GRSQVSTPRF	PTTG1/PTTG2		1	OvCa 53
B*27	QRMTTQLLL	FOLR1		1	OvCa 103
B*27	SRTEVISSR	MUC16		3	OvCa 53 OvCa 103 OvCa 110
B*35	LPSPVDAAF	MMP11	-	3	OvCa 104 OvCa 65 OvCa 121
B*35	DAYPEIEKF	PTTG1/PTTG2	-	8	OvCa 53 OvCa 54 OvCa 58 OvCa 110 OvCa 120 OvCa 121 OvCa 132 OvCa 150
B*35	NPSVREFVL	IDO	-	3	OvCa 13 OvCA 104 OvCa 109
B*35	APDAKSFVL	LGALS	-	5	OvCa 12 OvCa 13 OvCa 135 OvCa 102 OvCa 121
B*35	YPDPSKASSAM	MUC16		6	OvCa 65 OvCa 104 OvCa 107 OvCa 121 OvCa 126 OvCa 151
B*35	FPHSEITTL	MUC16		5	OvCa 12 OvCa 13 OvCa 53 OvCa 121 OvCa 132
B*35	LPHSEITTL	MUC16		4	OvCa 12 OvCa 13 OvCa 121 OvCa 135
B*35	SPQNLRNTL	MUC16		8	OvCa 23 OvCa 72 OvCa 84 OvCa 104 OvCa 107 OvCa 126 OvCa 148 OvCa 151
B*35 (auch B*07)	TPGNRAISL	MUC16		11	OvCa 23 OvCa 72 OvCa 84 OvCa 104 OvCa 107 OvCa 109 OvCa 111 OvCa 126 OvCa 148 OvCa 151 OvCa 167
B*40	GEVAPDAKSFVL	LGALS		4	OvCa 99 OvCa 136 OvCa 142 OvCa 151
B*40 (auch B*18)	YEFKFPNRL	LGALS		5	OvCa 153 OvCa 109 OvCa 116 OvCa 142 OvCa 151
B*40	SESPSTIKL	MUC16		2	OvCa 13 OvCa 70
B*44 (auch B*18)	TETEAIHVF	MUC16		4	OvCa 111 OvCa 114 OvCa 41 OvCa 80
B*44	AESIPTVSF	MUC16		5	OvCa 114 OvCa 118 OvCa 142 OvCa 157 OvCa 162
B*44	NEIERVFVW	EYA2		1	OvCA 139 (Zystadenom)
B*51	FPFQPGSV	LGALS		2	OvCa 141 OvCa 130
B*51	DALVLKTV	MUC16	**1 / 3**	7	OvCa 41 OvCa 73 OvCa 74 OvCa 79 PC2011-14 OvCa 126 OvCa 141
B*51	DPYKATSAV	MUC16	**3 / 3**	7	OvCa 10 OvCa 41 OvCa 69 OvCa 73 OvCa 74 OvCa 79 PC2011-14